TECHNICAL AND ECONOMIC FEASIBILITY STUDY OF METAL 3D PRINTING IN THE CHEMICAL INDUSTRY: APPLICATION TO PUMP IMPELLERS

Felix Hernández Hernández

UNIVERSITAT ROVIRA i VIRGILI

TECHNICAL AND ECONOMIC FEASIBILITY STUDY OF METAL 3D PRINTING IN THE CHEMICAL INDUSTRY: APPLICATION TO PUMP IMPELLERS

FELIX HERNÁNDEZ HERNÁNDEZ

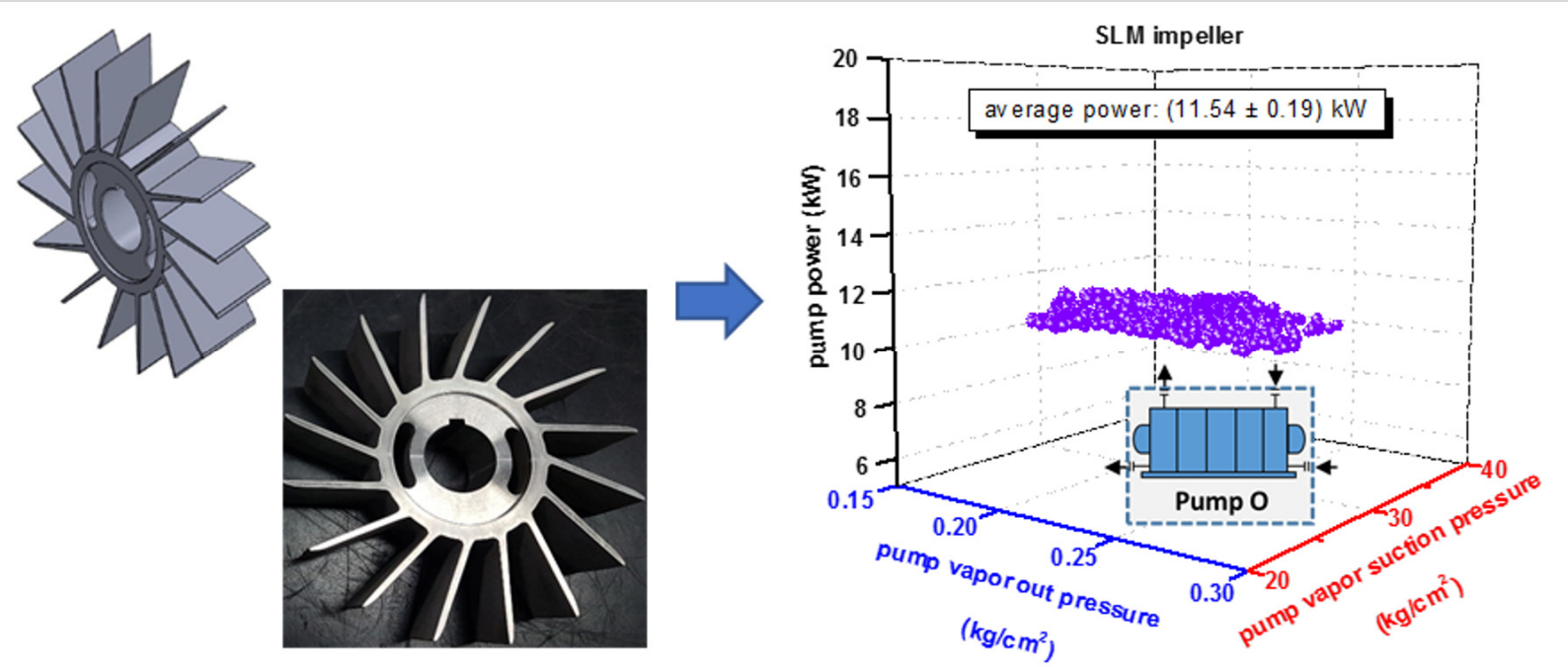

DOCTORAL THESIS
2023

Felix Hernández Hernández

Technical and Economic Feasibility Study of Metal 3D Printing in the Chemical Industry: Application to Pump Impellers

Dissertation submitted to obtain the degree of
Doctor from Universitat Rovira i Virgili
Supervised by: Dr. Alex Fragoso Sierra

UNIVERSITAT
ROVIRA i VIRGILI
Departament d´Enginyeria Química

Tarragona
February 2023

UNIVERSITAT ROVIRA I VIRGILI

Departament d'Enginyeria Química
Universitat Rovira i Virgili
Campus Sescelades,
Avda. Països Catalans, 26
43007 Tarragona
Tel: 977 55 85 79
Fax: 977 55 96 67

Dr. Alex Fragoso

CERTIFIES:

That the present study, entitled "Technical and Economic Feasibility Study of Metal 3D Printing in the Chemical Industry: Application to Pump Impellers" presented by Felix Hernández Hernández for the award of the degree of Doctor, has been carried out under my supervision at the Department of Chemical Engineering of Universitat Rovira i Virgili,

Tarragona, February 1st, 2023.

Dr. Alex Fragoso

ACKNOWLEDGEMENTS

This thesis would not have been possible without the support of, in particular, two people to whom the author would like to express his sincere gratitude.

On the one hand, to Dr. Alex Fragoso for his work as a tutor throughout the entire doctorate, during which he has shown me great empathy and patience. Without them, the work would not have been possible.

And, on the other hand, to my wife for her patience and encouragement through difficult times, especially those moments when "drop out the PhD" was very close to reality.

I also do not want to miss this opportunity to mention the support and learnings from my parents, such as strong capacity for the effort and to work hard in adverse circumstances. Without being close to me in my day-to-day life, I know that they taught me many things that myself do not even know that I know.

Esta tesis no hubiera sido posible sin el apoyo de, especialmente, dos personas a las que el autor quiere mostrar su especial agradecimiento.

En primer lugar, al Doctor don Alex Fragoso por su labor como tutor a lo largo de todo el doctorado durante el que ha me demostrado una gran empatía y paciencia sin las que el trabajo no hubiera sido posible.

Y, en segundo lugar, a mi esposa por su paciencia y motivación en los momentos difíciles, sobre todo en aquellos momentos en los que "dejarlo" fue un pensamiento muy próximo a la realidad.

Tampoco quiero perder esta ocasión para mencionar el soporte y eternas enseñanzas de mis padres (como la capacidad de esfuerzo y trabajo en circunstancias adversas) que, sin estar allí en mi día a día, sé que me enseñaron muchas cosas que ni yo mismo sé que las sé.

Table of Contents

ABSTRACT

(English version)

The Metal 3D Printing fabrication techniques, also named Metal Additive Manufacturing (AM) Technology, are in its birth starting point from the perspective of industrial applications and worldwide massive divulgation. It is noteworthy that there are high hopes in the near future for this technology, hopes from a technological and from an economical point of view.

The emergence of additive manufacturing is renovating the landscape of available production technologies. These technologies have multiple different and potential uses. Among them, in the Industrial field, as an alternative to the process of materials purchasing and price negotiations, manufacturing obsolete (not yet in the market) or new pieces and storage / custody of technical spare parts for the chemical industry.

The purpose of this study will be focuses on the application of Additive Manufacturing in metal (3D printing) for pump impellers, rotating equipment widely used around the world and with a high criticality in the chemical industry - origin of this project - but also in many other types of Industry. The scope of the project includes the construction of 2 metallic pump impellers, according to strategies 1 and 2 indicated below:

Strategy 1: Manufacture a metallic pump impeller using molds with additive technology 3D sand printing, additive technology type BJ (Binder Jetting).

Strategy 2: Manufacture a metallic impeller for a pump with 3D additive technology type SLM (Selective Laser Melting).

The development of the present work will be based on next steps: design - scanning, drawing / elaboration of constructive 3D plans -, manufacturing, pump assembly and commissioning of two impellers (*strategies 1 and 2*) in two different pumps (pump P and pump O) made of metal with two completely different 3D technologies.

Next will be analysis of the results / work data once the pump is assembled and put into operation in the plant, and after a minimum of 4 months of service.

And finally, make a comparison - under normal operating conditions - with the same previous service and with the same type of metal impeller but manufactured in a conventional way: AM vs conventional manufacturing methods.

On *Strategy 1* we describe the fabrication of a closed vane pump impeller (ϕ 206 mm, height 68 mm, weight 4 kg) by Binder Jetting (BJ) 3D printing of a sand mold followed by casting using stainless steel 316 to create an identical copy of a part in service in a chemical plant in Tarragona, Spain. The original part – from manufacturer KSB - was reverse engineered and used to create a sand mold by BJ 3D printing on which new impellers were fabricated by casting. Metallographic studies showed an austenitic matrix with 6.3% of ferritic phase and 40 μm × 8 μm ferrite grains without precipitated carbides. The impeller was put into operation in a centrifugal pump at a polyol/polyglycol plant belonging to Dow Chemical Ibérica SL from October 30, 2020 to April 2021, 6 months. Process variables related to the pump behavior were compared with the same variables obtained in previous cycles with the original impeller for three different product viscosities (30, 180 and 500 cSt). At 500 cSt, the average current consumption was 9,34 A as compared with the 9,41 A measured with the original impeller. Similarly, the pump pressure remained essentially constant during process operation with both impellers (3,97 bar with the new impeller vs. 3,99 bar with the old). Other monitored parameters (product flow, tank level) were similar in both cases, validating the fabrication strategy from an operational point of view.

Regarding *Strategy 2*, we describe the manufacture of an open pump impeller (ø 230 mm, height 60 mm, original weight 5.247 kg reduced to 2.99 kg in metal 3D printing) using Selective Laser Melting (SLM) 3D printing technology in material Ti6Al4V titanium alloy (original impeller was made of stainless steel 1.4027.05, but this metal powder is not yet available for AM technology) to create an identical copy of a part in service at a chemical plant in Tarragona, Spain. The original part – from manufacturer Flowserve SIHI - was reverse engineered and used to create a 3D digitized CAD drawing from which the new SLM impellers were manufactured. The impeller was put into operation in a vacuum pump in a hydrocarbon plant of Dow Chemical Ibérica SL from June 16, 2022 to October 2022, 4 months. The process variables related to the behavior of the pump were compared with the same variables obtained in previous cycles with the original SIHI impeller. Results obtained with both impellers show typical values between 11 and 12 kW. The pump power should remain constant since a decrease would indicate a malfunction of mechanical parts of the pump in which the impeller is located, indirectly measuring the performance of the pump throughout the process. The average values in

all cases were around 11,5 kW with low standard deviations, indicating similar behaviour of both impellers.

On the one hand, there are many potential competitive advantages that this technology offers. But, on the other hand, it is in its initial status of technical validation of the technology and it is needed to ensure its viability and reliability. This work further demonstrated that the implementation of metal additive manufacturing technologies in chemical process engineering is a useful solution to fabricate spare parts that could be difficult to replicate with other technologies, providing potential economic benefits.

3D technology is presented mainly as a complement to traditional manufacturing, it does not come to replace it, but it is also true that in some cases it is really a serious replacement alternative. If the prospect of potential improvement that metal 3D printing offers is confirmed, it opens a very relevant new path for better maintenance and reliability perspective of Chemical plants, as well as significant economic savings.

The future is coming closer…

ABSTRACT

(Spanish version)

La técnica de fabricación 3D en metal, también llamada fabricación aditiva (Additive Manufacturing – AM), está en un momento incipiente y muy novedoso. Hay muchas esperanzas futuras depositadas en esta tecnología, tanto desde un punto de vista tecnológico como económico.

La aparición de la fabricación aditiva está renovando el panorama de las tecnologías de producción disponibles. Estas tecnologías ofrecen múltiples aplicaciones y, entre ellas, en el terreno industrial, son alternativa al proceso de compra y negociación de precios de materiales, fabricación de piezas nuevas u obsoletas (que ya no se encuentran en el mercado) y almacenamiento/custodia de recambios técnicos para la Industria Química.

El proyecto se centra en la aplicación de la fabricación aditiva en metal (3D printing) para impulsores de bombas, equipos rotativos de uso muy extendido y crítico en la Industria Química - origen de este proyecto - pero también igualmente en muchos otros tipos de Industria. El alcance del proyecto abarca la construcción de 2 impulsores metálicos de bomba, según las estrategias 1 y 2 a continuación indicadas:

Estrategia 1: fabricación de un impulsor de bomba en metal usando moldes hechos con tecnología aditiva 3D sand printing tipo BJ (Binder Jetting).

Estrategia 2: fabricación de un impulsor de bomba en metal hecho con tecnología aditiva 3D tipo SLM (Selective Laser Melting).

El desarrollo del trabajo tendrá varias etapas bien diferenciadas. La primera será el diseño – escaneado, dibujo/elaboración planos 3D constructivos -, a continuación la fabricación del rodete, montaje en la bomba y puesta en funcionamiento en una planta química de acuerdo a las *estrategias 1 y 2*, en sendas bombas (bombas P y O) con los impulsores fabricados en metal con tecnología aditiva 3D.

En la siguiente etapa se hará un análisis de los resultados/datos de trabajo una vez la bomba es montada y puesta en funcionamiento en planta, con un mínimo de 4 meses de servicio.

Finalmente, como última etapa, se establecerá una comparación con el mismo servicio previo y con el mismo tipo de impulsor metálico pero fabricado de forma tradicional.

Referente a la *Estrategia 1*, describimos la fabricación de un impulsor de bomba cerrado (ø 206 mm, altura 68 mm, peso 4 kg) mediante la impresión 3D Binder Jetting (BJ) de moldes de arena seguido de una fundición tradicional con acero inoxidable 316 para crear una copia idéntica de una pieza en servicio en una planta química en Tarragona, España. Se realizó ingeniería inversa de la pieza original que se usó para crear un molde de arena mediante la impresión 3D BJ en el que se fabricaron nuevos impulsores por fundición. Los estudios metalográficos mostraron una matriz austenítica con 6.3% de fase ferrítica y granos de ferrita de 40 μm × 8 μm sin carburos precipitados. El impulsor se puso en funcionamiento en una bomba centrífuga en una planta de producción de poliol/poliglicol de Dow Chemical Ibérica SL desde el 30 de octubre de 2020 hasta abril de 2021 (6 meses). Las variables de proceso relacionadas con el comportamiento de la bomba se compararon con las mismas variables obtenidas en ciclos anteriores con el impulsor original (fabricante KSB) para tres viscosidades de producto diferentes (30, 180 y 500 cSt). A 500 cSt, el consumo medio de corriente fue de 9.34 A frente a los 9.41 A medidos con el impulsor original. De manera similar, la presión de la bomba se mantuvo esencialmente constante durante la operación del proceso con ambos impulsores (3.97 bar con el impulsor nuevo frente a 3.99 bar con el anterior). Otros parámetros monitoreados (flujo de producto, nivel del tanque) fueron similares en ambos casos, validando la estrategia de fabricación desde un punto de vista operativo.

Referente a la *Estrategia 2*, describimos la fabricación de un impulsor de bomba abierto (ø 230 mm, altura 60 mm, peso 5.247 kg original reducido a 2.99 kg en impresión 3D) mediante tecnología de impresión 3D Selective Laser Melting (SLM) en aleación de titanio Ti6Al4V (el impulsor original está fabricado en inoxidable 1.4027.05, pero este polvo metal no está aún disponible en AM technology) para crear una copia idéntica de una pieza en servicio en una planta química en Tarragona, España. Se realizó ingeniería inversa de la pieza original del fabricante Flowserve SIHI que se usó para crear un plano digitalizado 3D en CAD con el que se fabricaron los nuevos impulsores por SLM. El impulsor se puso en funcionamiento en una bomba de vacío en una planta de hidrocarburos de Dow Chemical Ibérica SL desde el 16 de junio de 2022 hasta octubre de 2022 (4 meses). Las variables de proceso relacionadas con el comportamiento de la bomba se compararon con las mismas variables obtenidas en ciclos anteriores con el impulsor original. Los resultados obtenidos con ambos impulsores muestran valores de 11 a 12 kW. La potencia de la bomba debe permanecer constante, una disminución de

potencia podría indicar un mal funcionamiento de la misma. Los valores medios de potencia, en todos los casos, son siempre alrededor de 11.5 kW, comportamientos similares en ambos impulsores.

Por un lado, son muchas las potenciales ventajas competitivas que esta tecnología ofrece. Pero, por otro lado, en su actual status inicial se necesita una validación técnica de la tecnología para asegurar su viabilidad y su fiabilidad. Este trabajo demostró que la implementación de tecnologías de fabricación aditiva en metal en la ingeniería de procesos químicos es una solución útil para fabricar repuestos con otras tecnologías, proporcionando potenciales beneficios económicos.

La tecnología 3D se presenta principalmente como un complemento de la fabricación tradicional, no viene para sustituirla, pero cierto es también que en casos puntuales se está convirtiendo en una seria alternativa a la manufactura convencional. Si se confirma la perspectiva de mejora potencial que la impresión 3D en metal ofrece, se abre un camino nuevo muy relevante con perspectivas para un mejor mantenimiento y fiabilidad de las plantas químicas, así como un relevante potencial ahorro económico.

El futuro está más cerca…

Keywords: 3D, metal 3D printing, additive manufacturing (fabricación aditiva), binder jetting, sand mold (molde de arena), SLM (Selective Laser Melting), impellers (impulsores, rodetes), titanium (titanio), stainless steel (acero inoxidable), mechanical properties (propiedades mecánicas).

Chapter 1: Introduction and literature review

1.1. General overview about metal manufacturing processes

Conventional manufacturing methods are mainly limited by the total volume of the production run and the physical complexity of the different parts machined and, as a result, it can be needed - from time to time - to use other processes and software that increase the total cost of the piece of our interest to be produced with a more expensive result. Additive manufacturing (AM) solutions have recently emerged to provide a major competitive advantage in some cases, as described below in Sections 1.6. and 1.7, and are seen as one of the major revolutionary industrial processes for the next years (Romero L. et al., 2019).

From a global and generic point of view, there are 3 main types of metal manufacturing processes (Galindo M., 2016):

1.- Subtractive manufacturing (e.g. computer numerical control machining, turning or drilling).

2.- Formative manufacturing (e.g injection molding, metal casting, stamping and forging).

Both processes (Figure 1.1) form the traditional manufacturing methods that include casting, machining, sintering (pressing-compacting under pressure with temperature), injection, forging, stamping (compression of a metal between 2 molds). In general, non-additive processes shape the metal by means of molds or inner molds or, on the other way, by starting of metal blocks that are shaped through processes of turning (machining used to make cylindrical parts), milling (cutting the material that is machined with a rotary tool), drilling, grinding (mechanical process of correction of wear in the cylinder interior walls), etc...

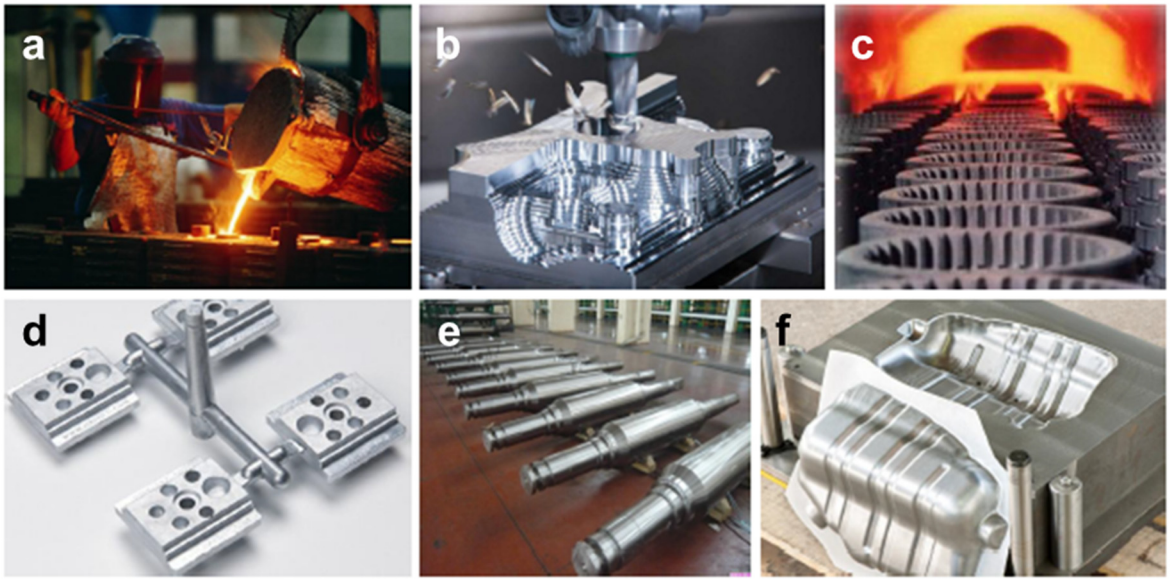

Figure 1.1. Traditional manufacturing methods. a) casting, b) machining, c) dies, d) drilling, e) turning, f) molding.

These different processes of traditional manufacturing are developed basically using a high-capacity resources combined with electronic systems or informatics tools to arrive to very high levels of precision, reliability and production efficiency.

3.- Additive Manufacturing (3D Printing) (Figure 1.2), which complements and/or replaces the other two conventional processes. It uses – as raw material - metals in powder, filament or laminated form.

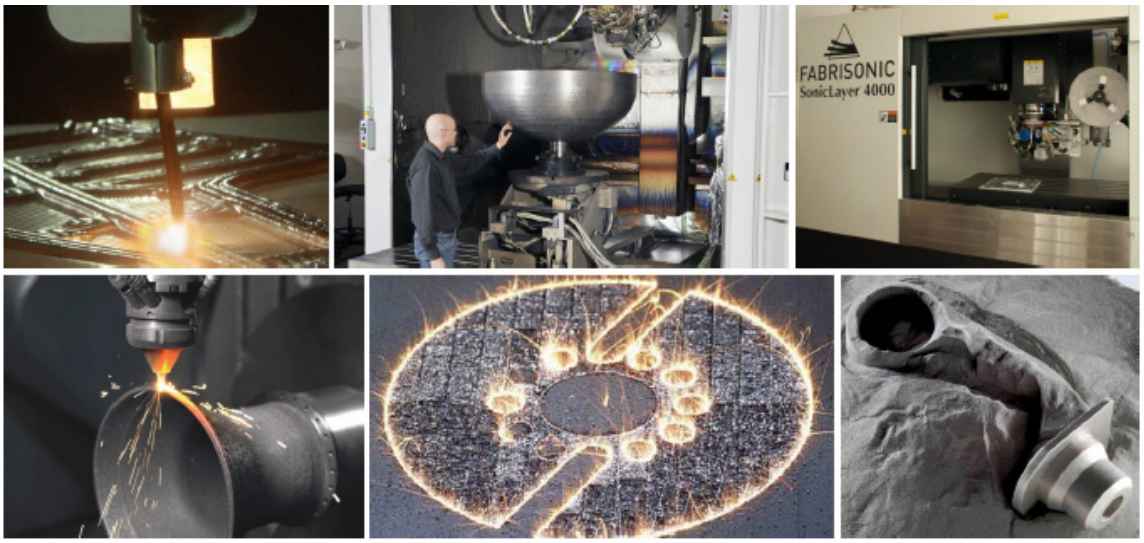

Figure 1.2. Some examples of additive manufacturing methods (3D Printing) on metal substrates. Source: Leitat 2016.

If attention is focused on the application of the different manufacturing technologies used for obtaining rapid prototypes or manufactured pieces, the current technologies can be classified as additive (stereolithography, laser sintering, fused deposition modelling, etc.) and non-additive (incremental forming, high-speed machining, pressure injection molding, lost wax, laminating and contouring, etc.) (Frazier W.E., 2014) (Galindo M., 2016) (Romero L. et al., 2019). These techniques are applicable in a wide range of materials, from polymers to ceramics (Table 1.1).

Table 1.1. Materials and techniques in AM processes, highlighting in gray those used for metal processing.

Category	Technology	MATERIALS			
		Polymers	Metals	Ceramics	Composites
VAT Photo-polymerization	Stereo Lithography	x			x
	Digital Light Processing	x			
Material Jetting	Multijet Modeling	x			x
	Poly Jet	x			
Material Extrusion	Fused Deposition Modeling	x	x	x	x
Powder Bed Fusion	Electron Beam Melting		x		
	Selective Laser Melting		x		
	Direct Metal Laser Sintering		x		
	Selective Laser Sintering	x	x	x	
	Multi Jet Fusion	x			
Binder Jetting	Powder Bed and Inkjet Printing	x	x	x	x
Sheet Lamination	Laminated Object Manufacturing	x	x	x	x
	Ultrasonic Consolidation		x		x
Direct Energy Deposition	Laser Metal Deposition		x		x
	Direct Metal Deposition		x		x

1.2. Additive manufacturing. History, concept, and scope.

Additive manufacturing (AM), also simplified as "3D printing", is a family of manufacturing technologies that use computer-aided created designs or 3D scanners to guide the layer-by-layer deposition of material, which creates a physical object in a precise geometric form (Gao W. et al., 2015).

The first 3D printer was launched on the market in 1986 by Chuck Hull, who founded the company "*3D Systems*" and used the stereolithography (SLA) process (Redwood B. et al.,

2021) to create a 3D object by photopolymerization (Talamona D. et al., 2020). The process uses mirrors, known as galvanometers or galvos (one on the x-axis and one on the y-axis) to quickly point a laser beam across a vat, the printing area, curing and solidifying the resin as it progresses.

In the 1990s and early 2000s, other 3D printing technologies were released, such as FDM from "*Stratasys*" and SLS from "*3D Systems*". These printers were very expensive and were used primarily only for industrial prototyping (Redwood B. et al., 2017).

As early as 2009, ASTM Committee F42 published a document containing standard terminology on additive manufacturing. This is an important milestone because it established 3D printing as an industrial manufacturing technology.

In the same year, the Fused Deposition Modeling patents expired and desktop 3D printers were born with the *RepRap project*. Thus, printers that up to that date used to cost up to *$ 200,000*, became available for less than *$ 2,000* from one day to the next.

According to Wohlers (Wholers report 2020), the adoption of 3D printing continues to grow: more than 1 million desktop 3D printers were sold worldwide between 2015 and 2017, and sales of industrial metal printers almost doubled in 2017 compared to the previous year (Figure 1.3). Now, AM is a quickly expanding technology with many application possibilities such as consumer products, space missions, and rapid prototyping, among others. They offer high design freedom that enables the fabrication of structures with complex internal features that are difficult to achieve with traditional manufacturing techniques (Wholers report 2020).

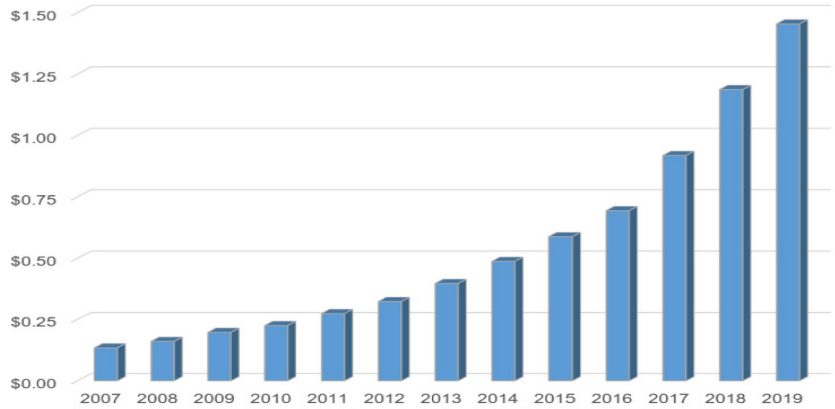

Figure 1.3. Annual worldwide expenditure on final part production using AM technologies. Values in billions of dollars ($\times 10^9$ USD). Source: Wohlers Report 2020

An example of this is the recent announcement that the Italian company "*Isinnova*" has designed and produced many valves for artificial respirators in less than 2 days (Wholers report 2020). This effort has been as a consequence of the emergency situation experienced due to the Covid-19 pandemic and, thanks to "*Isinnova*", many patients could breathe through artificial respirators thanks to their manufactured 3D valves.

Meanwhile, 3D metal fabrication techniques are at a very starting point (Wholers report 2020) (Vaezi M., et al., 2020) but they have already a large number of applications. It is noteworthy that there are high hopes in the near future for this technology, hopes from a technological and from an economical point of view (Wholers report 2020) (Redwood B. et al., 2021).

1.3. Understanding the basics: additive manufacturing vs. conventional manufacturing methods

Metal Additive Manufacturing is a novel and high potential technology for manufacturing a wide variety of spare parts and materials adapted to the client as never traditional manufacturing tools could do it in the past. This is where the alternative term Additive Manufacturing comes from. 3D printing is a fundamentally different way of producing parts compared to traditional subtractive (CNC machining) or formative (injection molding) manufacturing technologies. In 3D printing, no special tools are required (for example, a cutting tool with certain geometry or a mold). Instead, the part is manufactured directly onto the built platform layer-by-layer, which leads to a unique set of benefits and limitations. This unique feature allows the manufacture of complex geometries that are almost impossible to fabricate using conventional systems (Vafadar A. et al., 2021).

To choose between an AM production process or a subtractive or formative manufacturing process, there are a few basic rules to follow before taking that decision.

As a rule of thumb:

"*3D printing is the best option when a single (or only a few) parts are required at a quick turnaround time and a low-cost or when the part geometry cannot be produced with any other manufacturing technology*." (Redwood B. et al., 2021).

The different processes used to manufacture conventional parts and components could be influenced by several production conditions and limitations in relation to obtain certain complex and customized forms where specific and special manufacturing conditions are a limitation to make an effective production.

In the case of subtractive manufacturing process, to make it more profitable the following conditions should be considered:

- medium production volumes (~100 – 500 uds).
- relatively simple geometries.
- high dimensional accuracy.
- For larger production (> 1000 parts), formative technologies (like injection molding) are more cost effective and usually make the most financial sense.

It can thus be said that 3D printing offers geometric flexibility and can quickly produce customized parts at low cost, but when large volumes, tight tolerances and/or demanding material properties are required, traditional manufacturing technologies are often the better option (Redwood B. et al., 2021).

Two important features take the main differences to differentiate between the 3D Printing manufacturing techniques and their traditional counterparts. These makes really the difference between both technological areas to make them more competitive or not, or to make them more or less expensive:

(1) the geometrical complexity of the part to be manufactured.
(2) the customization of the part to be manufactured.

These two characteristics can give important profits in different sectors like, for instance, energy / education / industrial / medical / entertainment. Examples are:

- lightweight products.
- multi-material products.
- ergonomic products.
- integrated mechanisms.

As far as the production of industrial components is concerned, there are many obvious benefits offered by AM with respect to conventional techniques. Among them we can indicate:

(i) a reduction of the time new designs takes to reach the market.
(ii) short production runs.
(iii) a reduction of assembly errors and their associated costs.
(iv) a reduction of tool investment costs.

(v) possibility to combine different manufacturing processes in hybrid processes. In this case, combining additive manufacturing processes with conventional processes might be interesting to make the most of the advantages offered by both.
(vi) optimum usage of materials.
(vii) a more sustainable manufacturing process.

But, on the other side, some inconvenient should also be balanced before choosing AM technologies such as: (Romero L. et al., 2019)

(i) the "*stepping effect*", i.e. complications due to the shaping of geometrical curves and an extremely rough surface finish.
(ii) the manufacturing operation itself can be slow in some technologies.
(iii) can be applied in limited types of materials
(iv) the deposition of layers produces anisotropic materials.
(v) the tolerances obtained may be low.

It is evident that, in recent years, AM has been expanding into several industrial sectors due to the technology provide new opportunities in terms of improved functionality, productivity and competitiveness. Furthermore, while metal AM technologies have almost unlimited potential and the range of applications has increased in recent years, industries have faced challenges in the adoption of these technologies in a turbulent market. Despite the extensive work that has been completed on the properties of metal AM materials, the results clearly indicates that there is still a need of a robust understanding of processes, challenges, application-specific needs, and considerations associated with these technologies like material standard certifications or legal issues (Vafadar A. et al., 2021).

1.4. Understanding the basics: manufacturing steps and materials

Every 3D printer builds pieces based on the same main principle that consists on the transformation of a digital model into a physical three-dimensional object by the sequential layer-by-layer addition of material (Redwood B. et al., 2021).

AM has, as per ASTM F2792-12a "Standard Terminology for Additive Manufacturing Technologies", a terminology which includes terms, definitions of terms, descriptions of terms, nomenclature and acronyms associated with additive-manufacturing (AM) technologies (Bhuvanesh Kumar M., Sathiya P., 2021) in an effort to standardize

terminology used by AM users, producers, researchers, educators, and/or press/media and it is explained as a 3D model created in CAD software and sliced into layers and then, the layer data goes to a specific format (usually standard tessellation language - STL) that is given to the 3D Printing machine. (Frazier W.E., 2014) (F2792 − 12a Standard Terminology for Additive Manufacturing Technologies, 2013). The machine then adds material upon the material in a layer by layer fashion to create the 3D objects based on the STL information (Kumar Das A., Anand M., 2021).

3D printing starts with a digital file derived from computer aided design (**CAD**) software. Once a design is completed, it must then be exported as a standard tessellation language (**STL**) file, meaning the file is translated into triangulated surfaces and vertices. The STL file then has to be sliced into hundreds – sometimes thousands – of 2-D layers and then turned into a set of instructions in machine language (**G-code**) for the printer to execute and form a three-dimensional object. All design files, regardless of the 3D printing technology, are sliced into layers before printing. Layer thickness – the size of each individual layer of the sliced design – is determined partly by technology, partly by material, and partly by desired resolution and your project timeline; thicker layers equates to faster builds, thinner layers equate to finer resolution, less visible layer lines and therefore less intensive post-processing work (Romero L. et al., 2019) (Table 1.2).

Table 1.2. Phases in additive manufacturing processes (Romero L. et al., 2019).

Conceptual Process	Description
1.- Conceptual development	1.- Conceptual development of the idea.
2.- 3D CAD application	2.- Design of the model in a 3D CAD application.
3.- Generation of the .stl file	3.- Generation of an .stl or .amf file to enable the additive manufacturing equipment to interpret the geometrical information (triangulation) modelled in CAD.
4.- Generation of the G code	4.- Orientation within the machine and generation of the NC code (G code) by the additive manufacturing equipment.
5.- Manufacturing	5.- Manufacturing of the component.
6.- Cleaning	6.- Cleaning. Removal of the support material (if the technology uses support material and the component so requires).
7.- Post-processing	7.- Post-process phase: improving the finish and hardening. Some technologies do not require this.

3D printing enables fast and cheap fabrication, but AM does not refer to one kind of manufacturing or technological process. 3D printing refers to any manufacturing process which additively builds or forms 3D parts in layers from CAD data. The technology is a significant change because it offers direct manufacturing, it means that from a design it goes to a physical product through a computer and a printer. And, inside 3D printing technologies, metal additive manufacturing is a specific and independent world to explore quite different from other additive materials used.

1.5. AM technologies: Advantages, disadvantages, materials available, how do they work?

As stated above, 3D Printing is not only one technology, it is a compendium of various technologies with different characteristics, advantages and disadvantages, range of applications, etc. (Frazier W.E., 2014). Figures 1.4, 1.5 and 1.6 show a compilation of the AM processes available for polymers, metals and other materials (i.e. composites, sand, wax, etc.).

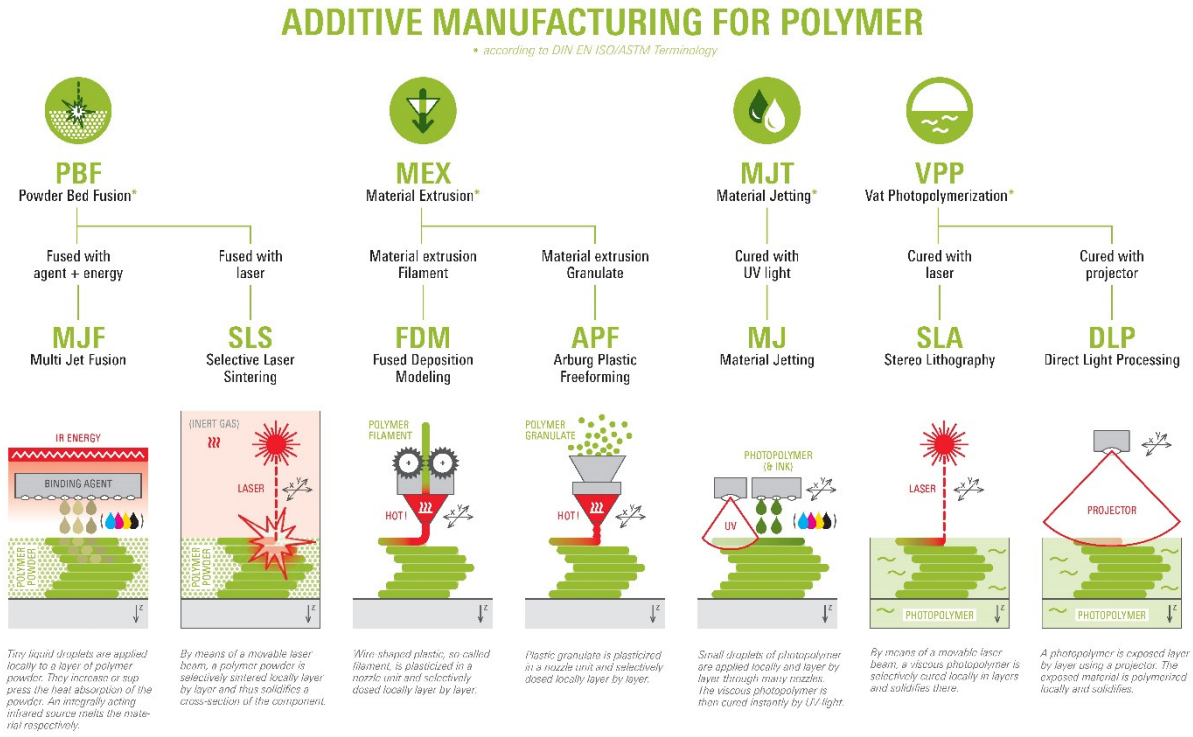

Figure 1.4. Additive manufacturing processes for plastics (Ritter S., 2018).

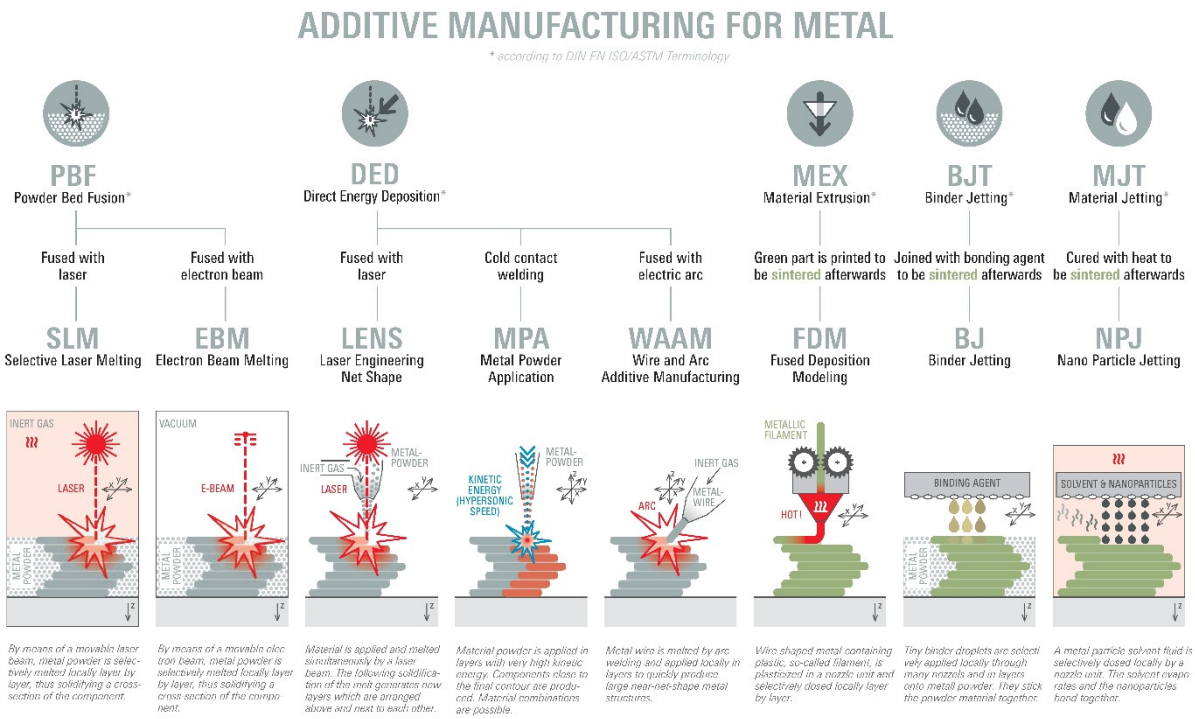

Figure 1.5. Additive manufacturing processes for metals (Ritter S., 2018).

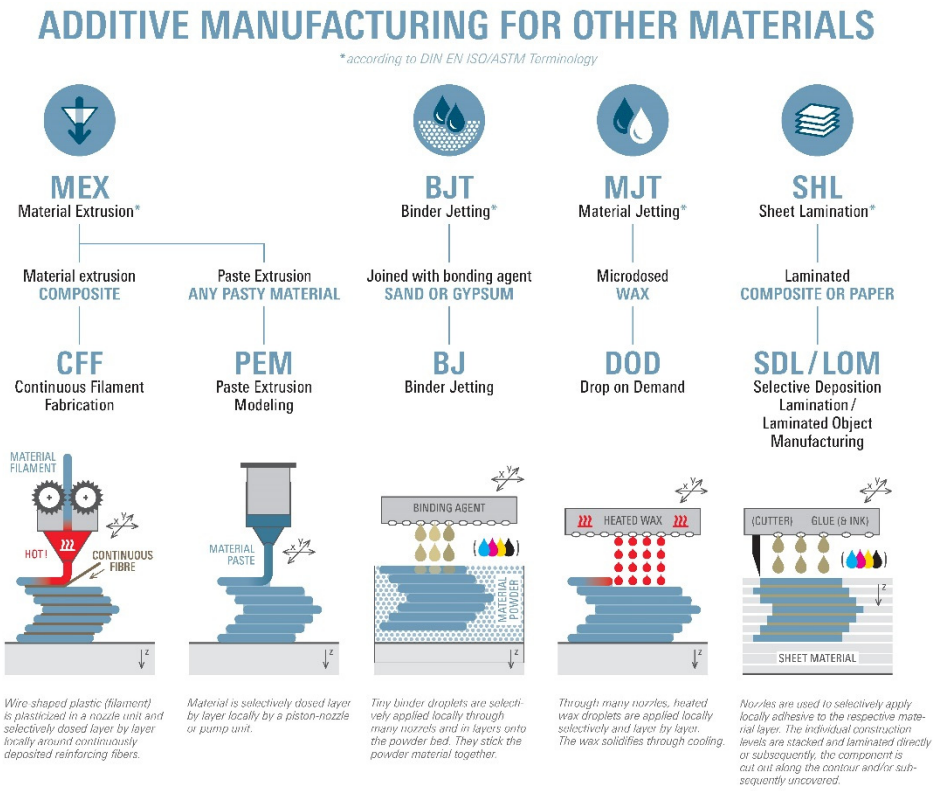

Figure 1.6. Additive manufacturing processes for other materials (Ritter S., 2018).

Here we present in some details the most relevant for metal additive fabrication in their current status.

1.5.1 Material Extrusion

This technology includes: Fused Deposition Model (FDM) or Fused Filament Fabrication & Bound Powder Extrusion (FFF & BPE) and was patented in 1989 by *Stratasys, Ltd.* (Bhuvanesh Kumar M., Sathiya P., 2021).

Advantages:

Economic, fast, wide range of materials (Vafadar A. et al., 2021) (Vaezi M. et al., 2020) (Bhuvanesh Kumar M., Sathiya P., 2021).

Disadvantages:

Post-processed work could be required (support structures that dissolve in water or some type of solvent, but it does not require machining), poor accuracy and precision, surface quality (roughness), anisotropy. The resulting part does not look like pure metal (Vafadar A. et al., 2021) (Vaezi M. et al., 2020) (Bhuvanesh Kumar M., Sathiya P., 2021).

How does it work?

FDM is an additive manufacturing process in which material is selectively dispensed through a nozzle or orifice (F2792 − 12a Standard Terminology for Additive Manufacturing Technologies, 2013). In 2009, the patents expired, and other manufacturers started to build new versions of FDM, which are called Fused Filament Fabrication (FFF) (Vafadar A. et al., 2021). In FDM, a spool of filament is charged to the 3D printer and then fed to the header for extrusion which is equipped with a heated nozzle. At the moment the nozzle reaches the optimal temperature, a motor moves the filament inside and melts it.

The printer moves the extrusion header, placing the molten material in exact places, where later it cools, dries and solidifies - like a very precise hot glue gun. When a layer is finished, the build deck moves down and then the process repeats again and again until the piece is done.

Moreover, after printing, the part is usually ready for using but it may require some post-processing tasks such as removal of support structures or smoothing of the surface (Redwood B. et al., 2021) (Frazier W.E., 2014). FDM needs support materials for over-hanging features of the build part. After the part is built, support materials should be

removed or washed away. The support materials must be easily breakable or water/ solvent-soluble (Bhuvanesh Kumar M., Sathiya P., 2021).

One of the recent developments in the metal AM market is the development of metal filled filaments, which can be printed using FFF machines. In this filament, the metal powder is infused in a standard ABS or PLA filament, and the powder percentage can vary. The prints made using these filaments are not pure metal parts (Vafadar A. et al., 2021). The first metal extrusion 3D printers were launched in 2018. The technology is also known as Bound Metal Deposition (BMD) or Atomic Diffusion Additive Manufacturing (ADAM). Like FDM in plastic, a piece is built layer by layer by extruding material through a header. The difference with FDM is that the material is not plastic, but a metallic powder that is joined together with a polymer binder. The result of this first printing step is a "*green*" part ("*draft*" printed) that needs to be removed the embed and sintered to become fully metallic.

FDM is the most cost-effective way to produce custom thermoplastic prototypes and pieces. It also has the shortest lead times, as fast as overnight delivery due to the high availability of technology. A wide range of thermoplastic materials are available for FDM suitable for both applications, prototyping on the one side and some functional applications on the other side. FDM is perhaps the main competitor of SLA in the market. The obvious advantages of using FDM are the low cost of consumables and machines compared to SLA, the wide range of machines and easiness of pattern preparation (Talamona D. et al., 2020).

As a limitation, FDM has the lowest dimensional accuracy and resolution compared to the other 3D printing technologies. FDM constructions have visible coating lines, so post-processing is often required to obtain a smooth surface finish. In addition, the adhesion mechanism of the layer makes the FDM piece inherently anisotropic (different behavior depending on the direction). This means that they will be weaker in one direction and generally not suitable for critical applications.

High surface roughness (Ra), being the major drawback of FDM technology, has been one of the major challenges for the AM industry. It has been found that process parameter optimization can solve the problem partially. For example, layer thickness is the most important parameter to ensure better surface quality (Talamona D. et al., 2020).

Constructive characteristics:

- Layers + supports + % infill.
- Dimensional accuracy: ± 0.5 mm with a lower limit of ± 0.5 mm (± 0.020")
- Typical build size: 300 x 200 x 200 mm (-20% effective build size after sintering)
- Common layer thickness: 50 - 200 μm
- Support required for printing and sintering
- Internal porosity: 2.0 - 4.0%

Materials of construction:

Filaments such as acrylonitrile butadiene styrene (ABS), Nylon®, acrylonitrile styrene acrylate (ASA), resins, polycarbonate (PC) and polylactic acid (PLA) with metal incrustations can be used. When FDM is used, it is assumed that ABS is superior to PLA, due to its better surface finish (Talamona D. et al., 2020) (Bhuvanesh Kumar M., Sathiya P., 2021). About metal material selection is currently very limited, although filaments of austenitic stainless steel mixed with plastic have been reported (Vaezi M. et al., 2020).

1.5.2 Direct Metal Laser Sintering (DMLS) and Selective Laser Melting (SLM)

This technology was patented by Pierre Ciraud in the 1970's and first tested in 1994 (Frazier, 2014). It is currently manufactured by EOS GmbH.

Advantages:

It can print metal and complex parts, has less weight and material requirements and very remarkable mechanical characteristics (outdoors included). It is also fast and of high precision with details and finishes for functional prototypes that are isotropic and have no internal porosity (Kumar Das A. Anand M., 2021) (Vafadar A. et al., 2021) (Vaezi M. et al., 2020) (Bhuvanesh Kumar M., Sathiya P., 2021).

Disadvantages:

High costs, less available technology, mitigating oxygen contamination (Pauzon C. et al., 2021) limit of the size of the piece and supports, post-processed work (cleaning, polishing or painting) and it needs heat treatment (Kumar Das A. Anand M., 2021) (Vafadar A. et al., 2021) (Vaezi M. et al., 2020) (Bhuvanesh Kumar M., Sathiya P., 2021).

How does it work?

SLM/DMLS are additive manufacturing processes in which thermal energy selectively fuses regions of a powder bed (F2792 − 12a Standard Terminology for Additive Manufacturing Technologies, 2013). Direct laser sintering of metals (DMLS) and selective laser melting (SLM = LMF Laser Metal Fusion) produce pieces in a very similar way to SLS: a laser source selectively binds the powder particles layer by layer (Frazier W.E., 2014). The main difference, of course, is that DMLS and SLM produce metal parts (Redwood B. et al., 2021). The powder used during SLM/DMLS operation varies from source to source, in terms of quality, and has a considerable effect on the mechanical properties (Deng S. et al., 2021). The chemical composition of the powder has also a major impact on melting point, thermal conduct and weldability. The size of the powder particles affects the flow ability and density. Defect-free components can be achieved by using good quality powder with appropriate powder particles (Kumar Das A. Anand M., 2021).

The difference between the DMLS and SLM processes is subtle: SLM achieves a complete fusion of the powder particles, while DMLS heats the metal particles to a point where they fuse at the molecular level. DMLS produces parts from metal alloys, while SLM makes parts from single element metals such as e.g. titanium (Vafadar A. et al., 2021).

Qualification and certification has been repeatedly identified as a challenge to widespread adoption of AM structurally critical components; and SLM normally makes critical pieces, the current process is too costly and takes too long. Hence, technological alternative means of accelerated qualification are needed. Ultimately, the business case assessment will determine the success of AM. SLM is currently favored in small production lots in which the higher cost of specific raw materials is offset by a reduction in fixed costs associated with conventional manufacturing. Further, there is a value to be placed on the speed, versatility, and adaptability of SLM as it allows for just in- time manufacturing. The economic viability of producing large production lots of AM parts depends heavily on the reduction of reoccurring costs (Frazier W.E., 2014).

These are the basic steps of the DMLS/SLM 3D printing process (Figure 1.7):

1. The chamber is first filled with inert gas (nitrogen or argon) and then heated up to the optimum printing temperature - just below the metal melting point (Mathew M. T. et al., 2021) (Pauzon C. et al., 2021).

2. A thin layer of metallic powder (typically 50 µm) is spread on the building platform.

3. The laser scans the cross section of the piece selectively binding the metal particles (sintered or melted) (Mathew M. T. et al., 2021).

4. When the entire area is scanned/printed, the building deck moves down one layer and the process repeats layer after layer until the entire build is completed.

5. After printing, the part must first be cooled down and then the rest of the powder (not printed) is removed.

6. Finally, the supports must be removed and the surface polished.

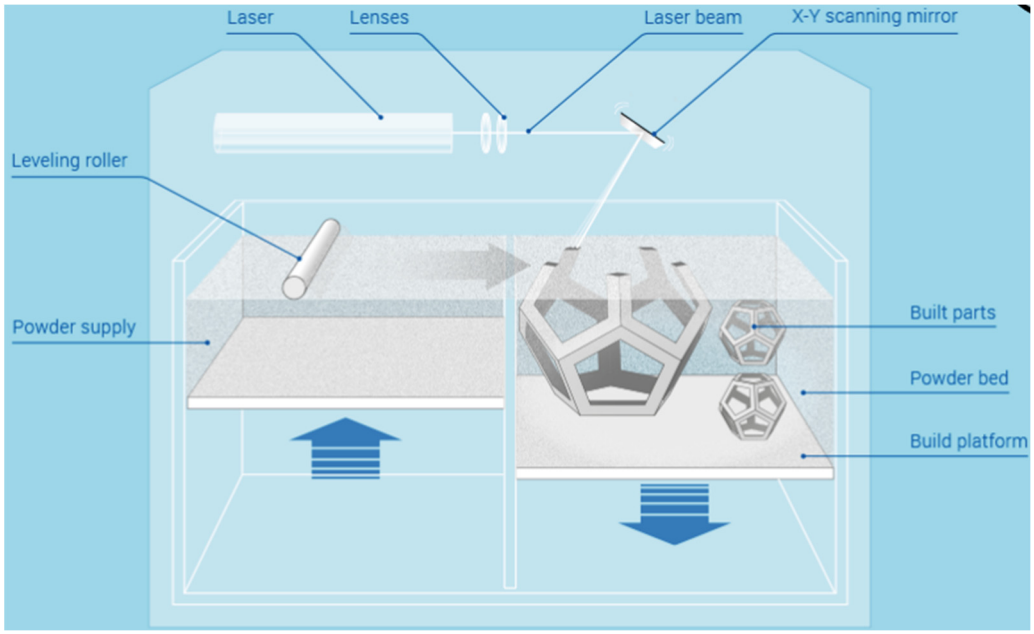

Figure 1.7. Diagram of the operation of SLM technology. Source: additively.com, accessed Feb/2022.

The 3D printing is just part of the DMLS/SLM manufacturing process. After printing is complete, several post-processing steps (required or optional) may be needed before the construction parts are 100% ready to use (Alvarez B.J. et al., 2021).

In case of mandatory post-processing steps, these include:

1. Stress Relief: Due to the very high processing temperatures during printing, internal stresses are developed. Pieces need to be heat treated (Hoon Kang S. et al., 2021) to remove residual stresses (heat treatment or hot isostatic pressing (HIP).

2. Removing the construction parts: In DMLS/SLM the parts are essentially welded to the building platform. A cutting band saw or wire cutter is used here.

3. Support structures are always required in DMLS and SLM to minimize distortion caused by the high temperatures required to fuse metal particles. After printing, the metal supports must be removed manually or by CNC machining.

To meet engineering specifications, additional post-processing steps are often required. These may include:

1. CNC machining: Machining can also be used to improve the accuracy of critical features (for example holes). When tighter tolerances than the standard ± 0.1mm are required, machining is used as the finishing step. Like this, only a minimum material is removed.

2. Smoothing / Polishing: Certain applications require a smoother surface than the standard 10 µm RA printed with DMLS / SLM. CNC machining and manual, vibratory or chemical polishing are the available solutions (Mathew M. T. et al., 2021).

DMLS / SLM is ideal for manufacturing metallic pieces with complex geometries, which traditional fabrication methods cannot produce. DMLS / SLM construction parts can (and should) be topology optimized to maximize their performance while minimizing their weight and the amount of material used. DMLS / SLM construct with excellent physical properties (Deng S. et al., 2021), often exceeding the strength of raw metal (Mathew M. T. et al., 2021). Many metal alloys that are difficult to process with other technologies, such as metal super alloys, are available in DMLS / SLM (Stratasys, web consulted in Feb-2021) and also multi-material additive manufacturing – MMAM (Wei Ch. et al., 2021).

The AM process offers several advantages but still, there are several issues or challenges which need to be addressed simultaneously. Firstly, SLM/DMLS processed parts may experience physical defects like porosity (Mathew M. T. et al., 2021) and delamination and thus, deteriorate the mechanical properties and microstructural behavior of the processed components. Secondly, the heat treatment and high cooling rate lead to the formation of dendritic martensitic. Thus, the tensile strength of the SLM/DMLS

processed parts can be enhanced but the ductility of the sintered parts will be poor. Another challenge is to investigate the tension and compression behavior of the processed componentsAnother issue is to examine the fatigue behavior of the material (Mathew M. T. et al., 2021) which can be accomplished by conducting fatigue test (low cycle fatigue test as well as high cycle fatigue test). In addition, crack initiation needs to be examined as well. The next issue is to investigate the residual stresses associated with the SLM/DMLS process. Due to the high thermal gradients associated with the process resulted in high residual stress which needs to be relieved to avoid the dimensional accuracy and component distortions. Another challenge is to examine the corrosion behavior (Kumar Das A. Anand M., 2021).

The costs associated with DMLS / SLM 3D printing are high - parts produced with these processes typically cost between *$5,000* and *$ 25,000*. For this reason, DMLS/SLM should only be used to manufacture parts that cannot be produced by any other method. Furthermore, the building size of modern metal 3D printing systems is limited as the precise manufacturing conditions required (Wei Ch. et al., 2021) are difficult to maintain for larger build volumes (Hoon Kang S. et al., 2021).

Constructive characteristics:

- Dimensional accuracy: ± 0.1 mm
- Typical build size: 250 x 150 x 150 mm (up to up to 500 x 280 x 360 mm)
- Common layer thickness: 20 - 50 μm
- Typical surface roughness: 8 - 10 μm
- Support always required
- Internal porosity: lower than 0.2 - 0.5%

Materials of construction:

A wide range of material selection is currently available (Kumar Das A. Anand M., 2021) Metals such as titanium alloys (Ti-6Al-4V) (Frazier W.E., 2014) (Mathew M. T. et al., 2021) (Sun G.F. et al., 2021), stainless steel of different grades like 304 or 316L (Deng S. et al., 2021), Inconel® 718 (austenitic Ni-Cr-based alloy), aluminum and aluminum alloys ZL104), cobalt-chromium alloys, nickel super alloys, precious metals, etc. (Hoon Kang S. et al., 2021). It is also applicable in multi-material additive manufacturing (MMAM) (Wei Ch. et al., 2021).

1.5.3 Binder Jetting (BJ)

The principle of BJ was first developed at the Massachusetts Institute of Technology in the early 1990s (Vaezi M. et al., 2020).

Advantages:

Low cost metal print, color prototypes, no limit due to thermal effects (Fernández-Abia A. et al., 2020). No need of supports, can print complex geometries and allows the production of small/medium batches (~100 units). No machining (except for sand casting) and lower quantity of powder raw material with lower costs (Miyanaji H. et al., 2020). Excellent repeatability. BJ can print sand molds of any size for foundry (Cai D., et al., 2021) (Hedberg Y. S. et al., 2020) (Vafadar A. et al., 2021) (Vaezi M. et al., 2020) (Bhuvanesh Kumar M., Sathiya P., 2021).

Disadvantages:

Low mechanical characteristics of the metal (except with sand casting molds), porous and brittle parts and need of post-process work. In some cases, there is an inhomogeneous contraction, difficult to predict (Cai D., et al., 2021) (Hedberg Y. S. et al., 2020) (Vafadar A. et al., 2021) (Vaezi M. et al., 2020) (Bhuvanesh Kumar M., Sathiya P., 2021).

How does it work?

BJ is an additive manufacturing process in which a liquid bonding agent is selectively deposited to join powder materials (F2792 − 12a Standard Terminology for Additive Manufacturing Technologies, 2013). Binder Jetting is a flexible technology with diverse applications, ranging from low-cost metal 3D printing, to full-color prototyping and the production of large sand casting molds or inner molds. BJ is a technology that uses a powdered material (i.e. metal or sand) alongside a liquid-state binder to print the desired metal parts in layers. In this process, the binder droplets consolidate the powdered materials within and between sliced layers (Vafadar A. et al., 2021) (Figure 1.8).

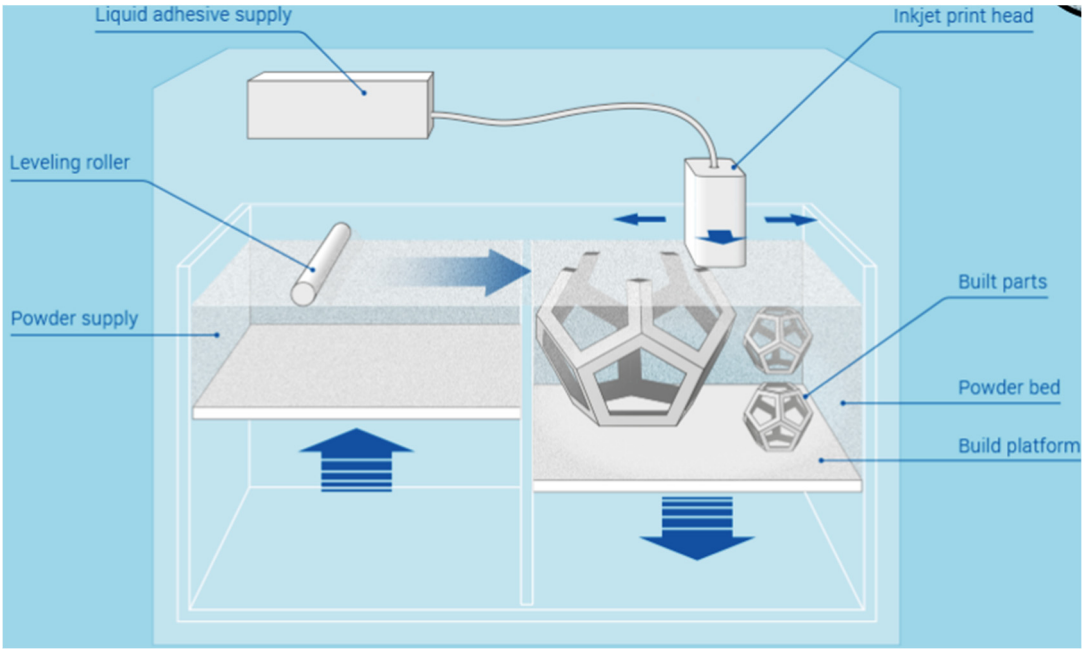

Figure 1.8. Diagram of the operation of *Binder Jetting* technology. Source: additively.com, accessed Feb/2022.

In Binder Jetting, a thin layer of dust particles is first deposited on the building deck (Miyanaji H. et al., 2020). Then, the adhesive drops (liquid binding agent) are ejected by an ink jet print header to selectively bond the powder particles and build a piece layer by layer (Redwood B. et al., 2021). The effects of layer thickness and inkjet concentration density, compressive strength, bending strength, surface roughness, and dimensional accuracy are closely related. When the binder content is constant, the strength decreased, and the roughness increased with the increase of the layer thickness. A correlation between layer thickness and binder saturation on the properties of BJ-printed 316 L stainless has been reported recently (Cai D., et al., 2021).

The interaction between binder droplets and the metal powder/feedstock characteristics are highly critical (Sharon Nai M. et al., 2020). Also important is that BJ is done at atmospheric temperature, this means that thermal effects (such as deformations and internal stresses) are not a problem as they are in DMLS/SLM technology, and no supports are then required. It was originally used to create full-color sandstone prototypes and models. Currently, a variation of the process is gaining popularity due to its batch production capabilities (Sharon Nai M. et al., 2020).

After printing is complete, the dust is removed from the piece and it is cleaned as well. At this stage it is very fragile and requires additional post-processing, there are two options for post-processing (Talamona D. et al., 2020) (Vaezi M. et al., 2020):

1. Infiltration: The "*green*" part is first washed off the binding agent to create a "*brown*" piece with significant internal porosity (~ 70%). This "*brown*" piece is then heated in an industrial furnace in the presence of a low melting point metal (usually bronze). The internal voids are filled resulting a bimetallic piece, while the full-color parts are infiltrated with cyan acrylate adhesive.

2. Sintering: For metallic parts, thermal sintering (similar to injection molding of metal). The "*green*" part is placed in an industrial oven. There, the binder is burned out first and then the remaining metal particles are sintered together. The result is an all-metal piece with dimensions that are approximately 20% smaller than the original "*green*" part. To compensate for this shrinkage, parts are originally printed larger.

Binder Jetting can produce full color metal parts and prototypes at a fraction of the cost of DMLS/SLM or Material Jetting, respectively. Very large sandstone parts can also be manufactured with Binder Jetting, as the process is not limited by thermal effects (Sharon Nai M. et al., 2020). Since no support structures are needed during printing, binder jetting metallic parts can have very complex geometries and, like SLS, batch production is possible by filling the entire building volume container.

In the case of stainless steel, the blasting and superfinishing treatment substantially reduces the surface roughness and level of surface porosity. Blasting has a detrimental effect on the pitting corrosion resistance of the printed surface. The superfinishing process induced an enrichment of chromium in the surface oxide that improved its resistance for pitting corrosion (Hedberg Y. S. et al., 2020).

However, metal binder injection pieces have lower mechanical properties than bulk material, due to their porosity. The Young's modulus and compression properties of 316L stainless steel parts decreased with increasing porosity (Sharon Nai M. et al., 2020). According to the special post-processing requirements of Binder Jetting, special design restrictions apply. For example, very small details cannot be printed as parts are very fragile outside of the printer and can easily break. Metal construction parts can also deform during the sintering or infiltration step if they are not held correctly.

The properties of binder jetting printed parts can be controlled by different factors, such as printing parameters (printing speed, layer printing delay, and layer thickness), powder parameters (particle size, composition, humidity, flow ability and wettability) and binder parameters (concentration, activator content, and binder type) (Fernández-Abia A. et al., 2020).

Constructive characteristics:

- Dimensional accuracy: ± 0.2 mm (± 0.1 after trials).
- Typical build size: 400 x 250 x 250 mm (-20% effective build size after sintering)
- Common layer thickness: 35 - 50 μm
- Typical surface roughness: 6 μm
- Support not required for printing
- Internal porosity range: 0.2 - 2.0%

Materials of construction:

The materials that solidify thanks to the binder are usually plaster, sand, ceramics, metals and polymers in granules. It is also possible to use metal alloys (stainless steel, tool steel, tungsten carbide), super alloys, cobalt-chrome, sand with resin, ceramics and a wide variety of polymers (Vaezi M. et al., 2020).

1.6 Additive manufacturing of metallic materials

Many of the manufacturing techniques described in Section 1.5 have now been adapted for the use of metallic precursors with very satisfactory results. This is due to their superior mechanical characteristics, stability, variety and wide range of potential applications that make 3D-printed metals a priority development target in many chemical industries.

Metallographic analysis of laser-fabricated AM parts has shown comparatively dense microstructures as compared to parts made by traditional methods, with improved mechanical properties. This is an important finding since anisotropy and porosity are still weak points that must be examined in order to avoid premature failure of stress or mechanical fatigue (Bhuvanesh Kumar M., Sathiya P., 2021).

Currently there is a wide range of ferrous and non-ferrous alloys employed in metal 3D printing:

- Stainless and tool steels: Different types of steels such as austenitic, ferritic and martensitic, and also tool steels are those that encompass this category of materials. Their main characteristics are a high resistance and hardness. Taking into account that 3D printing processes involve high temperatures, cooling and tempering steps, as well as stress relief, these types of steels have a capital importance to avoid mechanical failures, as well as to achieve accurate dimensional results (Frazier W.E., 2014). In particular, stainless steel 316L belongs to the family of austenitic steels developed over last decades. Among its main virtues is that it has excellent mechanical properties (Deng S. et al., 2021), ease of being machined and/or welded and, finally, high resistance to corrosion that make SS 316L to have high prestige and has many potential applications, that is the reason because it is well recognized and broadly applied in installations with critical applications in all types of industries such as the chemical industry.
- Titanium alloys: Titanium alloys have excellent properties such as high strength and outstanding corrosion resistance. These superior characteristics make titanium an ideal material for those applications where work is carried out at high temperatures, or where a higher resistance is needed such as in the case of impellers for pumps or compressors in rotating machines for example. Working titanium alloys with traditional manufacturing systems has inconvenient such as low thermal conductivity or the large amount of waste material resulting from manufacturing processes. 3D printing solves these problems and is the ideal solution for working with this material (Frazier W.E., 2014) (Mathew M. T. et al., 2021) (Sun G.F. et al., 2021). Among the titanium alloys there are the Ti6Al4V, also called Ti64, Ti8Al1Er, TC11, TC21 and Ti5553. Ti64 has the widest acceptance (50% of the market, in particular in the chemical industry). The density of the material obtained by AM is even higher than that obtained with subtractive or formative manufacturing methods. Additionally, working Ti64 with the SLM technique provides great fusion stability, homogeneous microstructure, maximum density of 99.9%, a thermal expansion coefficient like forged titanium and minimal residual stress (Bhuvanesh Kumar M., Sathiya P., 2021).
- Aluminum alloys: There is a limited number of aluminum alloys used in additive manufacturing. The main reason is that it has poor weldability (difficulty to solder) but, on the other side, it has remarkable mechanical properties such as hardness, ductility, plasticity and high tensile strength. Excellent mechanical

properties of stiffness, yield strength or elongation even better than alloys achieved by conventional methods. Its main problem lie in the appearance of sporadic cracks or an irregular microstructure (Bhuvanesh Kumar M., Sathiya P., 2021) (Frazier W.E., 2014).

- Nickel-based superalloys: These alloys also contain Co and Cr, show high resistance, elastic limit and have the ability to work at very high temperatures. Their main application is in equipments that works under conditions of high mechanical stress and at high temperatures, such as compressors or gas turbines (Frazier W.E., 2014).

As can be seen, there is a wide range of metallic materials amenable for 3D printing. According to Ludivine Cherdo (Cherdo L, 2022), by 2019 laser-based techniques were the most commonly used in manufacturing metallic parts by AM (~70% of printers sold) , followed by BJ (16%) and extrusion (10%). This tendency is expected to continue in the near future as reflected in the number of AM machines available in the market (Figure 1.9).

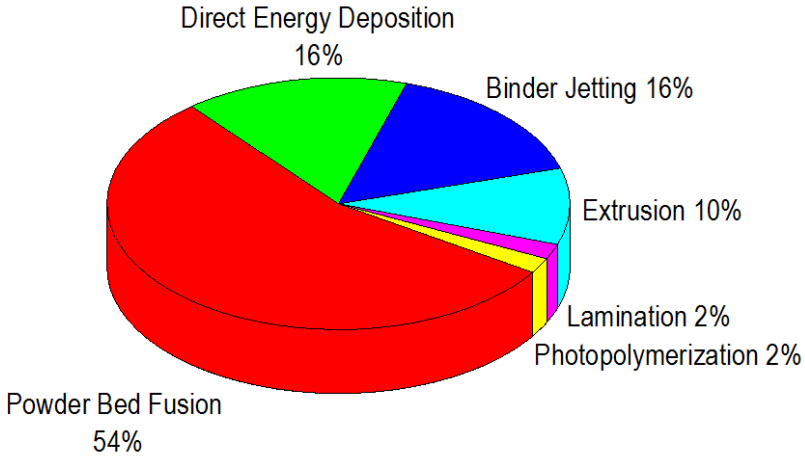

Figure 1.9. Metal AM printer market in 2019. Source: Cherdo L, 2022.

1.7. Potential 3D printing advantages.

The progress achieved over the last decades on 3D printing gives many industrial processes a remarkable potential improvement in maintenance and operations (Redwood B. et al., 2021), (Vafadar A. et al., 2021) (Romero L. et al., 2019). Here we present the main advantages of this technology:

- 3D printing offers a new negotiation tool for price negotiations and avoids having immobilized stock thus reducing the cost of purchasing materials with the consequent operational and maintenance cost reductions.
- Reliability improvement of chemical plants due to the possibility of having old spare parts that are no longer manufactured today (already out of the market).
- Greater flexibility for the manufacture and supply of materials.
- Reduction of delivery times of materials and available space for spare parts management.
- The use of electronic files instead of physically disposing of the materials represents a step forward towards virtual material inventories with the consequent economic savings.
- Possibility of manufacturing more complex materials and freedom of design in metal 3D printing:
    - 3D printing allows to create complex shapes and parts - many of which cannot be created with conventional manufacturing methods.
    - Complex geometries can be created and allows great design freedom.
    - 3D printing can produce complex models in one piece, without the need to produce smaller parts and then assemble them together.
- Customization and personalization at an affordable cost:
    - Metal 3D printing allows easy customization for optimization or enhancement. Each one of the products can be customized without additional manufacturing costs.
    - In case it should be a need to change the design of a particular product, the digital design would be changed fist but without costly manufacturing processes or additional tools.
- No need for specific or additional tools:
    - One of the advantages of 3D printing compared to traditional manufacturing is that the 3D printing process generally does not require any special tools to produce models or their parts.
    - Does not require additional costs or waiting periods while making a simple or complex object.
- Speed and cost savings:

- One of the biggest advantages of metal 3D printing is the speed of production compared to conventional manufacturing methods. Complex models can be printed in a relatively short time.
- Cost savings are also achieved by saving time.
- No correlation between item complexity and cost.
- Production on demand.

- Faster access to the market:
  - Since models or their parts can be produced in a short time, metal 3D printing can be used for quick checks and development of design ideas. It is cheaper to produce a 3D prototype, and then redesign it if necessary.
  - Therefore, 3D printing is a good choice to manufacture an idea product, because it is a less risky way before entering the market.
  - Metal 3D printing can also reduce risks associated with some manual manufacturing processes.
  - Simplification of the production chain.
- More sustainable and ecologic processes due to less waste, low material loss and weight reduction of the manufactured part:
  - Metal 3D printing is an additive process - an object is created from a raw material layer by layer. Additive manufacturing methods generally only use the amount of material they need to create that particular object.
  - Most processes use materials that can be recycled or reused for more than one figure, creating very little waste resulting from additive manufacturing processes.
- Production of a wide variety of products with a single printer.
- Possibility of making very small objects and reduction of assembled parts (all parts can be manufactured directly together).
- In metal fabrication with 3D molds:
  - Cast iron sands capable of withstanding ferric alloys - like a wide variety of stainless steel - and very high temperatures.
  - All kinds of sizes available, from 300 mm up to 4000 mm.

As can be seen, there are many potential competitive advantages that this technology offers and efforts continue today in the academic and industrial sectors towards a widespread implementation.

1.8. Potential 3D printing disadvantages.

On the other hand, 3D printing is in its initial status of technical validation and it is needed to ensure its viability and reliability (Romero L. et al., 2019) (Vafadar A. et al., 2021). There are currently several potential disadvantages that need to be dealt with in the future:

- Compared with subtractive and formative technologies, AM has lower costs for prototyping and production of few units but higher costs for large production (Redwood B. et al., 2021). This means that the price decrease due to an increase in production volume is much smaller than traditional technologies, in which the price per unit decreases dramatically (Figure 1.10).

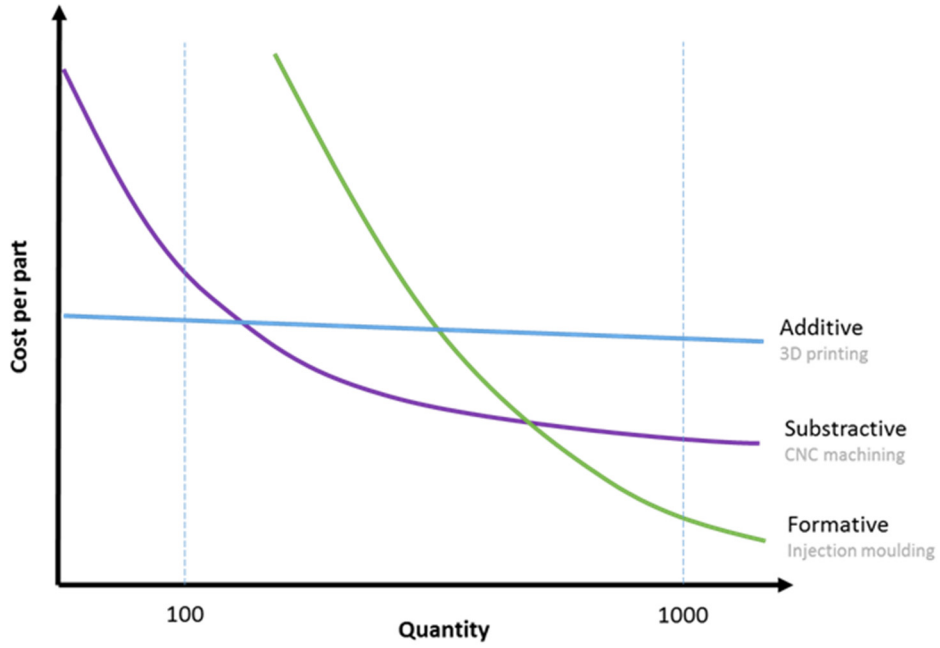

Figure 1.10. Cost of manufacturing 3D printing spare parts versus traditional methods and quantity. Adapted from Redwood B. et al., 2021.

- The price of printers for metal 3D printing is still extremely high.

- Raw materials also have a high cost, although the trend is that in the near future it will tend to decrease as printers are adapted to other materials.

- Still fewer choices of materials, colors or finishes, a process in constant improvement although there are still some limitations compared to the materials, colors and finishes with conventional methods.

- Not all printing technologies can ensure the strength of the objects they produce, and the strength is not uniform due to the manufacturing process from layer to layer (depending on the selected manufacturing process).

- The precision of printed objects needs to be improved.

- If there is a need to print precise parts or fine details it is still difficult to ensure the high precision capabilities of some metal fabrication processes. Others, on the other side have a high accurate precision.

- Most 3D printers are limited by scale and size.

1.9. Additive manufacturing in the chemical industry.

Chemical engineering has recently benefitted from the emergence of AM technologies, which are expected to transform process and reaction engineering and impact many chemical industries (Femmer T. et al., 2016) (Zentel K. et al., 2020) (Kotz F. et al., 2019). Advantages of their application include energy saving, increased reaction (Maier M. et al., 2019) and separation efficiency (Belka M. et al., 2021), novel (photo), catalysts (Zhu J. et al., 2022), etc., and further development can be expected in the future. Several examples of microfluidic devices (Chen C. et al., 2016), mixers (Hock S., 2020), and reactors (Zhao L. et al., 2019), among many others, can be found in the literature. Most of these printed devices have been made on polymeric materials such as fluorinated polyethers (Ligon S. et al., 2017), but glass (Gal-Or E. et al., 2019), ceramics (Gyak K. et al., 2019), and, more recently, metallic precursors (Vafadar A. et al., 2021) have also been employed (Figure 1.11).

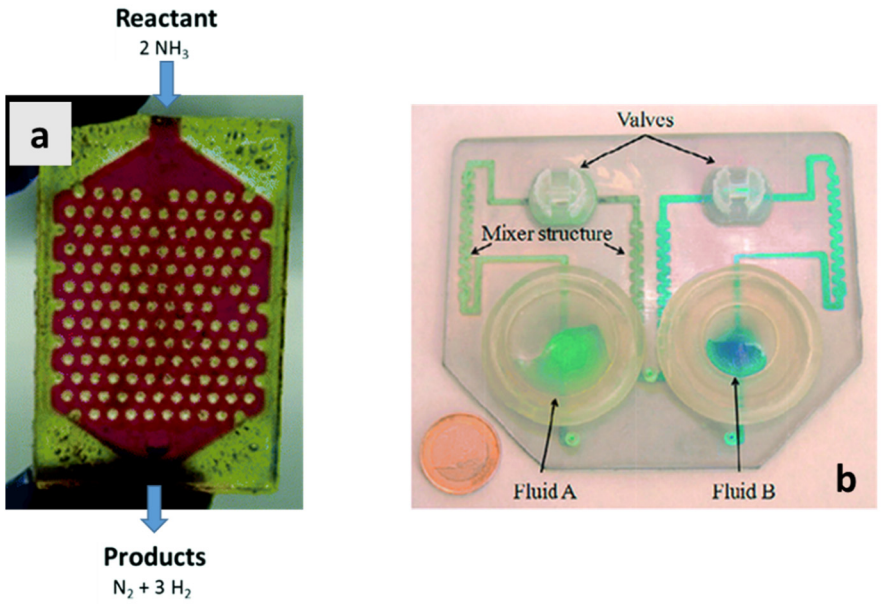

Figure 1.11. Examples of 3D-printed chemical operation devices. a) Ceramic (SiCN) ammonium cracking microreactor (adapted from Gyak K. et al., 2019), b) microfluidic mixer made of PDMS (adapted from Chen C. et al., 2016).

It is evident that the current integration of additive manufacturing (AM) in the industry is becoming lately very relevant (Vafadar A. et al., 2021). It should be noted that 3D technology is presented mainly as a complement to traditional manufacturing and it does not come to replace it, but it is also evident that in some cases it is a significant replacement alternative. While 3D printing is mostly amenable for prototyping and small-scale production of relatively small devices, large metallic components such as pump impellers are still challenging. As shown above, metallic parts can be 3D printed using powders or wires of a wide range of metals as starting materials by beam-based (mostly laser-based) or beamless techniques (Bandyopadhyay, A. et al., 2020) (Vaezi M. et al., 2020). Metal AM technologies enable the production of complex structures (Kladovasilakis, N. et al., 2021) (Ponticelli G. et al., 2021) with low residual stress, avoid oxidation, and allow control over the microstructure of the final product but have some disadvantages, such as high costs and energy consumption, the need for expensive manufacturing machines, and, in many cases, the need for post fabrication processing steps to generate the finished part (Shakil S. et al., 2022).

For this reason, hybrid manufacturing processes combining AM mold printing with metal casting constitute an alternative that increases design flexibility and reduces production times over traditional casting on sand molds (Lynch P. et al., 2020). Binder jetting (BJ)

3D printing is the most popular technology for producing sand molds for casting (Sivarupan T. et al., 2021) (Mostafaei A. et al., 2021) and has a series of advantages, such as better resource utilization, increased production efficiency, and reduced carbon footprint (Zheng J. et al., 2020). Unlike classical thick molds, the use of 3D printing offers great flexibility, allowing the fabrication of complex structures that would be difficult or even impossible to produce by conventional mold manufacturing processes (Figure 1.12). For example, lattice- or shell-type molds with varying thickness have network-like structures that result in increased cooling rates and reduced sand consumption, mold weight, and production times (Shangguan H. et al., 2018) (Deng C. et al., 2018). Another advantage is the possibility of using a multicomponent mold formed by the assembly of several parts to create the casting core and direct the molten metal in the desired filling direction. This was recently exemplified in the fabrication of a reduced-weight cellular structure made of an Al/Si alloy able to withstand several kN compressive and impact forces (Snelling D. et al., 2015).

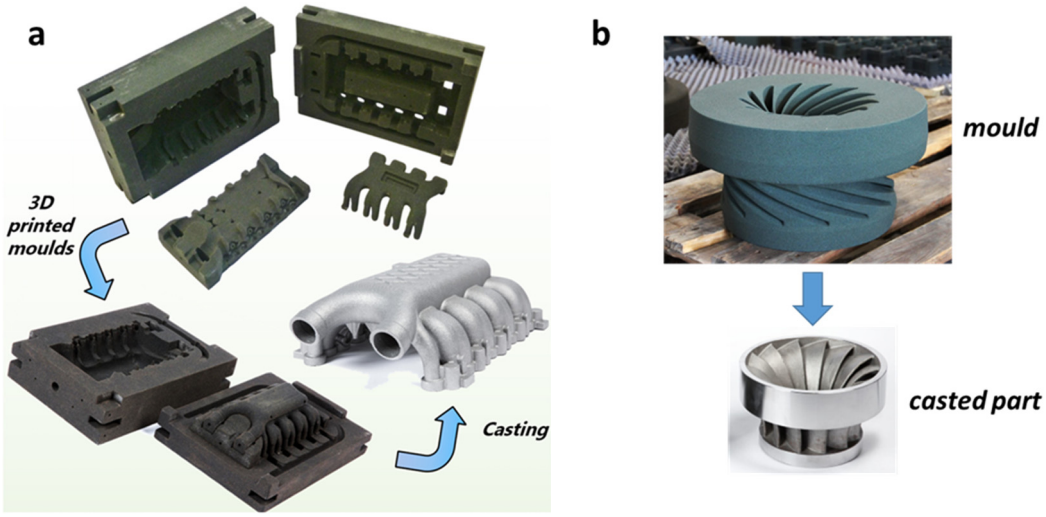

Figure 1.12. Examples of metallic parts fabricated by casting of sand molds printed by BJ. a) Engine cover, b) turbine. Adapted from Siravupan, et al, 2021.

Some reports on the fabrication of aluminium (Gill S. et al., 2009) (Shangguan H. et al., 2017) and stainless steel (Sama S. et al., 2019) parts exist in the literature and have highlighted the advantages of the hybrid AM/casting strategy in the manufacture of metallic elements. More recently, the application of artificial intelligence (Scime L. et al., 2019) and decision-making metrics (Pagone E. et al., 2021) in the mold-manufacturing

process has permitted addressing sustainability aspects that could, in the future, challenge traditional mass production technologies (Mitchel A. et al., 2018).

A very interesting example of the possibilities offered by AM is the case of the company Jabil Inc. that redesigned and 3D-printed an impeller in a single part using a fiber reinforced polymer composite instead of using 73 pieces assembled manually. As a result, up to fifty impellers can now be manufactured in the time needed before to manufacture only one (Wholers report 2020) (Figure 1.13).

Figure 1.13. 3D-printed composite impellers consolidating 73 parts into one produced by Jabil Inc. Source: Wohlers Report 2020.

Some other interesting examples include:

- Analytical chemistry enabled by 3D printing, sensors and biosensors: 3D printing offer tailor-shape devices with exquisite control in design and geometry and through the versatility of printable materials. Applications in analytical and bioanalytical chemistry have been on the rise, with microfluidics being one of the most represented areas of 3D printing towards this chemistry branch. Most stages of the analytical workflow comprising sample collection, pre-treatment and readout, have been enabled by 3D-printed components. Sensor fabrication for detecting explosives and nerve agents, the construction of microfluidic platforms for pharmacokinetic profiling, bacterial separation and genotoxicity screening, the assembly of parts for an on-site equipment for nucleic acid-based detection, the manufacturing of an online device for in vivo detection of metabolites, represent just a few examples of how additive manufacturing technologies have aided the field of (bio)analytical chemistry (Pumera M. et al., 2018).

- 3D printing technologies for chemical energy storage: Fabrication and assembly of electrodes and electrolytes play an important role in promoting the performance of electrochemical energy storage (EES) devices such as batteries and supercapacitors. 3D printing, a disruptive manufacturing technology, has emerged as an innovative approach to fabricating EES devices from nanoscale to macroscale, providing great opportunities to accurately control device geometry (e.g., dimension, porosity, and morphology) and structure with enhanced specific energy and power densities. Moreover, the "additive" manufacturing nature of 3D printing provides excellent controllability of the electrode thickness with much simplified process in a cost-effective manner (Zhou C. et al., 2017).
- 3D printing in chemical engineering for structured catalysts, mixers and reactors: Additive manufacturing closes the gap between theory and experiment, by enabling accurate fabrication of geometries optimized through computational fluid dynamics and the experimental evaluation of their properties. Computational modeling - as digital tools for the design and fabrication of reactors and structured catalysts – its contribution is to stimulate interactions at the crossroads of chemistry and materials science (Ameloot R. et al., 2018).
- 3D printing in food technology: although still in its infancy, 3D-printed foods are expected to revolutionize the food industry as it will be easier to customize ingredients, nutrients, shapes and appearance, minimize the use of additives and improve sustainability (Lipton J. I. et al, 2015; Nachal N. et al, 2019).

1.9. Applications and future prospects of additive manufacturing of metal parts

AM technologies start to have a significant potential perspective for future uses in the not only in the chemical industry but also in many other type of industries all over the world. As can be seen from Figure 1.14, there are many sectors that are currently benefitting from the adoption of AM technologies (Vafadar A. et al., 2021).

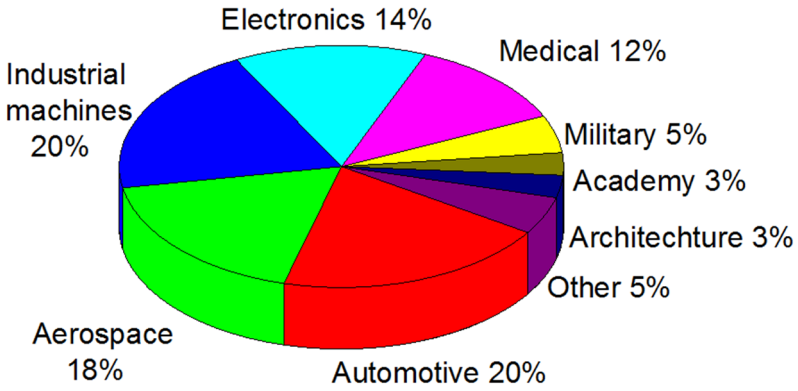

Figure 1.14. Distribution of AM revenues for the end-market in 2018 by sectors. Adapted from Vafadar A. et al., 2021.

In the specific case of metals, AM technologies start to have a significant potential perspective for future uses in the chemical and many other industries all over the world. The automotive, aerospace and medical sectors are the industry leaders for metal additive manufacturing. Other industries, including oil and gas, electronics, construction, and railway, have been paying close attention to AM in recent years as a way to make substantial advancements in the design and production of innovative components. Its adoption has been gradual because of the difficulties related to printing quality and price and, therefore, there is still room for new developments and additional research.

Chapter 2: Hypothesis and objectives

2.1. Hypothesis.

The main hypothesis of this work is to answer to the question if the replacement (total or partial) of the traditional system of purchasing technical spare parts such as pump impellers, which are critical for the chemical industry, by 3D-printed parts affords equal or similar technical and performance characteristics.

The hypothesis has two ways to be demonstrated: one way is a technical validation of 3D printing, essential to give validity to additive manufacturing technologies and expand their possibilities of application (Bhuvanesh Kumar M., Sathiya P., 2021), (Haghdadi N. et al., 2021), (Vafadar A. et al., 2021), (Wei Ch. Et al., 2021), (Talamona D. et al., 2020), and the other way is an evaluation of the associated economic impact (Romero L. et al. ., 2019).

2.2. Objectives.

The objective of the present work is the design (scanning, drawing, elaboration of constructive 3D plans), manufacturing, assembly and testing of two impellers (*strategies 1 and 2*) in two different pumps (pump P and pump O) made of metal with two different 3D printing technologies and a comparison of their performance with the original parts.

Strategy 1 involves the manufacture of a stainless-steel pump impeller using sand molds fabricated by binder jetting (BJ).

Strategy 2 comprises the manufacture of a Titanium alloy pump impeller by selective laser melting SLM).

In both cases, the printed parts are characterized by metrological and metallographic techniques analysis and analysis of the results and work data is carried out once the pump is assembled and put into operation in a chemical plant after several months of service.

Finally, a comparison of the operating conditions before (using the original part) and after (using the 3D printed part) is made, as well as an economic feasibility study with the aim to assess the possibility of using metal 3D printing techniques as alternative manufacturing methods in the chemical industry.

Chapter 3: Fabrication and testing of a close vane impeller by binder jetting (BJ) and casting. Performance tests in a polyol/polyglycol plant at Dow Chemical Ibérica SL (*Strategy 1*)

3.1. Introduction.

Conventional manufacturing methods are limited mainly by the total production volume. As described in the introductory chapter, 3D printing is a valuable alternative when few copies of a given part are needed. The aim of the first part of the work was to replace a very valuable old impeller used in the centrifugal pump (pump 'P' for confidential reasons) of a polyglycol plant at Dow Chemical Ibérica in Tarragona and compare the performances of the original and the 3D-printed copy. The pump is in a discontinuous service plant and has been in service for a long time with their original impeller manufactured by the German company KSB. The manufacture of the impeller (called BJ impeller) involved casting in sand moulds created by binder jetting - (Cai D. et al., 2021), (Miyanaji H. et al., 2020), (Manogharan G. et al., 2020), (Talamona D. et al., 2020), (Dong A. et al., 2018), (Sharon Nai M. L. et al., 2020), (S. Hedberg Y. et al., 2020) (Fernández-Abia A. et al., 2020).

The study began with an analysis of the original spare part (Galindo M., 2017) kept in stock as a pump inventory spare part at the company warehouse, a study that mainly includes identifying the critical dimensions, knowledge and validation of its construction material (Haghdadi N. et al., 2021) and subsequent 3D digitization in CAD. There were no original manufacturer drawings, which makes these initial steps more difficult. Once the scan is done, a plastic 'communication model' sample is manufactured for a first technical and visual evaluation of the results. After these first steps, the 3D mould design and manufacture continued (Manogharan G. et al., 2020) (Talamona D. et al., 2020) (Dong A. et al., 2018) using the binder jetting (BJ) technology followed by casting at an assigned foundry company in Barcelona. With the metal impeller already built, the final steps included machining and polishing work and performance tests to validate and certify the pump P impeller.

The sequential workflow is depicted in Figure 3.1 and involved the following steps:

- Step A) Analysis of the original part (KSB impeller)

- Step B) Part digitizing, CAD design and 3D printing of the plastic model
- Step C) Manufacturing CAD part
- Step D) Mould design
- Step E) Mould manufacturing
- Step F) Casting of the parts
- Step G) Finishing and testing
- Step H) Performance tests in a chemical plant and comparison with KSB impeller

In this chapter, we describe the methodology of fabrication and characterization of the BJ impeller and the performance results obtained after mounting the part in a chemical plant. To facilitate comprehension, the description has been made divided in the different steps presented above, followed by a conclusion section.

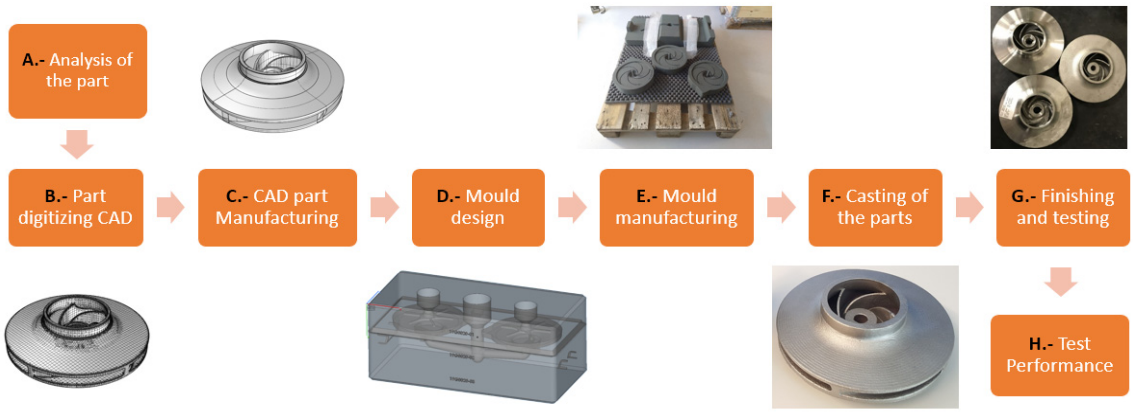

Figure 3.1. Workflow employed for the fabrication of the BJ impeller.

3.2. Step A. Analysis of the original part (KSB impeller).

The original KSB impeller was fabricated with EN 1.4408 (AISI 316) cast stainless steel. The composition is given in Table 3.1. This is an austenitic stainless steel specially formulated for casting and is widely used in the chemical industry. It has a good balance between corrosion resistance, mechanical strength, cost and availability in the market. The characteristics of 1.4408 steel are also due to the presence of a percentage of molybdenum, which improves the resistance of the material to corrosion due to sulfuric, hydrochloric and phosphoric acids. The presence of this alloying element improves the characteristics of mechanical resistance at high temperatures. This material was also used to manufacture the BJ impeller.

Table 3.1. Composition (%) of the cast stainless steel used in this work.

Element	Fe	Cr	Ni	C	Mo
%	63	19	11	0.7	2

The starting point is the material information obtained from the vendor (Figure 3.2).

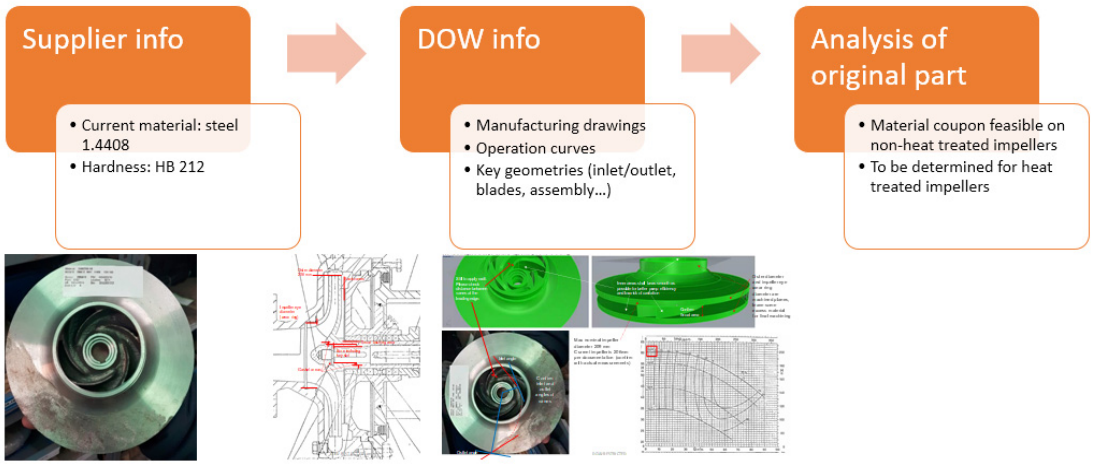

Figure 3.2. Schematic process of Step A.

There was no impeller original drawing from KSB manufacturer. Hence, initial support information was obtained from pump drawings (Figures 3.3 and 3.4) containing a few dimensional characteristics such as diameter (206 mm) and height (12 mm).

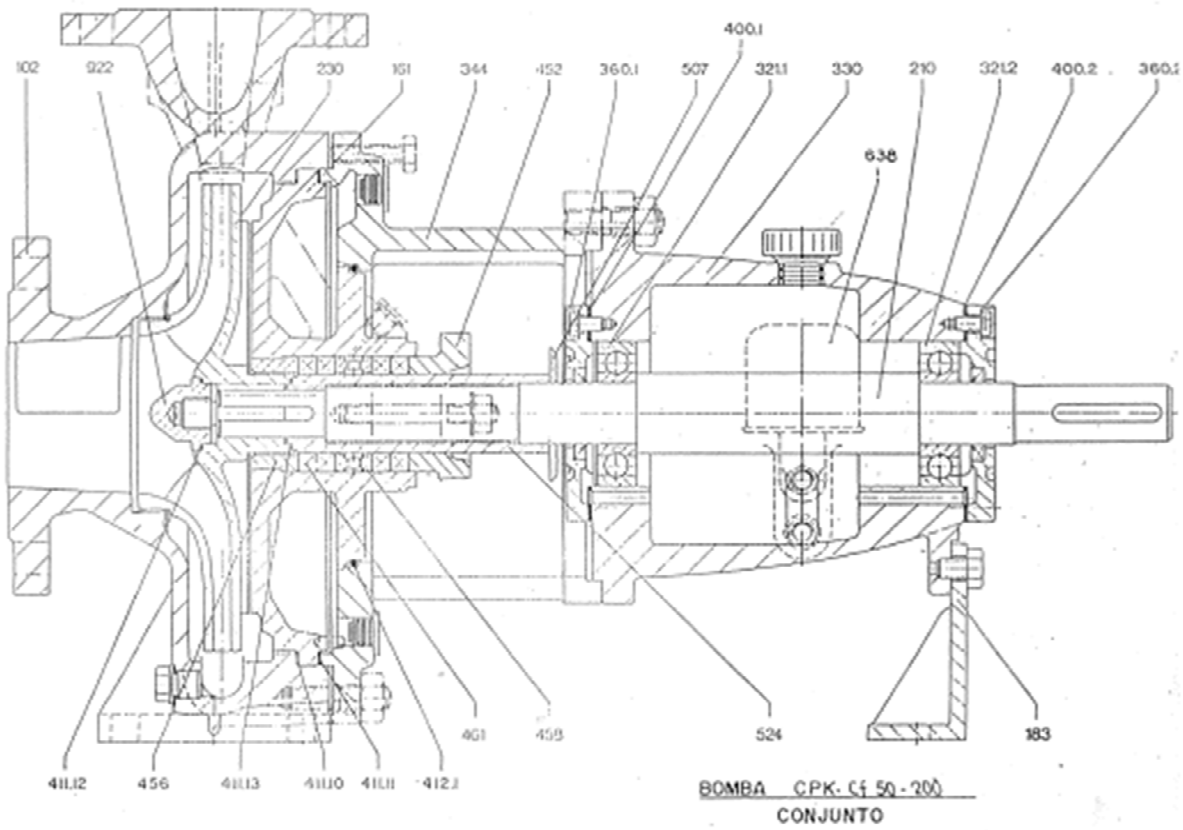

Figure 3.3. Pump P detail.

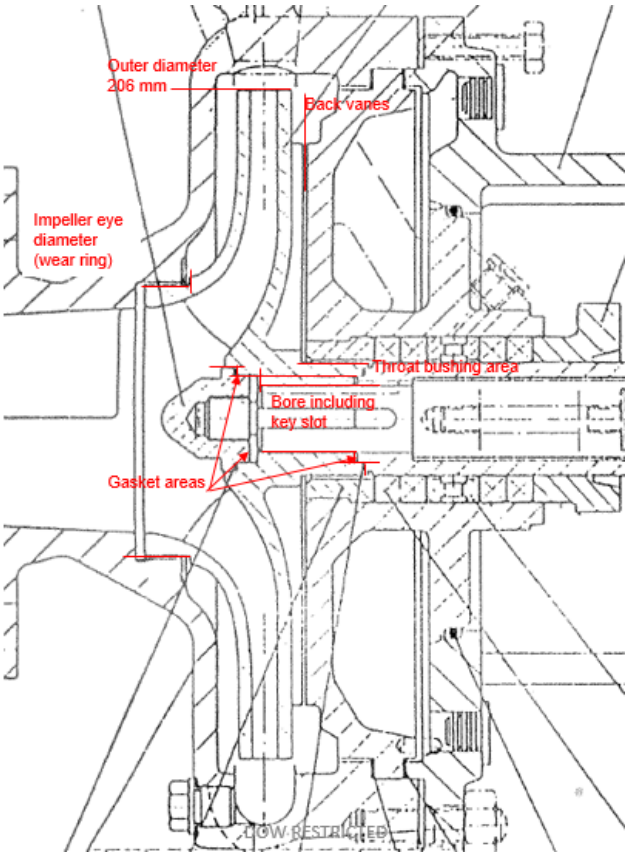

Figure 3.4. Detail of the impeller area in pump P.

These details, however, were not enough to fabricate the replicate and reverse engineering steps were then conceived.

3.3. Step B. Part digitizing, CAD design and 3D printing of the plastic model.

Figure 3.5 shows the process to obtain a virtual model from the KSB impeller.

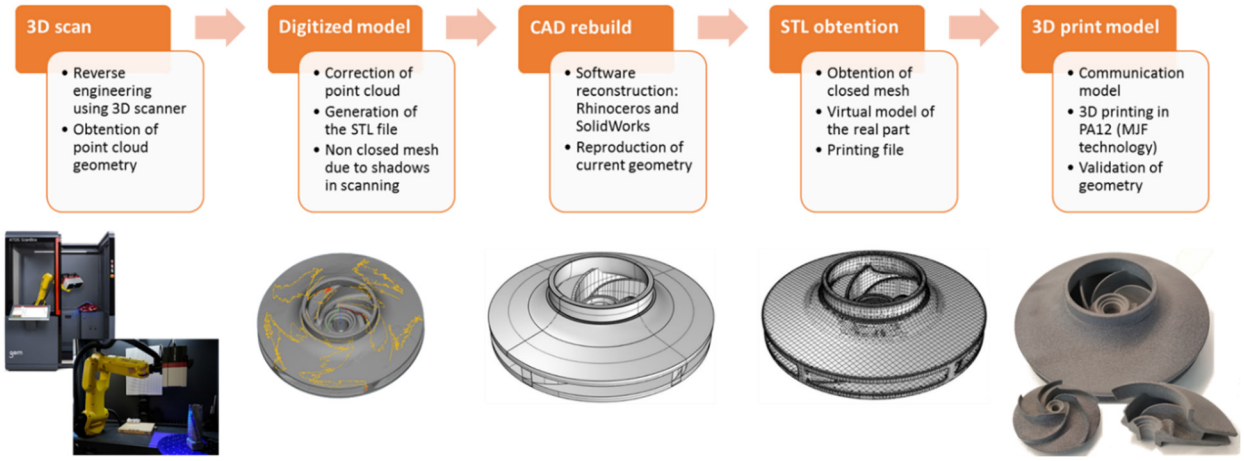

Figure 3.5. Schematic process of Step B.

Since there were no original drawings of the KSB impeller available, the part was reverse engineered using an industrial metrology 3D scanner bearing an optical automatic arm (ATOS Capsule in ScanBox series 4 model 4105, GOM GmbH, Braunschweig, Germany) adapted for measurement of small complex components up to 500 mm in size to obtain the point cloud geometry. These points were then used to extrapolate the shape of the impeller and finally a parametric CAD model was constructed. This is a useful strategy when a precise digital model of a mechanical component needs to be reproduced (Ponticelli G. et al., 2021).

After scanning, the small complex components were measured with an optical 3D coordinate measuring machine at up to 0.5 mm resolution to obtain the point cloud geometry. These points were then used to extrapolate the shape of the impeller, and finally, a parametric CAD model was made. Optical 3D coordinate measuring machines are replacing tactile measuring systems and gages because they capture more detailed and more easily interpretable information on an object in significantly shorter measuring times. Whereas old mechanical measuring systems captured data in a point-based or linear manner, optical measuring systems return full-field data about deviations between the actual 3D coordinates and the CAD data (Vora H. D., 2020).

The point cloud geometry was revised and corrected previous to generate the STL file, there are non-closed meshes due to shadows in scanning, that means the point clouds need to be converted in "closed surfaces" and that done by the Rhinos 7 software (McNeel Europe SL, Barcelona, Spain). Once the closed surfaces were prepared, the mechanical geometry was translated into dimensional parameters using the Solids Works software (Dassault Systèmes, Suresnes, France), and an STL file was created to be used by the 3D printer (Figure 3.6).

The last step of digitalizing and design is the virtual model construction - before the real part is made in metal - printed in polyamide (PA12) what is called a "*communication model*" at real size for visual inspection and geometry validation. The dimensions measured had relative standard deviations lower than 0.4%, thus validating the CAD model that was used to fabricate the mould (Figure 3.7).

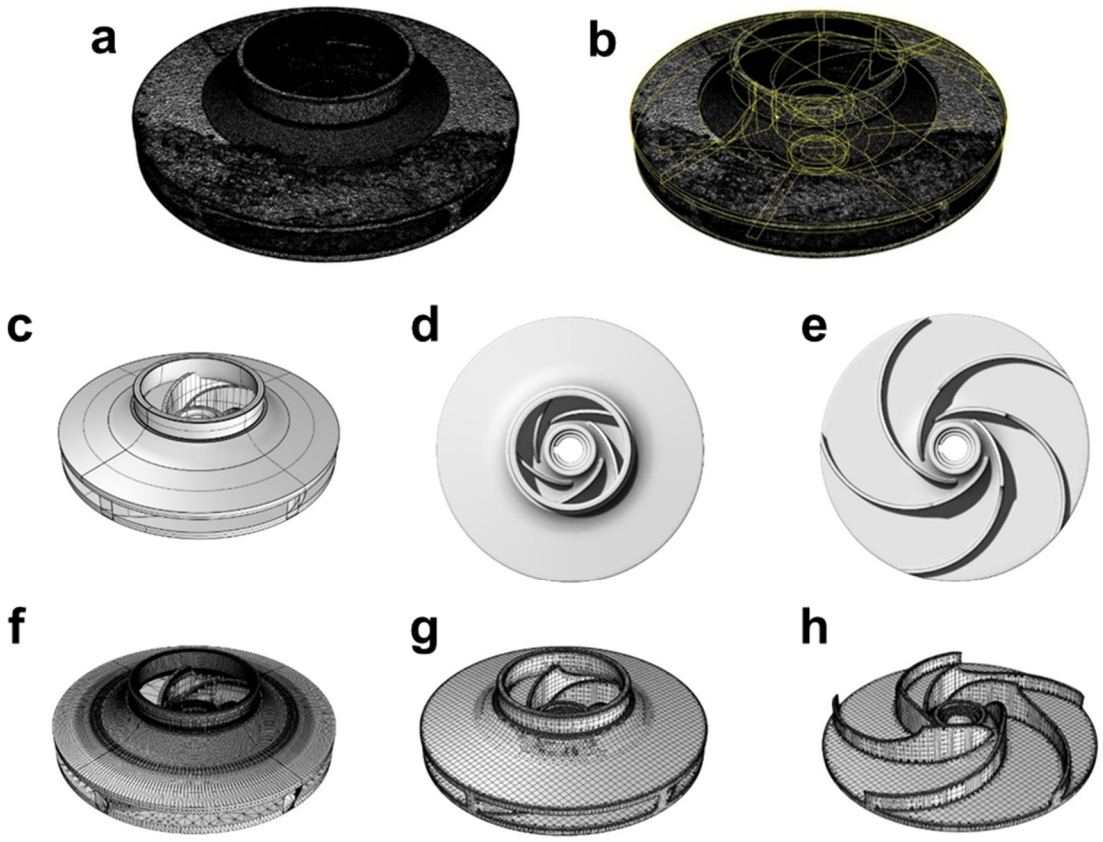

Figure 3.6. Flat impeller digitalizing and design: (a) impeller 3D scan, (b) impeller curves 3D scan, (c) surfaces solids design, (d) surfaces solids top view, (e) surfaces solids sectioned top view, (f) flat impeller meshes, (g) flat impeller surface meshes, (h) flat impeller surface meshes partial.

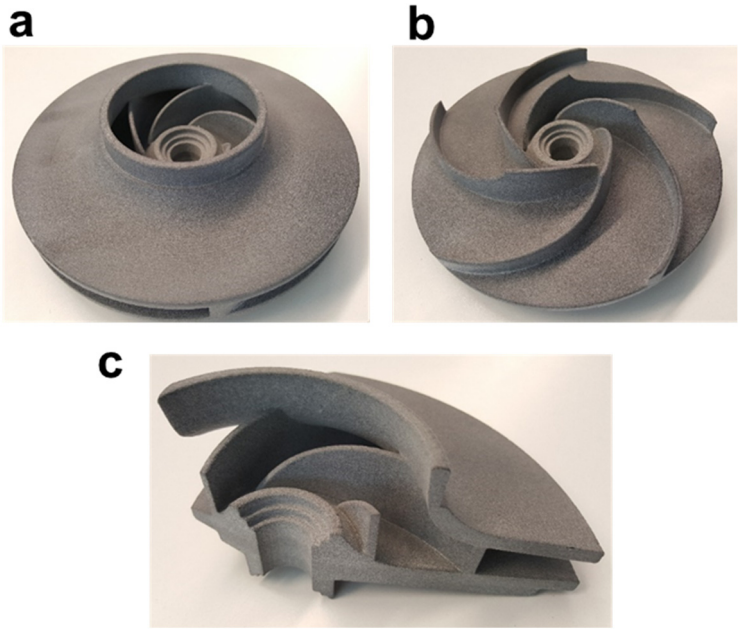

Figure 3.7. PA12 *communication model*": (a) Complete unit, (b) Partial (c) Sectional view

3.4. Step C. Manufacturing CAD part - from digitized part to casting geometry.

The final result of the previous step is the impeller CAD file (Figure 3.8).

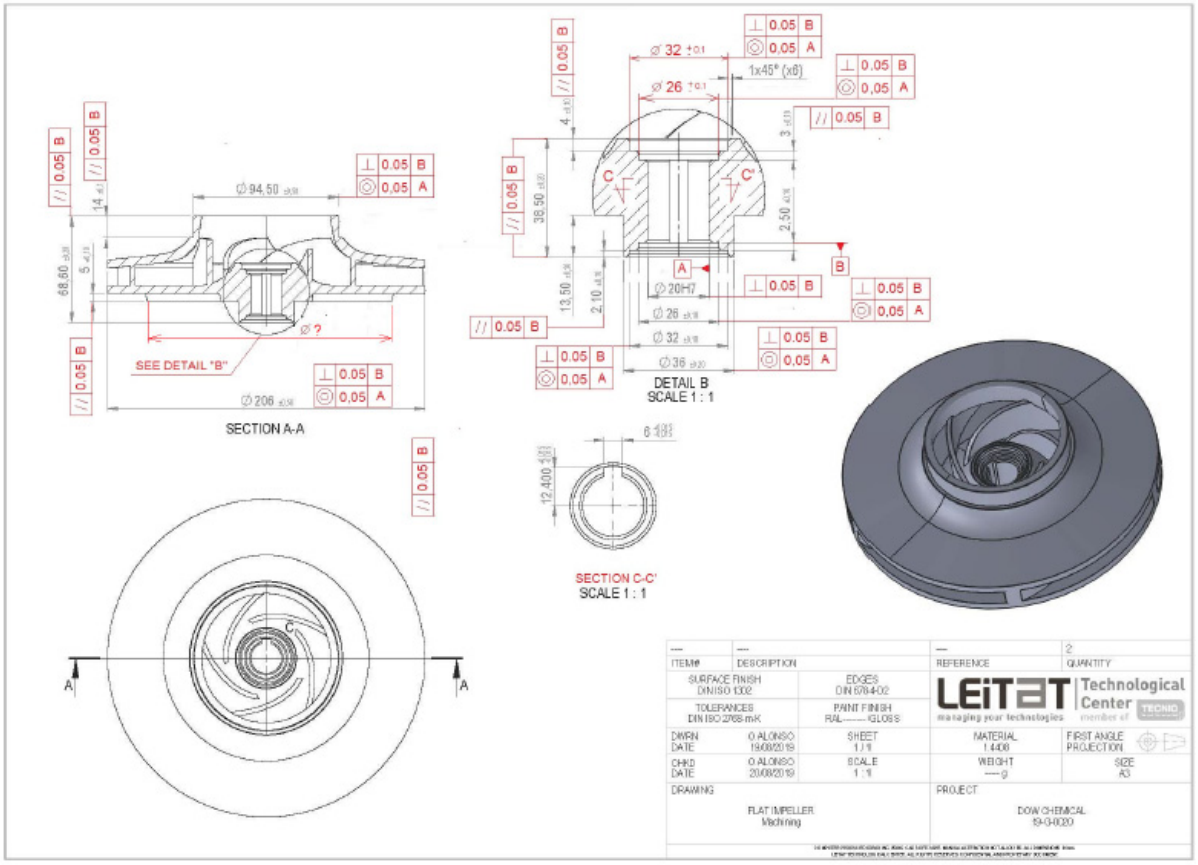

Figure 3.8. KSB impeller CAD file

To this model, the extra material needed for casting (pouring, gates, vents, etc.) was added and final dimensions were adjusted to account for the last step of manufacturing (machining, polishing and dimensional control) (Figure 3.9). For these modifications, the experience and recommendations of foundry company "Fondesal", where casting was to be realized, were crucial and strictly followed. "Fondesal" construction tolerance recommendation was 2.8% material excess for exterior parts and 1.2% material excess for interior parts.

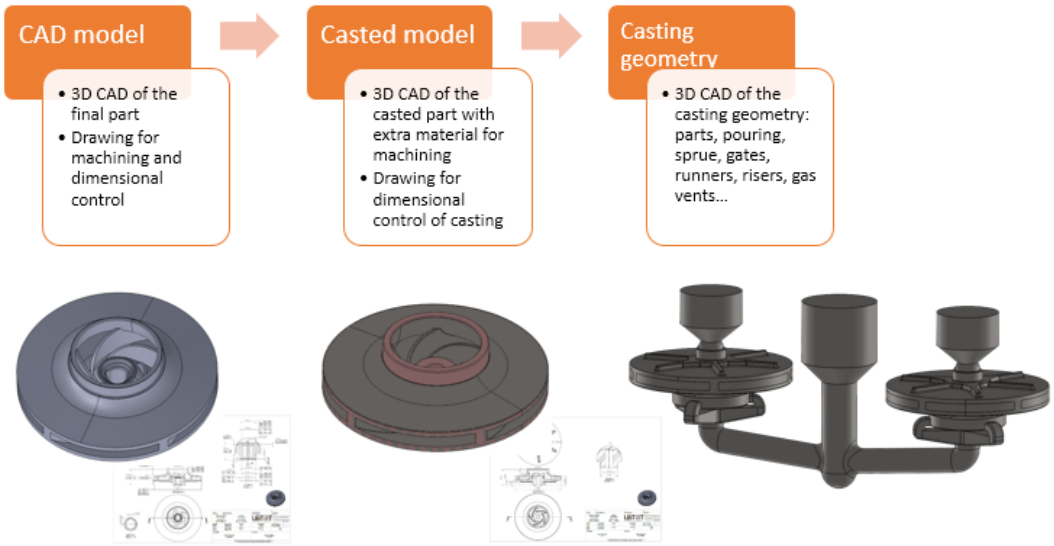

Figure 3.9. Schematic process of Step C.

3.5. Step D. Sand mould design - from the casting model to the mould.

Once the CAD file from the impeller and additional parts is well defined with measurements for machining and dimensional control, next step is the design of the 3D mould before manufacture. Design of the mould was based on criteria and conditions determined by the binder jetting technology, which prints the sand material sequentially layer by layer. Hence, the design took into account the position and orientation of the parts, core design, potential improvements, parting lines for non-consolidated sand removal and orientation geometry taking into account entrance and out flow of casting material (Figure 3.10).

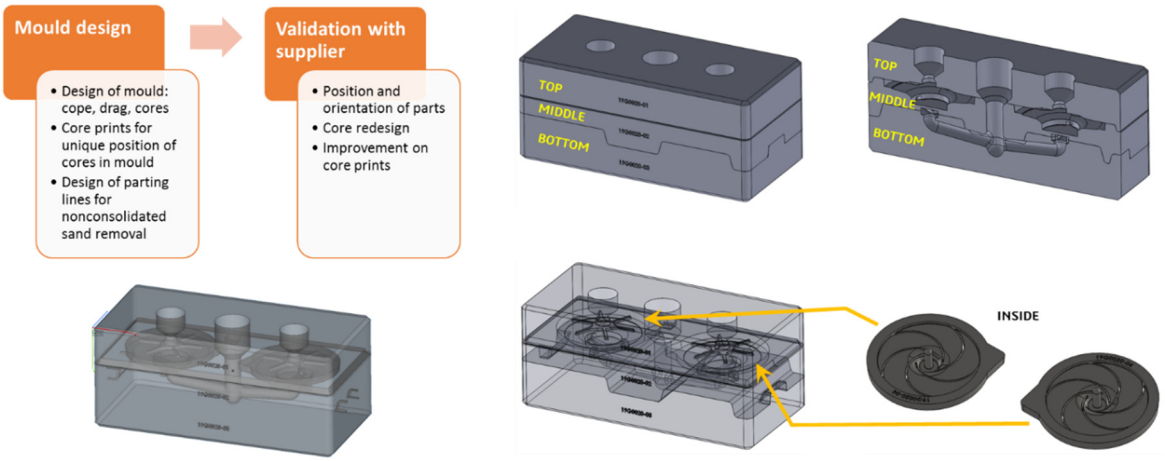

Figure 3.10. Schematic process of Step D.

The 3D mould was designed considering a rectangular box of 800 mm length, 300 mm width, and 450 mm height for the simultaneous manufacturing of two parts (Figures 3.11) to be assembled. A minimum sand wall thickness of 300 µm was considered, and 5 mm were added to account for both a volumetric contraction of 2.8% for stainless steel 316 after cooling from the molten state to room temperature and the removal of small amounts of material during finishing to reach the desired dimensions.

There were superior, intermediate, and bottom pieces that assembled like a puzzle. The fluid (liquid metal) entered through the superior part (cone shape inlet in Figure 3.11c) to fill internally, from down to top, the 3D features that generated the structure of the two impellers (Figure 3.12).

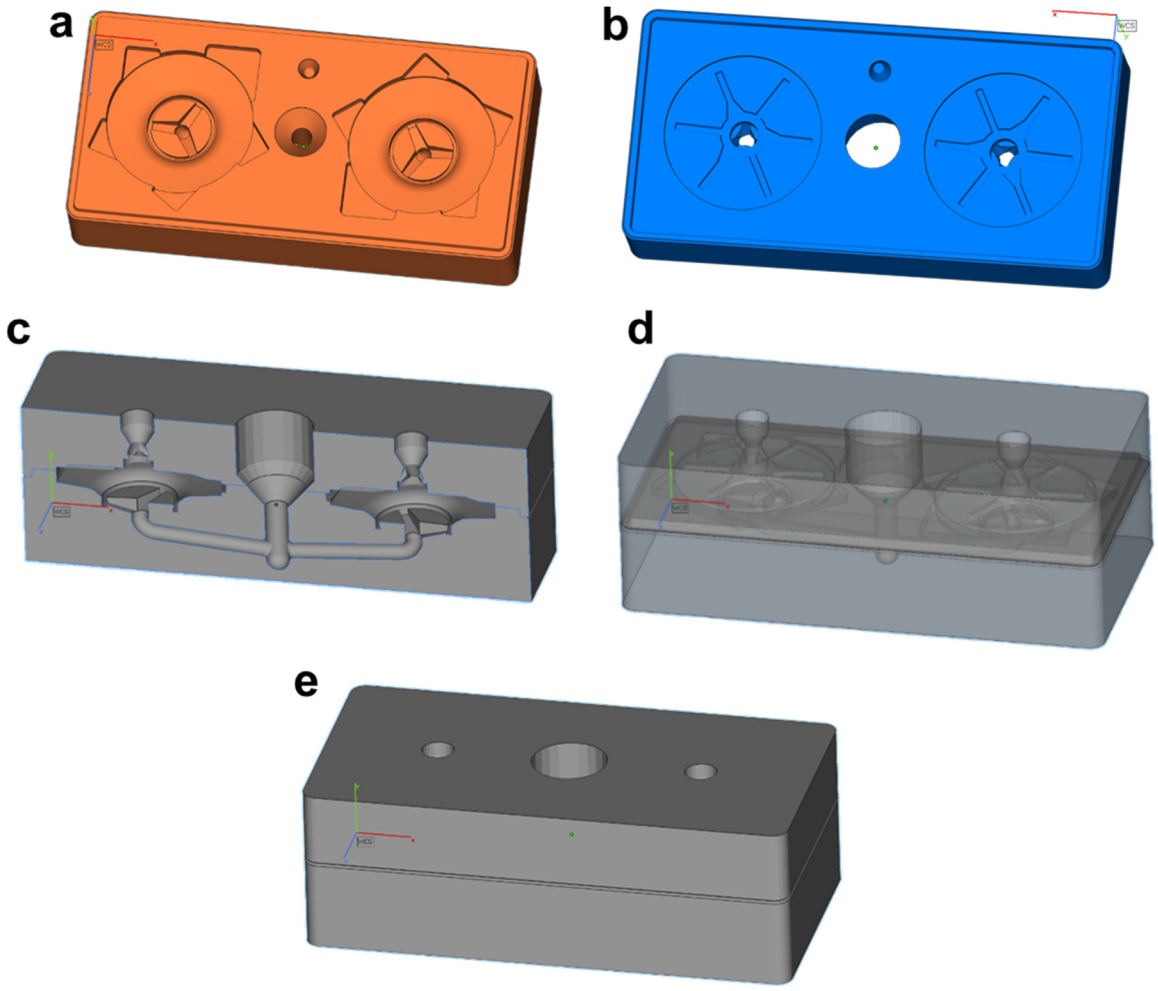

Figure 3.11. 3D views of the sand mould design: (a) lower mould cavity, (b) upper mould cavity, (c) mould cross section, (d) transparent mould view, (e) complete mould view.

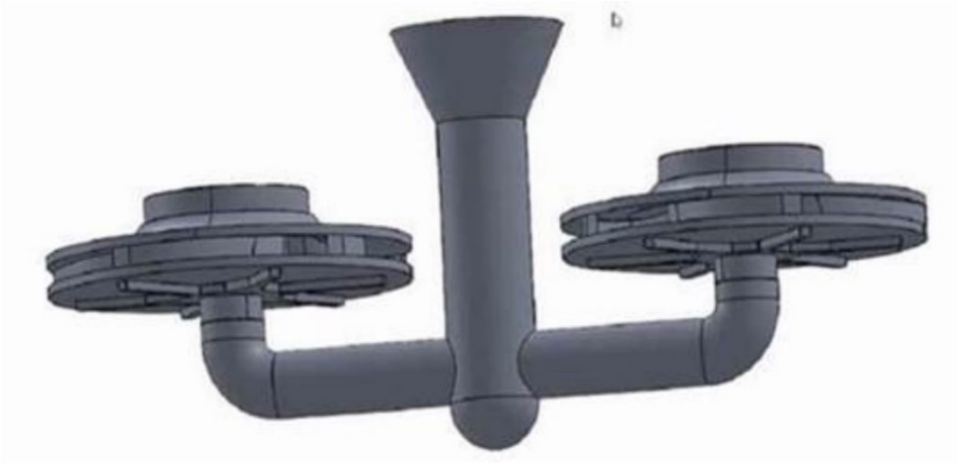

Figure 3.12. 3D model view of the impeller fill.

3.6. Step E. Sand mould manufacturing by binder jetting.

The material selected for mould manufacturing was rapid prototyping Silica GS14 (Voxeljet AG, Freiberg, Germany). The grain size was 0.14 mm. The compacting agent was a cold hardening furan resin. The 3D sand printer (Voxeljet VX1000) required 460 layers of 300 µm thickness to construct the complete mould. The total manufacturing time was 7 h 48 min, and each layer was deposited during 61 s. Finally, an epoxy resin infiltration was conducted to seal and close possible surface gaps. (Figure 3.13). Figure 3.14 shows photographs of the moulds after 3D printing.

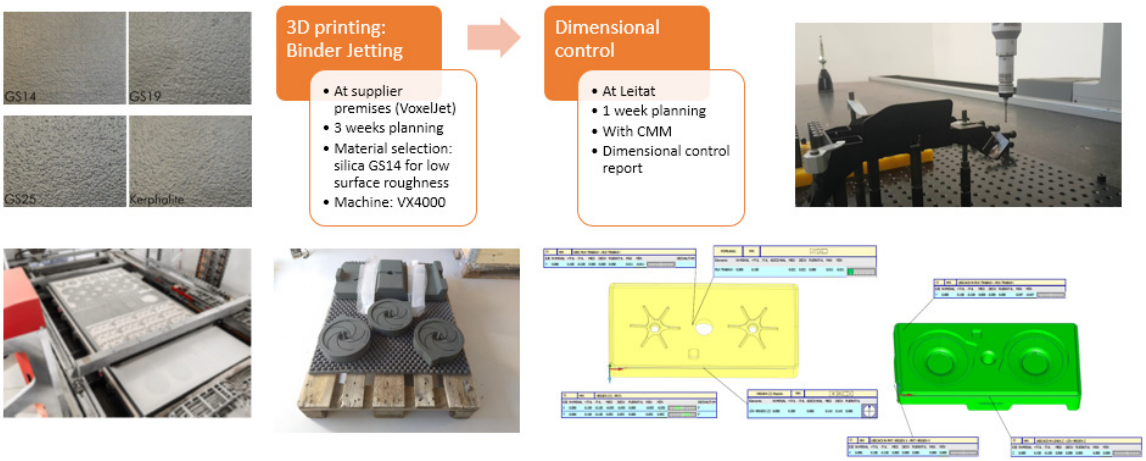

Figure 3.13. Schematic process of Step E.

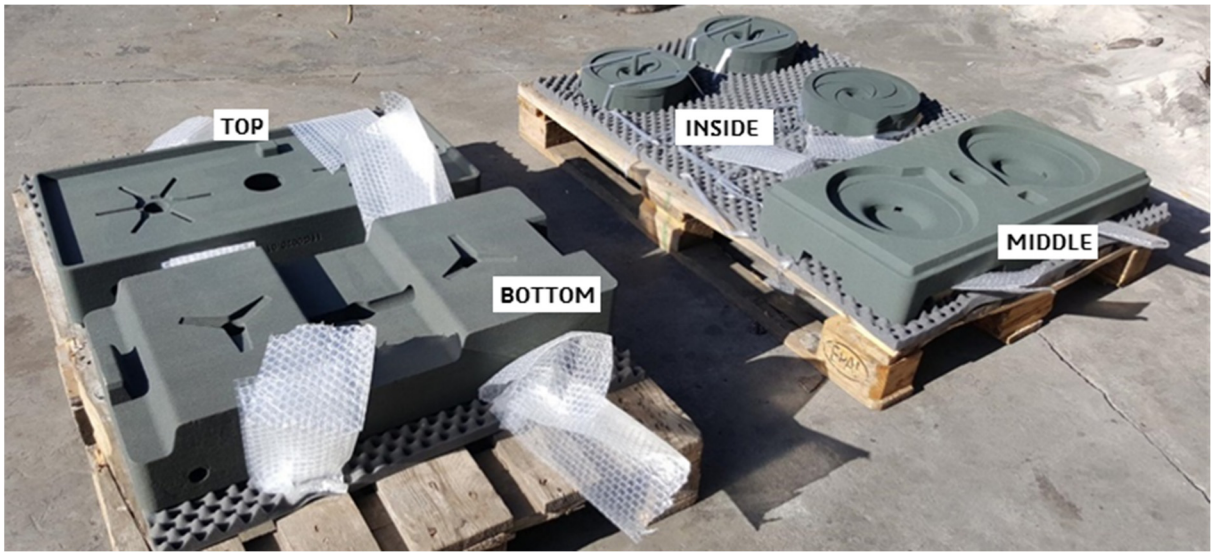

Figure 3.14. Photographs of the manufactured 3D sand moulds indicating the different parts.

3.7. Step F. Casting of the impellers using the 3D-printed sand moulds.

Casting of the BJ impellers was performed on the 3D sand mould at the premises of the Fondesal S.A. foundry company (Barcelona, Spain) using AISI 316 stainless steel. Figure 3.15 depicts 3D models of the time evolution of the casting process, while Figure 3.16 shows photographs of the resulting casted impellers after mould separation.

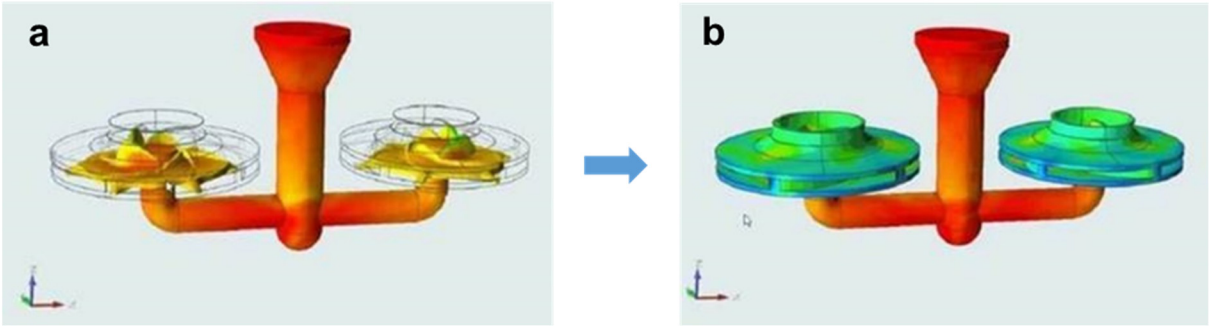

Figure 3.15. Casting impeller process: (a) fill in starting moment, (b) fully filled channels and structures.

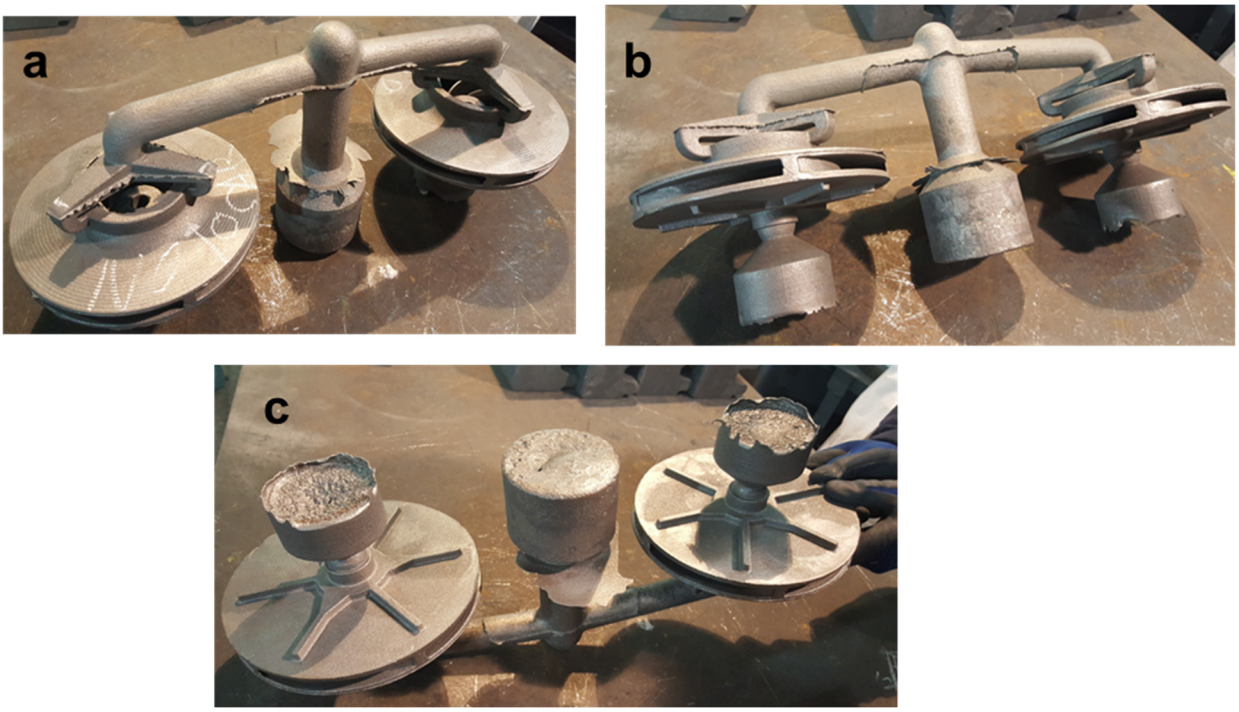

Figure 3.16. Casting impeller results: (a) upside view, (b) lateral view, (c) downside view.

3.8. Step G. Finishing and characterization of the fabricated impellers.

The next step of BJ impeller manufacturing involved finishing and testing steps (Figure 3.17).

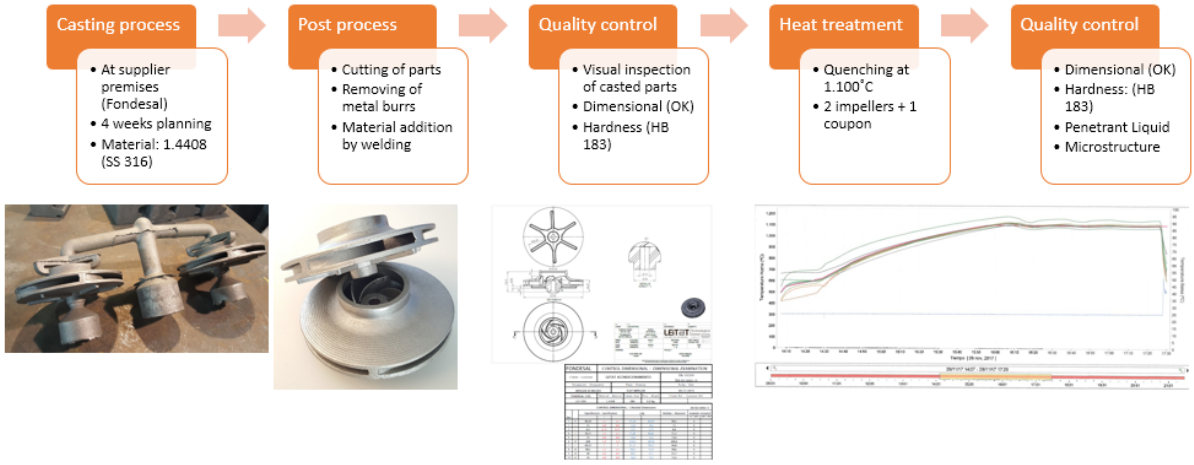

Figure 3.17. Schematic process of Step G.

Excess of casted material was removed, and the parts were machine finished to afford the individual parts (weight: 4.03 kg) ready for inspection, heat treatment and testing (Figure 3.18). The manufactured impellers were then thermally treated by heating the parts up to 1100°C at 5 °C/min for 120 min in a programmable oven initially set at 500°C. The austenization temperature was maintained for 90 min, and then the impellers were quickly quenched in water.

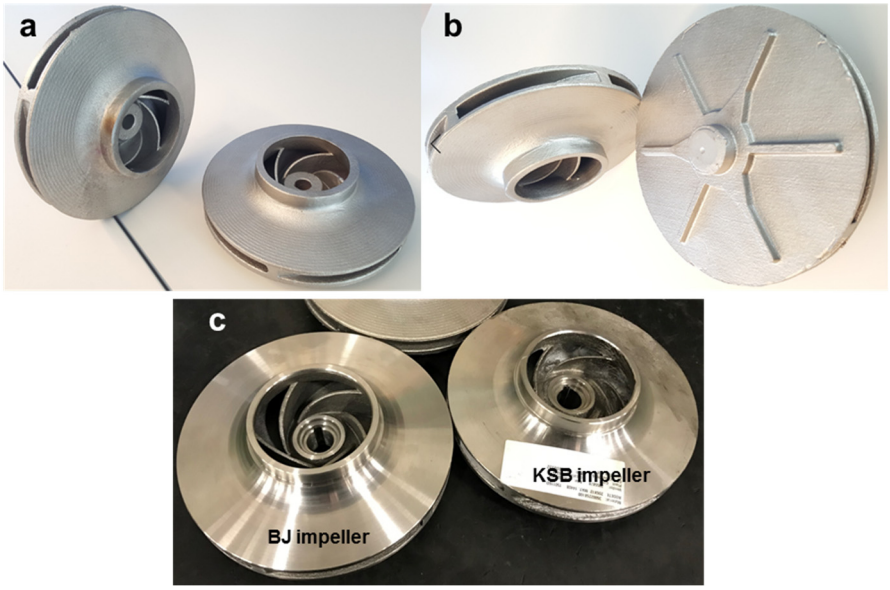

Figure 3.18. Casting impeller after first post process tasks: upside view, (b) downside view, (c) comparison with original *KSB* impeller after finishing.

After the heat treatment, a small portion of the material was examined at the optical microscope, and hardness (Brinell) gave a value of 183 as compared with the 212 of the original KSB impeller. The results of two-plane impeller dynamic balancing were within the permissible unbalance calculated according to ISO1940/1 for grade G 2.5 at an operating speed of 3000 rpm (Table 3.2).

Table 3.2. Mechanical properties of the BJ impeller.

Property		**Values** [1]
Relative Density (g cm^{-3})		7.89 ± 0.05
Hardness (Brinell)		183 ± 5
Dynamic Balancing [2]	Plane 1[3]	*Before balancing*: 6.5 g @ 90° (13 g·mm)
		After balancing: 0.3 g @ 93° (0.6 g·mm)
	Plane 2[3]	*Before balancing*: 17.8 g @ 160° (35.6 g·mm)
		After balancing: 0.9 g @ 150° (1.8 g·mm)

[1] Average of two measurements. [2] Calculated permissible unbalance per plane (G 2.5): 15.9 g·mm. [3] See inset figure in Table 3.3.

Table 3.3 shows the results of the dimensional characterization of the BJ impeller using a Brown & Sharpe DEA Scirocco measuring unit and a comparison with the dimensions specified by the manufacturer of the KSB impeller. A geometrical precision of ±0.1 mm was obtained with standard deviations for each dimension lower than 1%. The highest absolute dimensional discrepancy was obtained for dimension B, corresponding to the outside diameter of the impeller inlet, which may have been due to the finishing operations carried out after casting and removal of the excess materials (although in relative values, the deviation was only 0.28%). These results suggest that the 3D printing of the sand mould and subsequent metal casting are appropriate for generating relatively complex parts with sufficient precision to pass dimensional testing.

Table 3.3. Dimensional characterization of the BJ impeller.

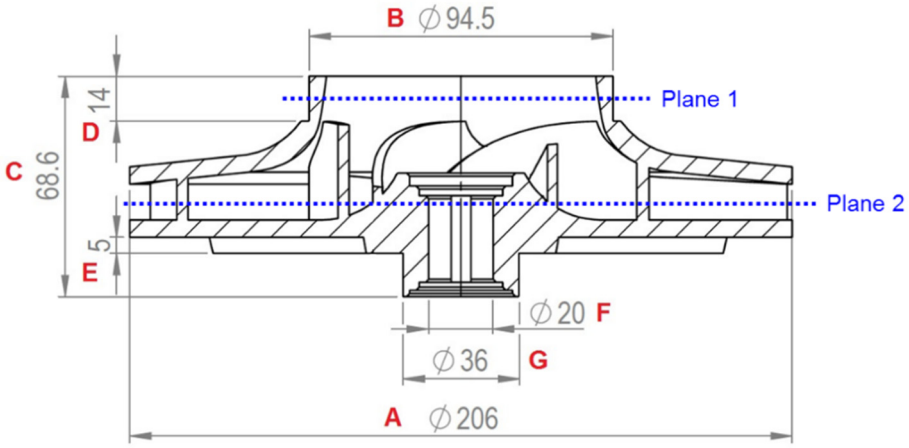

Dimension	Specification (mm)	Measured (mm)	Difference (mm)[1]	% Deviation[2]
A	206.0 ± 0.5	205.99 ± 0.01	−0.01	0.01
B	94.5 ± 0.5	94.23 ± 0.26	−0.27	0.28
C	68.6 ± 0.3	68.70 ± 0.13	0.1	0.19
D	14.0 ± 0.2	14.07 ± 0.07	0.07	0.50
E	5.0 ± 0.1	5.05 ± 0.05	0.05	0.99
F	20.0 ± 0.1	19.94 ± 0.05	−0.06	0.25
G	36.0 ± 0.2	36.02 ± 0.04	0.02	0.11

[1] Difference between measured and specification. [2] (standard deviation - measured dimensions) × 100.

Examination via scanning electron microscope of the surface of a residual portion of casted material revealed the presence of cavities due to metal contraction during the cooling process that followed casting (Figure 3.19). These shrinkage voids (Khalajzadeh, V.; Beckermann, C, 2020) had variable shapes and sizes, from a few µm to ~400 µm, but accounted only for a very small portion of the surface (less than 0.5%). Assuming that these discontinuities were also present in the finished BJ impeller, they did not affect its performance.

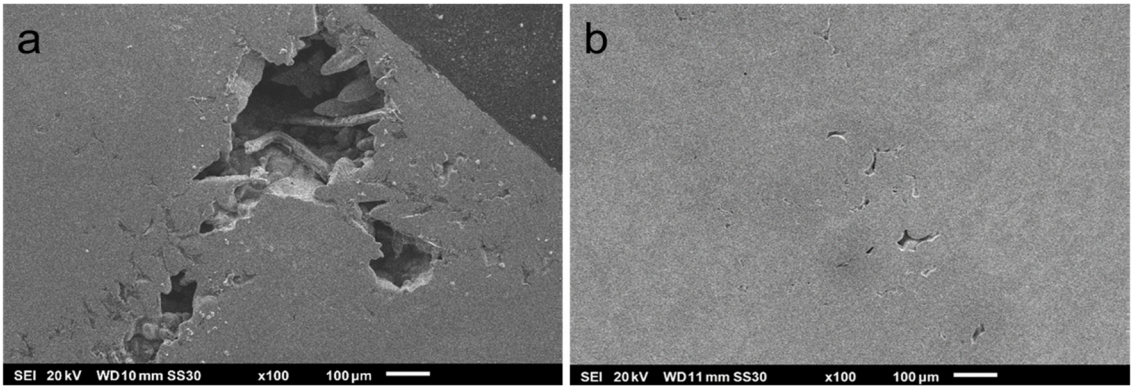

Figure 3.19. SEM images of BJ impeller surface showing (a) large (~400 μm) and (b) small (~50 μm) shrinkage voids due to metal contraction.

Metallographic inspection at 200× magnification was conducted using saturated $FeCl_3$ in concentrated HCl as an etchant after polishing and mounting in an epoxy resin. Analysis of the resulting images (Figure 3.20) showed a microstructure typical of a casting stainless steel 316 (Vander Voort, G et al., 2004), with an austenitic matrix and elongated ferrite grains of 40 ± 10 μm length and 6–8 μm width. The proportion of the ferritic phase was 6.3%, as suggested by image analysis, and no chromium carbide precipitation was observed (Astafurov, S.; Astafurova, E, 2021). Comparison of the microstructure with a sample of a discarded KSB impeller revealed a similar pattern of a Cr/C-free austenitic matrix with ferrite islands but differing in size (120 ± 30 μm long, 10–15 μm width) and proportion (8.1%). These variations, although not considerable, indicate a faster cooling rate in the BJ impeller, resulting in the formation of a smaller ferrite precipitate.

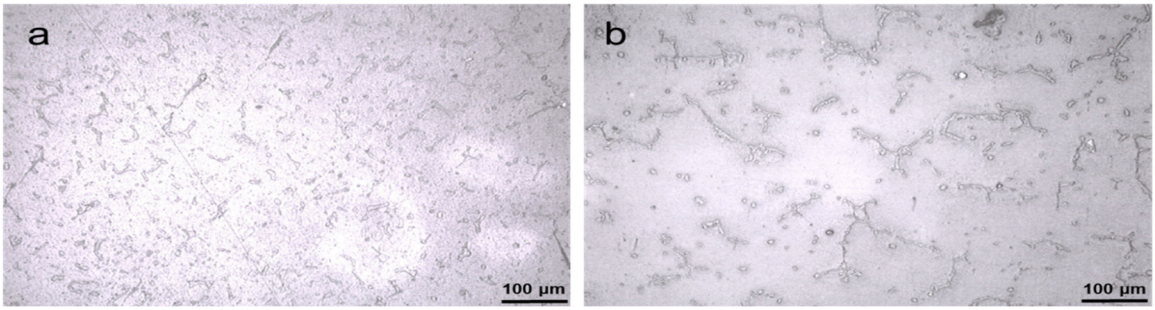

Figure 3.20. Microstructure images of (a) BJ impeller, (b) KSB impeller (200×, etchant: saturated $FeCl_3$ in concentrated HCl).

3.9. Step H. Performance tests in a chemical plant and comparison with KSB impeller.

The performance of the manufactured BJ impeller was then tested in a real scenario. The BJ impeller was mounted in a centrifugal pump (pump P, Figure 3.21) and put into service

on 30 October 2020 (reference date). The plant is located at ***Dow Chemical Ibérica*** (Tarragona Site, Spain) and produces aqueous polyol/polyglycol solutions of different concentrations and viscosity by adjusting the proportions of feed materials (a polyol/polyglycol precursor and an antioxidant solution) in a discontinuous process. Pump P is located immediately after the reaction tank T and pushes the product mixture towards distillation column D. The process is remotely supervised from a control room that collects several process parameters.

The pump was fed with three different product recipes that varied in the concentration and viscosity of the final product and started when the tower had a level higher than 40% and did not differentiate the product concentration or viscosity. Once the pump was in service, an automatic controller valve located on its impulsion side (V-B) regulates the pump with an amperage measurement that sent an alarm signal at 2.5 A and shut down the pump below 2 A. The pump also stopped if the level of tower D was lower than 15% and therefore had two "stop" set points, low amperage and low tower level.

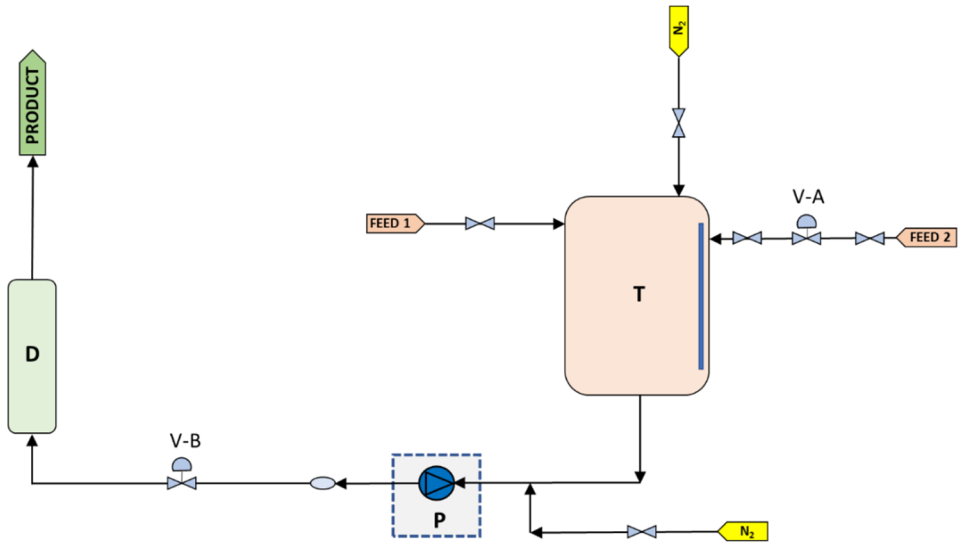

Figure 3.21. Work process flowchart at the polyol/polyglycol plant. The impeller was mounted in pump P. T: reaction tank, D: distillation column, V-A and V-B: fail-open valves.

For the purpose of this study, the process parameters were first collected using the original KSB impeller during specific periods of time for three product recipes of high, medium, and low viscosity, as indicated in Table 3.4. Afterwards, the KSB impeller was substituted (on 30 October 2020) for the BJ, which was set to operate in identical operational conditions for the three recipes in order to compare its performance with that of the original impeller.

Table 3.4. Product recipe compositions and test durations.

Recipe	Final Product Properties		Duration of Tests	
	Concentration (% *w*/*v*)	Viscosity (cSt)	KSB Impeller	BJ Impeller
1	80	500	January 2020–October 2020	November 2020–April 2021
2	50	180	August 2019–October 2020	November 2020–April 2021
3	20	30	May 2019–October 2020	November 2020–April 2021

Figures 3.22 to 3.24 show the results obtained for both impellers using the three recipes. Panels (a) and (b) in these figures show the dependence of pump amperage (current) on pressure and product flow, with typical values between 9 and 10 A. Since, in normal operating conditions, the electric tension of the pump is constant, a decrease in the current indicated a malfunction of mechanical parts of the pump in which the impeller was located and was thus an indirect measure of the performance of the pump. The average values in all cases were between 9.3 and 9.4 A, with low standard deviations, indicating similar behaviour of both impellers.

On the other hand, panels (c) and (d) in Figures 3.22 to 3.24 show comparisons of the data obtained with both impellers for one typical production cycle. Average values and standard deviations are also indicated over each trace. A normal run lasted about two days, and parameter readings were taken continuously every 20 min. Pump P was continuously monitored to maintain the level of tank T at ~40%, and the variations in pressure and product flow observed in the figures correspond to adjustments in the production according to the desired specifications and production volume. Although we did not carry out a detailed statistical analysis of these results, it was evident that the parameter readings with the BJ impeller were comparable to, and in some cases slightly more stable than, those obtained with the original KSB impeller. This general trend was observed for all production cycles monitored, and no failure of the BJ impeller was observed throughout the performance study.

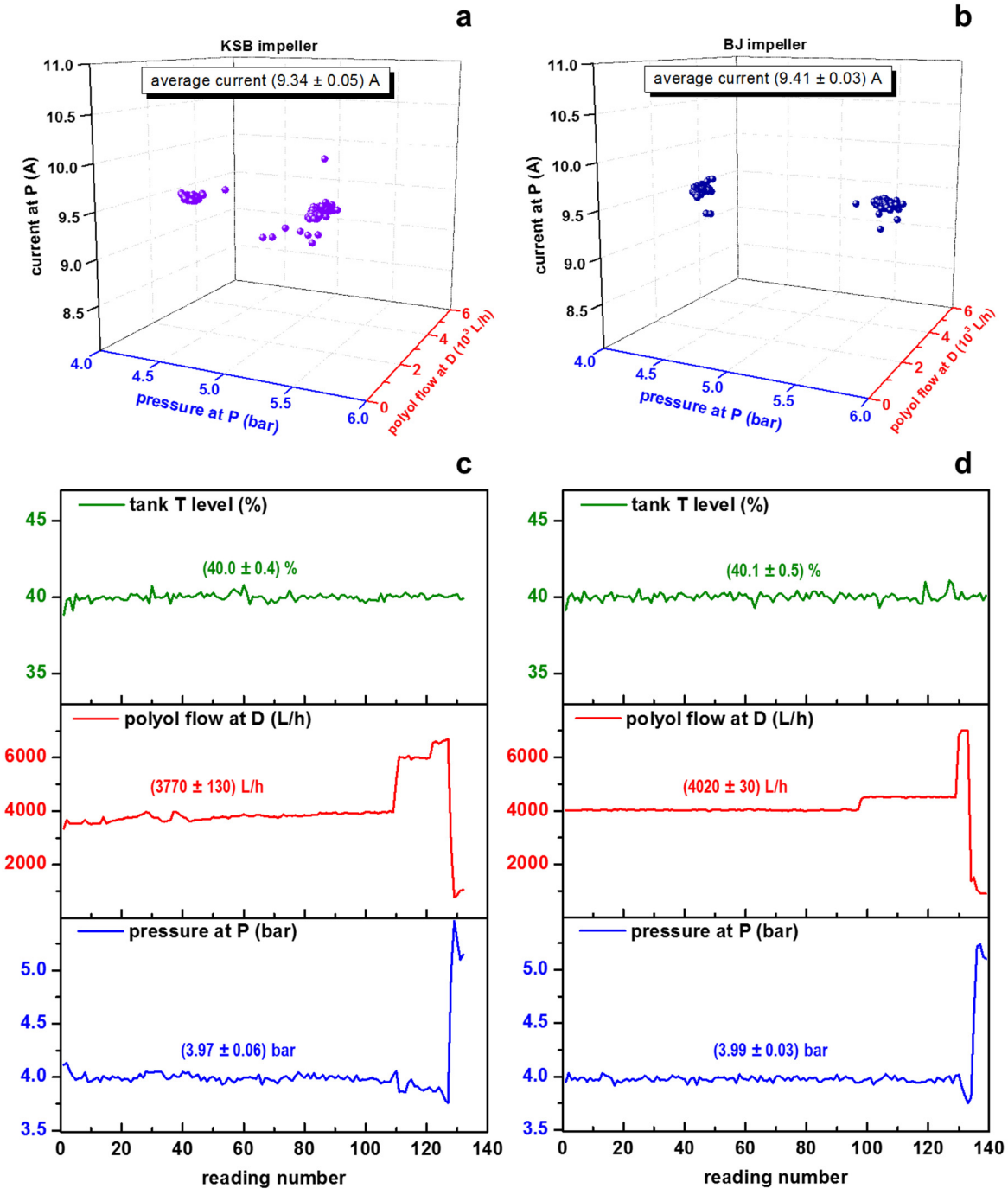

Figure 3.22. Recipe 1. (a,b) Dependence of pump amperage (current) on pump pressure and polyol flow for two consecutive production cycles. (c,d) Tank level, polyol flow, and pump pressure, read continuously for a complete production cycle. KSB impeller (a,c), BJ impeller (b,d).

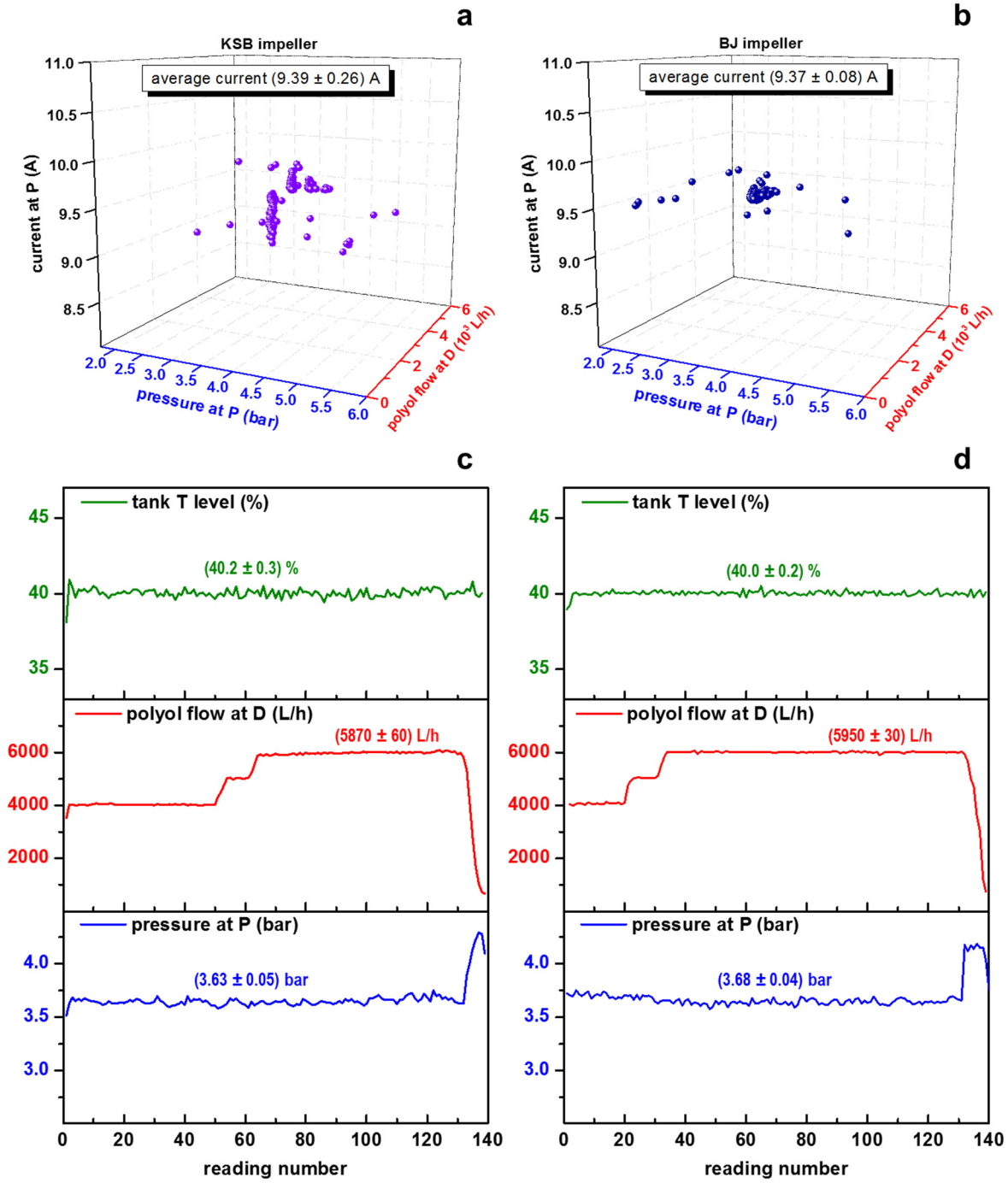

Figure 3.23. Recipe 2. (a,b) Dependence of pump amperage (current) on pump pressure and polyol flow for two consecutive production cycles. (c,d) Tank level, polyol flow, and pump pressure, read continuously for a complete production cycle. KSB impeller (a,c), BJ impeller (b,d).

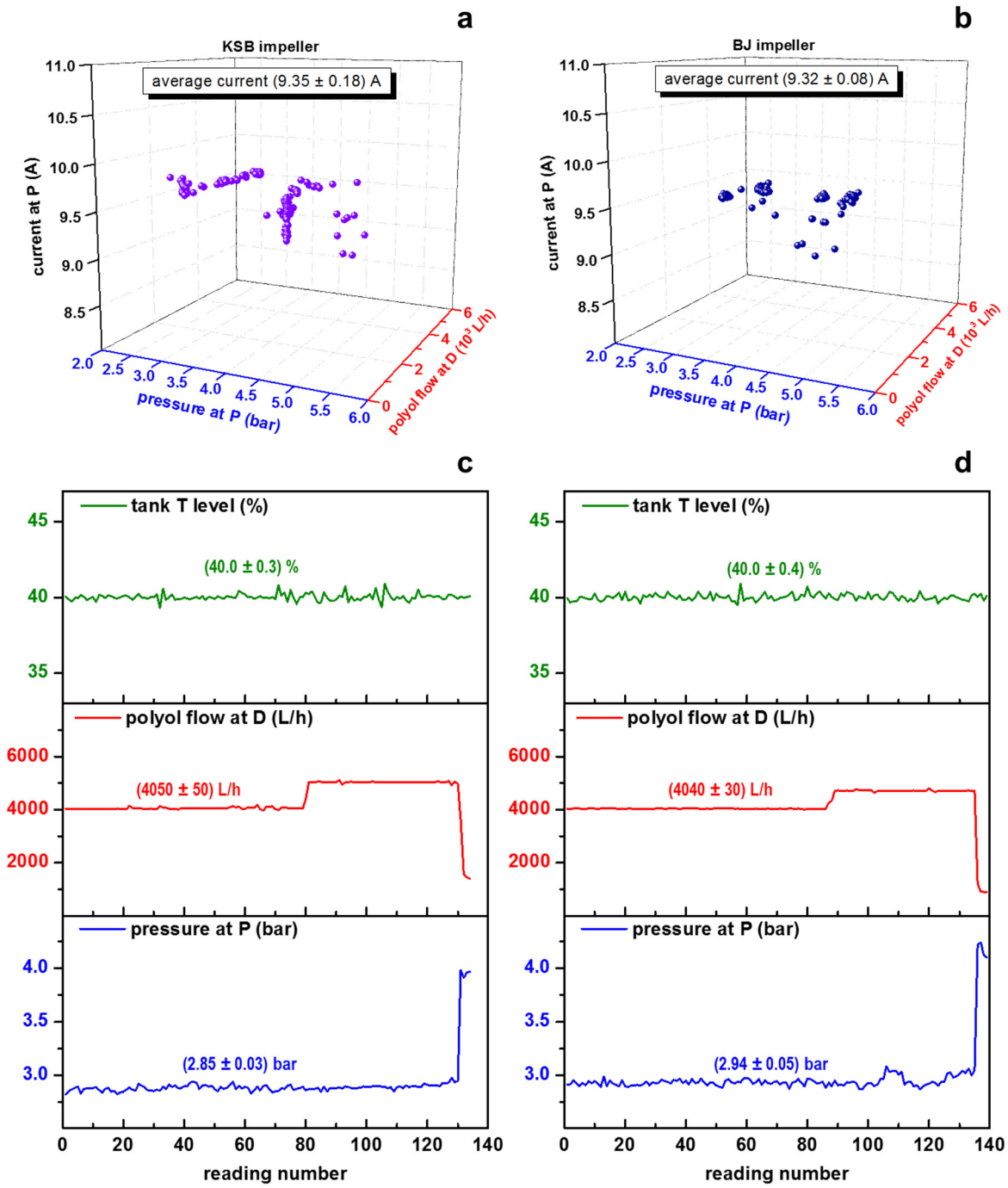

Figure 3.24. Recipe 3. (a,b) Dependence of pump amperage (current) on pump pressure and polyol flow for two consecutive production cycles. (c,d) Tank level, polyol flow, and pump pressure, read continuously for a complete production cycle. KSB impeller (a,c), BJ impeller (b,d).

The results obtained indicated that there were no differences between the original and the new BJ manufactured impeller and further demonstrated that the manufacturing strategy was technically validated, from a design/manufacture point of view to an operational/process point of view.

3.10. Economic evaluation of BJ impeller manufacture.

As an initial reference, to calculate the price of an element manufactured using additive technologies the following general model can be followed in which the final manufacturing cost of the prototype (C_p) of the 3D model has been calculated in accordance with the following equation (Romero L. et al., 2019):

$$C_p = C_e + C_m + C_t + C_a$$

where, C_e is the production cost (machine depreciation data), C_m is the cost of material, C_t is the processing cost of the 3D model and labor cost, and C_a is finishing (post-processing) cost.

However, this first estimation is not taking all cost elements into consideration once you go more into detail such as costs to study and develop any piece (engineering cost), and there is also a cost for material and manufacturing process for the 3D technology. Additionally, there are also costs associated to finishing and characterization tasks such as metallographic study, chemical analysis, impeller balancing, shaft hole machining and preventive supervision tasks once the pump is running in plant to assure correct service. Finally, stocking costs must be considered.

Hence, *Option 1* involves the calculation and economic balance in case the impellers are kept in stock in warehouse.

Alternatively, a very interesting option that should be also considered is to have no stock kept in warehouse, just material electronic files to print the impeller when actually needed it, not before (*Option 2)*. In such case, it must also be taken into consideration costs of having material stocked, which are:

1.- Operational costs: Labour costs, maintenance facilities, salaries…

2.- Taxes

3.- Capital charge:

a.- Use of inventory + accounts receivable

b.- Physical Assets (buildings, equipments)

c.- Intangible Assets (patents, intellectual property)

The results for both economic balance options are given below (Tables 3.5 and 3.6):

Option 1: **Project economic balance *keeping* units in stock in warehouse**.

Table 3.5. Project economic balance summary for *Option 1* (keeping units in stock).

KSB *vs*. first 3D impeller manufactured

Purchase order to KSB manufacturer	
Purchase order	3250
Total cost (€ / 1 impeller):	**3250**

3D manufactured 1st unit	
3D Development Cost - just once to pay (€)	5750
3D Manufacturing Print Cost (€/1 piece)	1560
Material analysis - replica (€)	222
Metallographic study (€)	500
Impeller balancing (€)	455
Shaft hole machining (approx. 2 h work) (€)	75
Total cost (€ / 1 impeller):	**8562**

2nd and 3rd 3D impeller manufactured

3D manufactured 2nd unit	
3D Development Cost - just once to pay (€)	0
3D Manufacturing Print Cost (€/1 pieces)	1560
Material analysis - replica (€)	222
Metallographic study (€)	0
Impeller balancing (€)	455
Shaft hole machining (approx. 2 h work) (€)	75
Total cost (€ / 1 impeller)	**2312**

3D manufactured 3rd unit	
3D Development Cost - just once to pay (€)	0
3D Manufacturing Print Cost (€/1 pieces)	1560
Material analysis - replica (€)	222
Metallographic study (€)	0
Impeller balancing (€)	455
Shaft hole machining (approx. 2 h work) (€)	75
Total cost (€ / 1 impeller)*	**2428**

* Considering an estimated IPC of 5%.

Total cost per impeller (€) ⇒	**1st unit**	**2nd unit**	**3rd unit**	**4th unit**
Purchase order to KSB manufacturer	3250	3412*	3583*	3762*
Cumulative cost	3250	6662*	10245*	14007*
3D manufactured units	8562	2312	2428*	2549*
Cumulative cost	8562	10874*	13302*	15851*

* Considering an estimated IPC of 5%.

The results indicate that the combination of 3D manufacturing and casting is economically profitable – comparing with traditional method from KSB manufacturer - taking into account the total cost invested from the first time study/evaluation and the total development work, but it is very interesting to mention that the 2nd unit is already profitable (cheaper than original KSB impeller, 2.312 € versus 3.250 €), so making cheaper the initial investment with, for example, a bigger amount of spare parts to evaluate together, it would make much more profitable 3D printing material.

Option 2: **Project economic balance *not keeping* units in stock in warehouse**.

Table 3.6. Project economic balance summary for *Option 2* (not keeping units in stock).

Purchase order to KSB manufacturer plus stocking costs	
Purchase order	3250
Cost of keeping stock for one year: 1.- Operational costs: Labor costs, maintenance facilities, salaries… 2.- Taxes 3.- Capital charge: a.- Use of inventory + Accounts receivable b.- Physical Assets (buildings, equipments) c.- Intangible Assets (patents, intellectual property)	
25-30% costs items	894
Total cost (€ / 1 impeller):	**4144**

Project economic balance: 3D impeller manufacturing but none stocked.

3D manufactured 1st unit/year - non stocked	
3D Development Cost - just once to pay (€):	5750
3D Manufacturing Print Cost (€/1 pieces):	0
Material analysis - replica (€)	0
Metallographic study (€)	0
Impeller balancing (€)	0
Shaft hole machining (approx. 2 h work) (€)	0
Cost of having stock (€)	0
Total cost (€ / 1 impeller):	**5750**

3D manufactured unit (only when needed it)	
3D Development Cost - just once to pay (€):	0
3D Manufacturing Print Cost (€/1 pieces):	1560
Material analysis - replica (€)	222
Metallographic study (€)	0
Impeller balancing (€)	455
Shaft hole machining (approx. 2 h work) (€)	75
Cost of having stock (€)	0
Total cost (€ / 1 impeller):	**2312**

Total cost per impeller (€) ⇒	**Year 1**	**Year 2**	**Year 3**	**Year 4**
Purchase order to KSB manufacturer - stocked	4144	894*	938*	4351*
Cumulative cost	4144	5038	5976	10327
3D manufactured units - non stocked	5750	0	0	2312
Cumulative cost	5750	5750	5750	8062

* Considering an estimated IPC of 5%.

The results indicate that *Option 2* is economically profitable – comparing with traditional method from KSB manufacturer - from the 2nd unit taking into account the total cost invested from the first time study/evaluation and total development work but making the 3D printing impeller just when you really need it in plant, not before. Additionally, it is interesting to indicate that 3D printing impeller fabrication (only the manufacture work) is cheaper than original KSB impeller, cost 2.312 € versus cost 3.250 €.

The estimation is done for a change of impeller in year 4.

3.11. Conclusions.

In this Chapter, we have presented the fabrication and performance study of a stainless-steel pump impeller manufactured by BJ printing of a sand mold followed by casting. The work is another example of the advantages of BJ sand printing in creating multicomponent molds able to recreate complex features of the original part. The main conclusions of the work can be summarized as follows:

- Reverse engineering of the original impeller allowed creating a polyamide copy, used to validate the CAD design by metrological characterization, with a dimensional accuracy higher than 99.0%.
- The casted material showed an essentially homogeneous surface, with a very small proportion (<0,5%) of shrinkage voids. The microstructure was similar to that of the original impeller, with 6,3% of ferritic phase.
- The operational performance of the produced impeller was tested in a real scenario by installing the impeller in a centrifugal pump. The pump operated in a polyol/polyglycol plant, and a series of process parameters related to the pump behaviour were measured continuously for three production recipes varying in final concentration and viscosity.
- For example, at 500 cSt of product viscosity, the average current consumption of the pump was 9,34 A, as compared with 9,41 A measured with the original impeller, with standard deviations of 0,3% and 2,7%, respectively, for a wide interval of pressures (4–6 bar) and flows (2000–6000 L/h).
- The parameters were also comparable when measured during a complete production cycle. This indicated that both impellers had equivalent performance, thus validating the fabrication strategy from an operational point of view.
- The combination of 3D manufacturing and casting is economically profitable for both stocking/non stocking options considered.

Therefore, this work demonstrated that the implementation of additive manufacturing technologies in chemical process engineering is a useful solution for fabricating spare parts of high added value that are difficult to replicate with other technologies, with consequent economic benefit. Further work should focus on comparing the initial mechanical and morphological properties of the BJ impeller with those obtained after one year of operation in order to understand possible changes induced by the stress associated with continuous operation.

In addition, the next step would thus involve the fabrication of an impeller by direct metal 3D printing and an economic study of the possible wider implementation of both 3D printing technologies in a chemical plant.

Chapter 4: Fabrication of a titanium alloy impeller by selective laser melting and performance tests in a hydrocarbon plant at Dow Chemical Ibérica SL (Strategy 2)

4.1. Introduction.

In the previous chapter we described the fabrication of a stainless-steel impeller combining binder jetting sand printing with casting. While this strategy proved to be successful with respect to the performance of the printed part in a real scenario and for a long period of time, the overall manufacture process required a relatively large number of steps.

As shown in Chapter 1, metals and alloys can be 3D-printed using a variety of techniques that can produce complex parts in short times with very good resolution. The aim of this second part of the work is directly print an impeller (called SLM impeller) by Selective Laser Melting technology, thus avoiding the need to fabricate a mold and a casting process, and compare its performance with the original part after continued use. The original impeller is used in a vacuum pump (called pump O for confidential reasons) installed in a hydrocarbon plant at Dow Chemical Ibérica SL in Tarragona Site (Spain) and was manufactured by Flowserve SIHI. The SLM technique (Deng S. et al., 2021; Frazier W. E. et al., 2014; Mathew M. T. et al., 2021; Alvarez B. J. et al., 2021), although it is still less available than other technologies, it has been used to print complex metallic parts with high precision and very remarkable mechanical characteristics.

The study also began with an analysis of the original part fabricated with stainless steel 1.4027.05. Since this material is not yet available in 3D printing technology, a construction material analysis was done to replace it by a titanium alloy (Ti6Al4V), which is widely used in the aeronautic industry due to its low density and good characteristics but less used – not yet - in the chemical industry, and it is also available for 3D printing. After 3D digitization in CAD, a plastic communication model was first manufactured for visual evaluation. The CAD design was then used to 3D-print the impeller in the titanium alloy. After machining and polishing, the impeller was mounted in pump O and tested for several months.

The sequential workflow is depicted in Figure 4.1 and involved the following steps:

- Step A) Analysis of the original part (SIHI impeller) and material selection.
- Step B) Part digitizing, CAD design and 3D printing of the plastic model.
- Step C) Manufacturing CAD part.
- Step D) 3D printing of the SLM impeller.
- Step E) Finishing and testing.
- Step F) Performance tests in a chemical plant and comparison with SIHI impeller.

In this chapter, we describe the methodology of fabrication and characterization of the SLM impeller, and the performance results obtained after mounting the part in a chemical plant. Similarly to the previous chapter, the description of methodology and results has been divided in the different steps presented above, followed by a conclusion section.

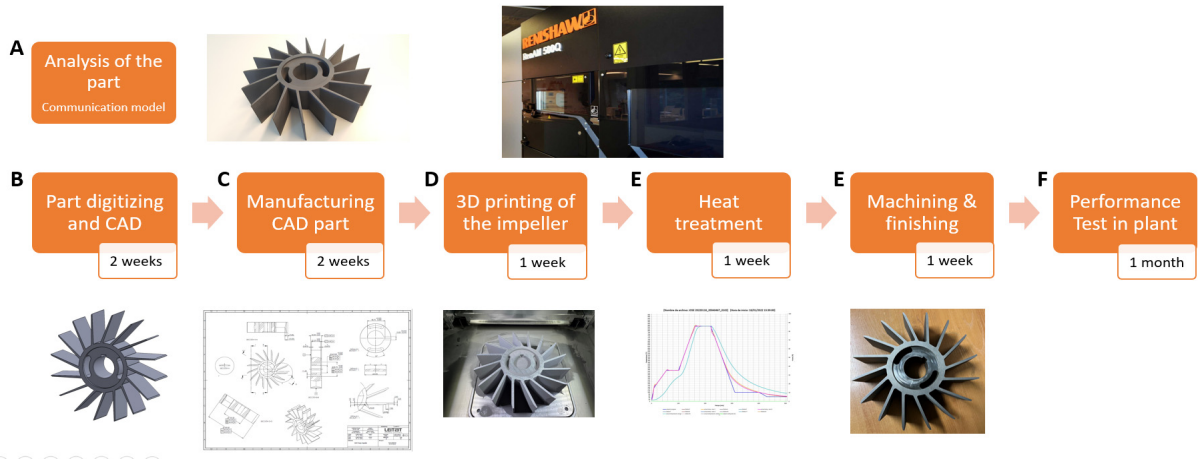

Figure 4.1. Workflow employed for the fabrication of the SLM impeller.

4.2. Step A. Analysis of the original part (SIHI impeller).

The original 16-vane SIHI impeller was fabricated with stainless steel 1.4027.05 with a hardness Brinell of HB 212. Since there was no impeller original drawing from Flowserve SIHI manufacturer, it was used a pump drawing (general overview) with a few dimensional characteristics that give some good support information such as impeller dimensions (230×60 mm) (Figure 4.2).

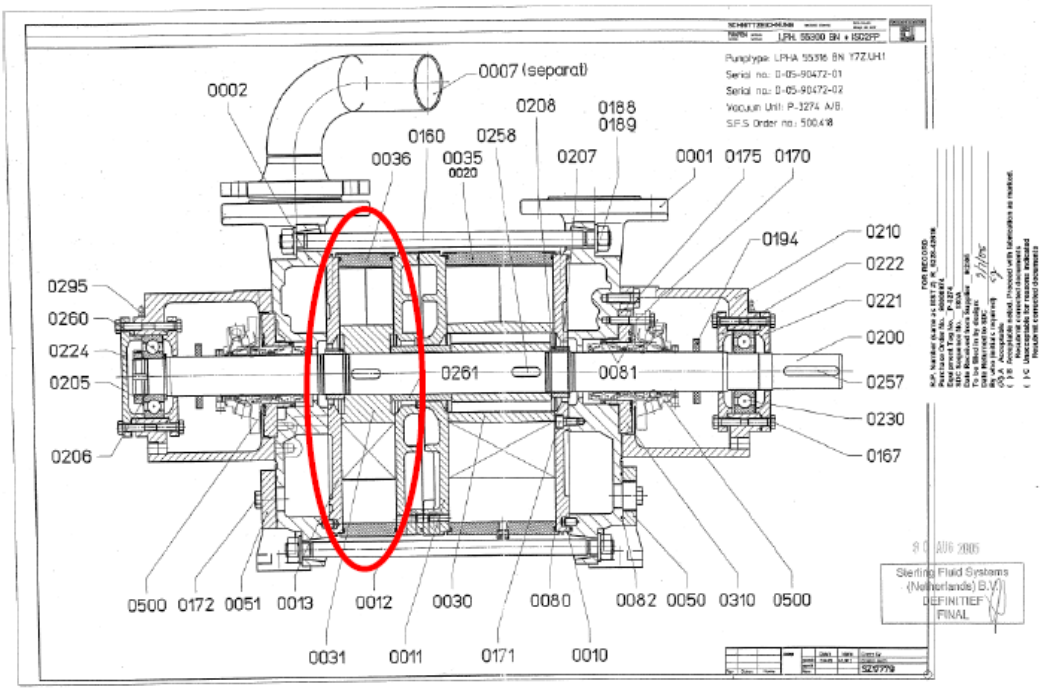

Figure 4.2. Pump O manufacturer sectional drawing with the high-pressure stage indicated in a red ellipse.

The SIHI impeller is mounted in the high-pressure stage of a pump (pump O) used to make vacuum in plant in certain process vessels in which the product is a mixture of liquid and gaseous phases. The pump consists of a low-pressure stage and a high pressure stage with flows connected in series and driven coaxially by the same electric motor. Both stages share radial dimensions, and their volumes difference is given by their different lengths.

Each stage consists of a cylindrical chamber, on one of whose sides there are suction and impulsion openings for the gas being pumped. The chamber is partially filled by the liquid phase of the same product that is being pumped. In both chambers an eccentric impeller with blades (12-vane for low pressure, 16-vane for high pressure) rotates inside the chamber so that it drives the liquid, leaving it uniformly distributed around the chamber wall (Figure 4.3). In this way, a gas phase cavity is left off-center with respect to the impeller. Due to this eccentricity, the gas remaining between the impeller blades expands and contracts once for each turn of the impeller, thus achieving suction through the inlet mouth and impulsion through the outlet.

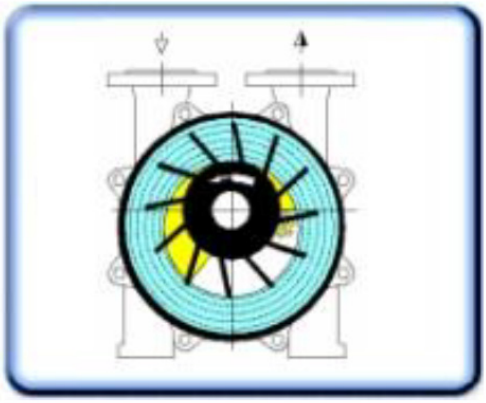

Figure 4.3. Pump O sketch with low pressure impeller position and workflow detail.

Given the impossibility of manufacturing stainless steel 1.4027.05 in a 3D technology, it was considered as the first option to use SS316 since it is a stainless steel with a very wide working range, well known and valued at an industrial level and for its ease of manufacture and subsequent machining. Hence, mechanical and physical properties were studied before to determine if it is a real valid alternative.

To determine its technical feasibility, we need first to perform a fluid dynamic analysis simulating the fluid behavior with a computer fluid dynamic (CFD) software (DualSPHysics) and, later on, next step is a mechanical analysis performed with an appropriate software (ANSYS).

DualSPHysics software was used to perform the fluid dynamics simulation. Rotor starts at steady (permanent) state, and it is slowly accelerated up to the speed of rotation, maintaining it until a permanent regime is reached in the fluid (the behavior is repeated in each cycle). Pressure values are taken at various points on the blade during various moments of a cycle and it is repeated in several cycles since the values are not exactly the same and thus the most unfavorable case can be taken.

Once the fluid pressures on the blade are obtained, a finite element model is made with the software ANSYS to be able to carry out the mechanical analysis. This model only needs the geometry of the blade, not the entire rotor. This simulation is also carried out over time, not in state regime, thus it is taking into account the inertial effects of the blade mass (resonance frequencies). The stresses in the three directions of each point and at each instant are obtained, and from them the Von Mises stress. The Von Mises stress values provide the allowable stress that the material would resist, then the “admissible

stress" is so obtained. And from the fatigue curves and that "admissible stress", it is determined the maximum number of cycles that the material resists.

Results of this analysis indicate the existence of a bubble implosion phenomenon that was repeated as each blade passed. At first moment, a wave forms on the surface in the gap between the blades. In the following moments, this wave hits the bottom of the drum, being confined in the form of a bubble and with the flow recirculating towards the center of it.

Finally, this recirculation produces the implosion of the bubble with the consequent sudden rise in pressure at that point (Figure 4.4 a). This sudden and local pressure rise spreads like a wave along the gap between the blades. During this propagation it is reflected on the walls of the blades, producing a pressure peak in each rebound (Figure 4.4 b,c).

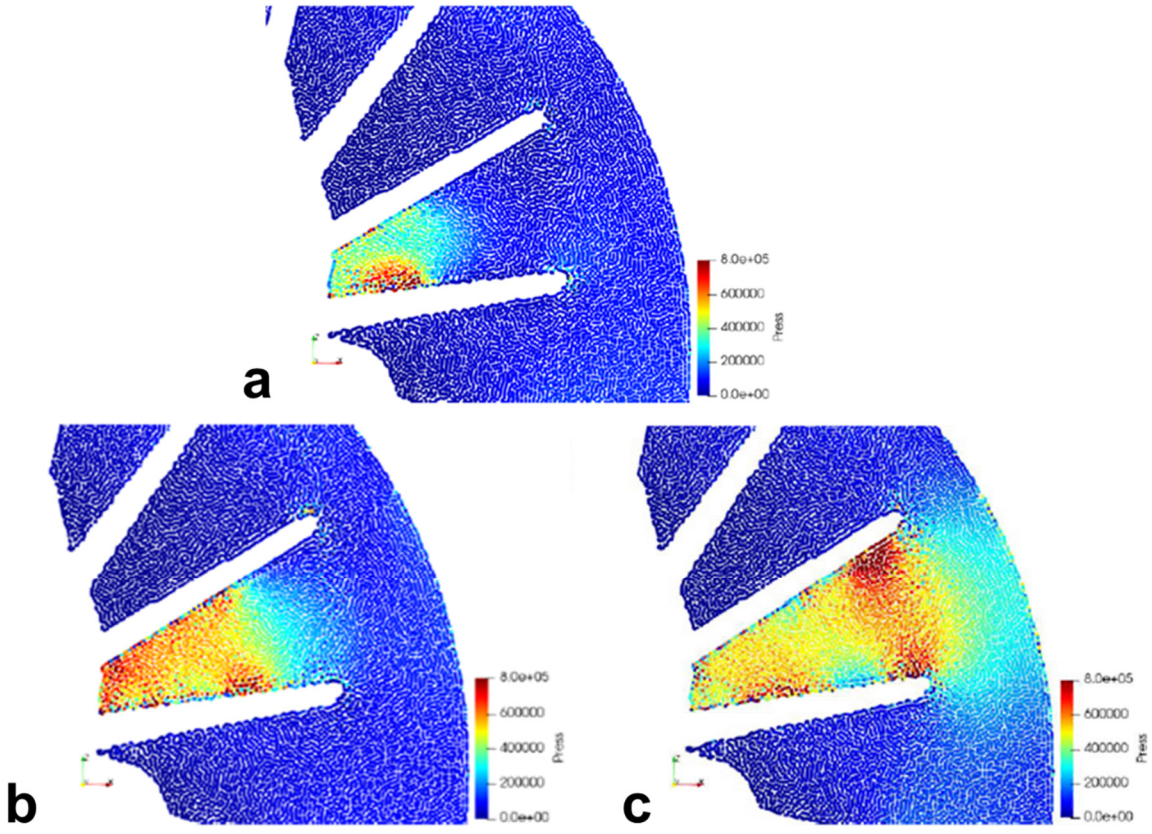

Figure 4.4. CFD study of liquid behavior in the blades as a function of time: a) sudden increase in pressure due to the implosion of the bubble, b,c) propagation of the pressure wave in the gap between blades and reflections in their blade walls.

Upon reaching the body of the pump, the wave collides, it is reflected in it and propagates towards the front and rear blades (Figure 4.5 a-c). The wave propagates towards its interior and the propagation cycle repeats but the pressure propagation to more distant holes is becoming increasingly weaker as can be seen in the reduced scale view of Figure 4.5 d. In these propagations within other holes, pressure peaks are also produced by reflection of the waves on the walls.

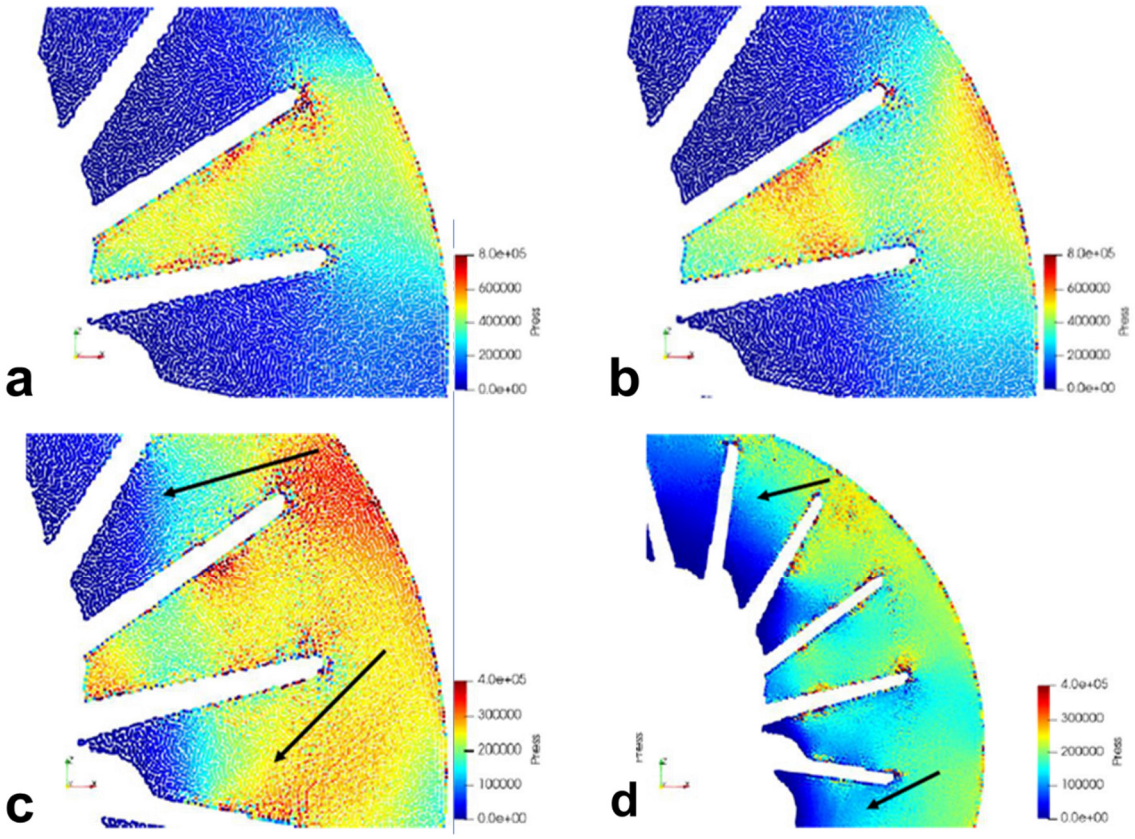

Figure 4.5. CFD study of liquid behavior in the blades as a function of time (3): a,b) propagation of the pressure wave outside the blade gap; c) reflection in the pump body; d) reduced scale view of pressure wave propagation to other gaps between vanes.

Once the presence of a cyclical phenomenon was detected with the frequency measured in the vibration measurement, the last step was to determine the structural behavior of the blade in the face of the stresses found and to evaluate whether the stress states produced are admissible or not.

With the measured stress data, fatigue behavior was estimated using the American Society of Mechanical Engineers Fitness-For-Service methodology (ASME FFS-1) and therefore,

it must be concluded that the design alternative proposed with stainless steel 316 is not viable as it is less resistant than current 1.4027 steel.

After a first evaluation of different material alternatives offered by the manufacturer Renishaw for 3D metal fabrication, several materials are discarded, leaving Inconel and titanium alloy as final viable alternatives.

Given the very high cost of Inconel and its difficulties in mechanizing due to its extreme hardness, it was decided to evaluate titanium alloys, in particular Ti6Al4V (Table 4.1), as per Renishaw manufacturer recommendation considering its high resistance, excellent chemical compatibility and that it is a well-proven and well-known material in multiple applications with a very stable - a priori - manufacturing process.

Table 4.1. Composition of the Ti6Al4V alloy employed in this work.

Element	Ti	Al	V	Fe
%	88.8	6.5	4.5	0.2

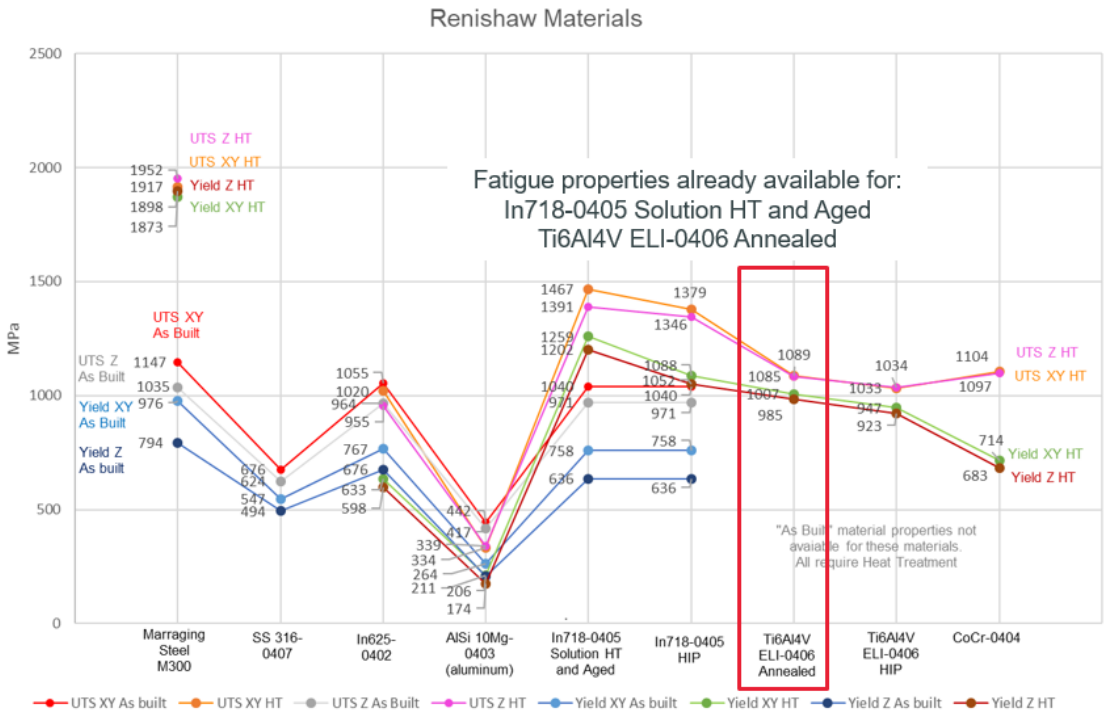

Figure 4.6. Renishaw manufacturer material alternatives and properties.

To evaluate the titanium material, several coupons (test probes) made by 3D printing were manufactured to analyze results (Figure 4.7a). All coupons are numbered from 1 to 12 and two models of coupons were manufactured: cylindrical bars and cube-like probes.

Figure 4.7. a) Renishaw manufacturer titanium coupons. b) Result of penetrant liquid test.

Several assays were done as described below:

- Compatibility Test: Immersion of the metal in 400 mL of the plant process product for 2 weeks to assess its chemical compatibility. Aliquots of the product were analyzed by ICP (Inductively Coupled Plasma) spectrometry to detect possible dissolved metals. The results indicated that no Ti, Al or V were found in the solution. Considering the detection limit of the analysis (0.5 mg/L), the assay time (15 days), the immersed surface of the material (70 cm^2) and the density of the alloy (6.1 g/cm^3), the corrosion rate limit was estimated to be lower than 13.3 mg/day, or $<1.1\times10^{-4}$ mm/year, which was considered satisfactory for the need of the plant process.
- Liquid penetrant testing: to locate possible surface discontinuities by inspection under white light after treatment with a red and fluorescent penetrant (MR® 68C). No fluorescence spots were observed indicating no surface defects for the 3D-printed test probes (Figure 4.7b).

4.3. Step B. Part digitizing, CAD design and 3D printing of the plastic model.

Similarly to the BJ impeller, the SLM impeller was designed through the digitalization of the surfaces and reverse engineering of the supplied component. An industrial metrology 3D scan was made with the original SIHI impeller using an optical automatic arm precision measuring machine ("*ATOS*" Capsule in ScanBox series 4 model 4105, "*GOM GmbH*", Braunschweig, Germany), adapted for measurement of small complex components up to 500 mm in size, to obtain the point cloud geometry. These points are then used to extrapolate the shape of the impeller and finally a parametric CAD model was constructed (Figure 4.8.a). After data acquisition has been performed, the software calculated a polygon mesh of the surface of the component as well as the actual values of the inspection feature plan. This data is compared with the nominal data and it is presented in a report. The measuring results are automatically saved in special export formats for statistical quality control. The measuring procedure for different components was performed fully automatically.

Point cloud geometry needs to be revised and corrected previous to generate the STL file, there are "non-closed mesh" due to shadows in scanning, that means the point clouds need to be converted in "*closed surfaces*" and that done by the Rhinos 7 software ("*McNeel Europe SL*", Barcelona, Spain). Once the closed surfaces were prepared, the mechanical geometry was translated into dimensional parameters using the Solids Works software ("*Dassault Systèmes*", Suresnes, France), and an STL file was created to be used by the 3D printer (Figure 4.8.b-d).

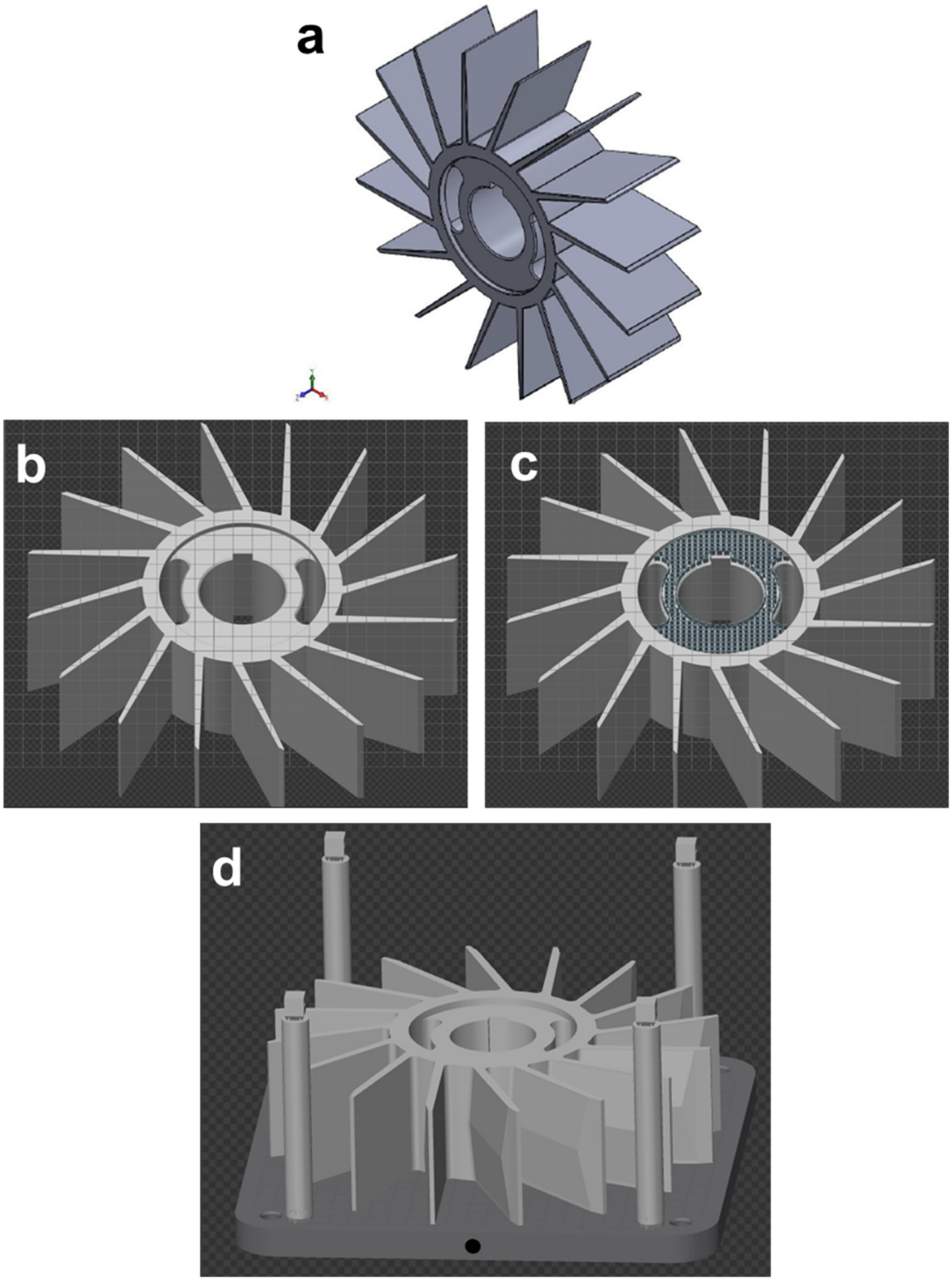

Figure 4.8. SLM impeller digitizing and CAD design: a) scanned geometry; b) scan view without supports; c) scan view with supports; d) 3D view with test coupons for material quality check.

The last step of digitalizing and design was to construct a "*communication model*" in polyamide PA12 at real size for visual inspection and geometry validation.

The dimensions measured validate the CAD model (Figure 4.9).

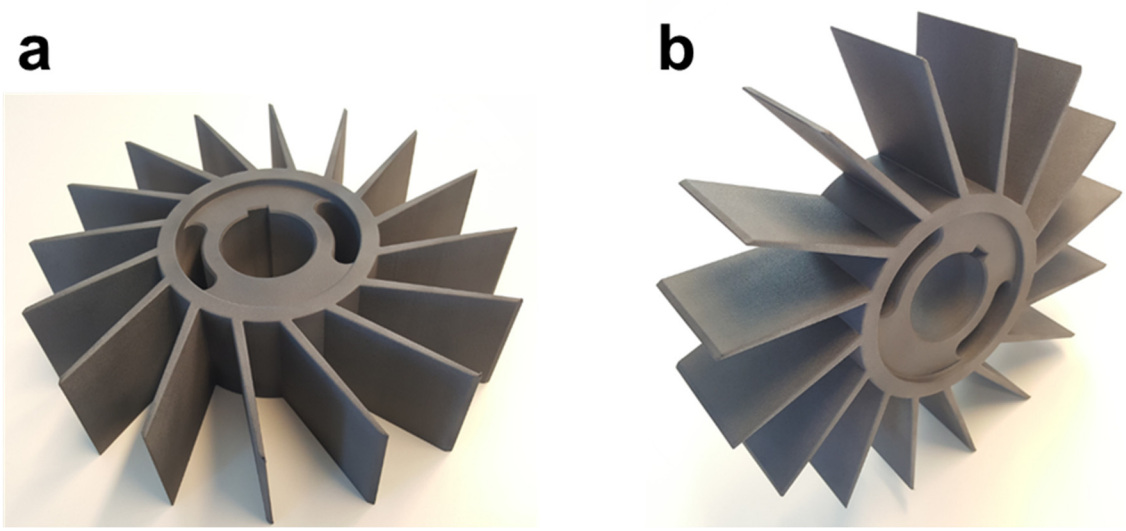

Figure 4.9. SLM impeller PA12 "*communication model*": a) upside view; b) side view.

4.4. Step C. Manufacturing CAD part.

The final result of the previous step is the impeller CAD file (Figure 4.10) where 0,5 mm extra material was added to account for last step of impeller manufacture (machining and dimensional control).

This value corresponds to the manufacturer recommendation for titanium alloys (Table 4.1).

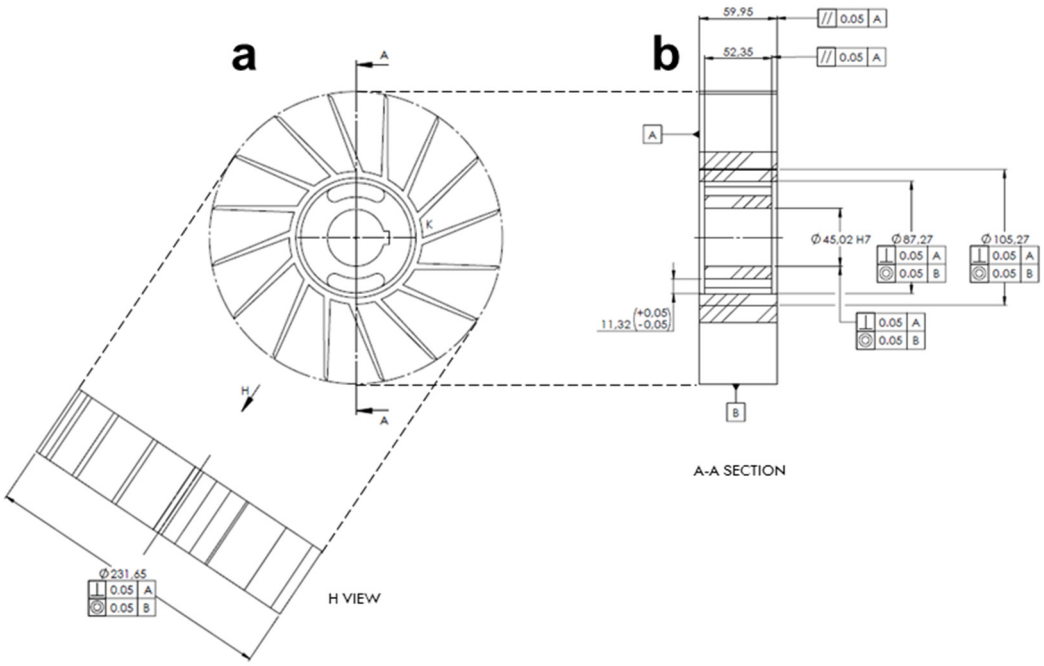

Figure 4.10. SLM impeller CAD file: a) front view and lateral (H) view; b) section view along the A-A axis.

4.5. Step D. 3D printing of the SLM impeller.

The SLM impeller was fabricated using a Renishaw RenAM 500 series metal 3D printer in Ti6Al4V alloy. A total of 2056 layers of 60 µm thickness were needed, for a total manufacturing time of 40 hours, 37 minutes and 36 seconds, including a cold down of 5 hours, 16 minutes and 53 seconds. The heater target temperature was 170°C and absence of oxygen was achieved with an argon flow of 189.9 m^3/h.

A total of 60.3 kg of metal powder were used (powder packing density 2.658 g/cm^3).

Figure 4.11 shows photographs of the different printing steps and the resulting SLM impeller compared with the original SIHI impeller.

The 3D-printed part had a weight of 2.990 kg, which is 43% lighter than the original from SIHI, see figure 4.12.

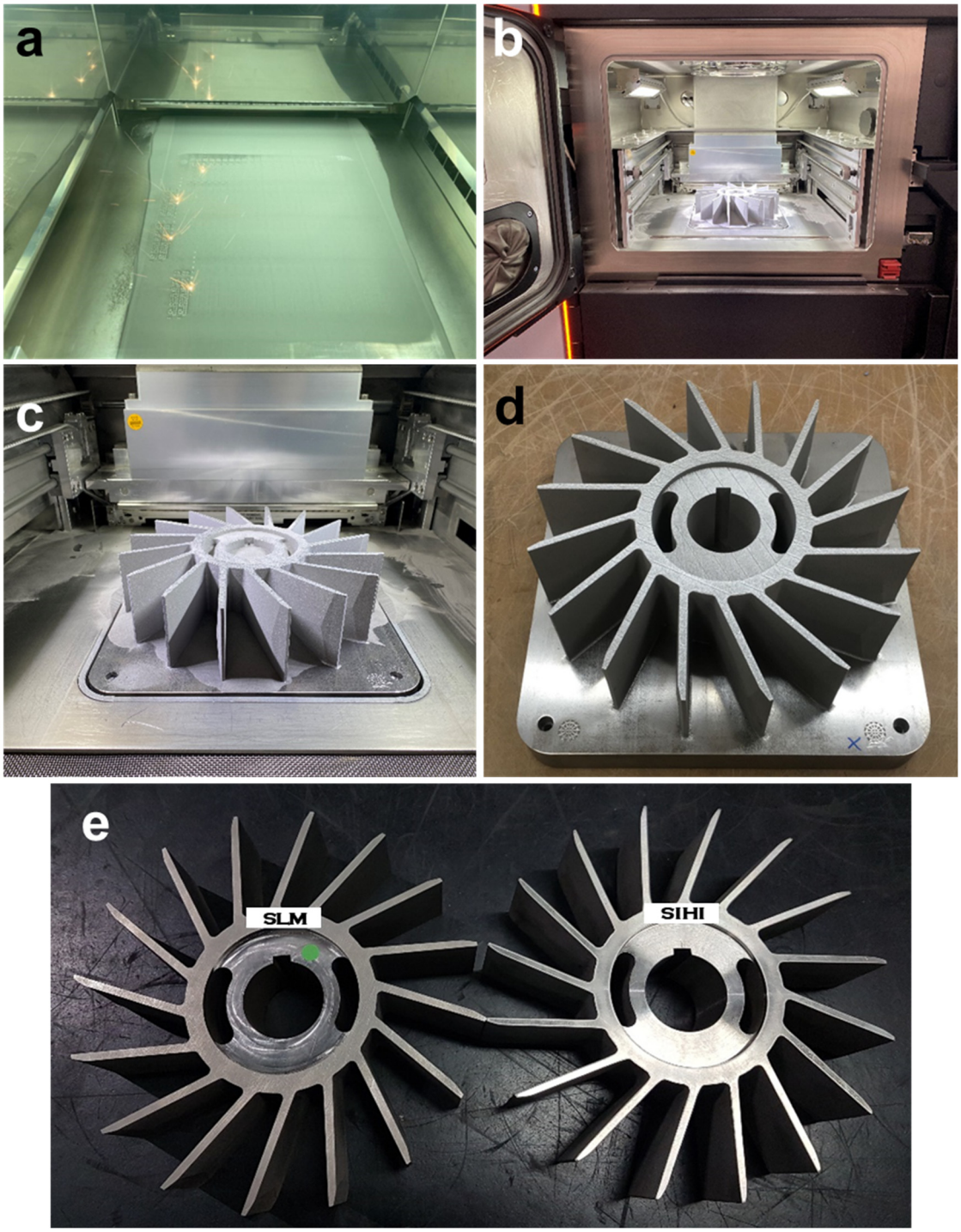

Figure 4.11. a-d) SLM impeller manufacturing steps 1, 2, 3, 4; e) visual comparison of SLM impeller (left) with the original part on the right.

Figure 4.12. Weight comparison of SLM and SIHI impellers.

4.6. Step E. Finishing and testing.

Once the impeller is manufactured, still last important tasks must be performed about the material itself and also about the impeller construction to prepare it to put in service in a properly rotating pump conditions. Machining of the impeller and final manufacturing operations are:

- Measurement and mechanization.
- Metrological analysis: Renishaw and Leitat dimensional control with satisfactory results. Very accurate tolerances adjustments (0.025 to 0.05 mm). Reports number AT21P3198-02 (Renishaw) and IN-00494/2022/1 (Leitat).
- Thermal heat treatment manufactured impeller and coupons with satisfactory results. Report number 20220118_20040467.
- Coupons destructive test (traction test) with satisfactory results. “Element” Report number LEIT1-2105101-0101.
- TUV NORD Qualicontrol NDT (penetrant liquids) with satisfactory results. Report number CCT0505PT2021XP01.
- MASA Impeller dynamic balancing report with satisfactory results according to ISO norm 1940, dynamic balancing speed of 750 rpm. Report number E22/018.

4.7. Step F. Performance tests in a hydrocarbon plant and comparison with SIHI impeller.

The SLM impeller was mounted in a centrifugal pump (pump O) and put into service on 16 June 2022 (reference date). This pump is needed to maintain vacuum in certain process vessels in which a product is in the liquid and gaseous phase. As with the case of the BJ impeller, the plant is located at Dow Chemical Ibérica SL (Tarragona Site, Spain) that produces a type of hydrocarbon (Figure 4.13.).

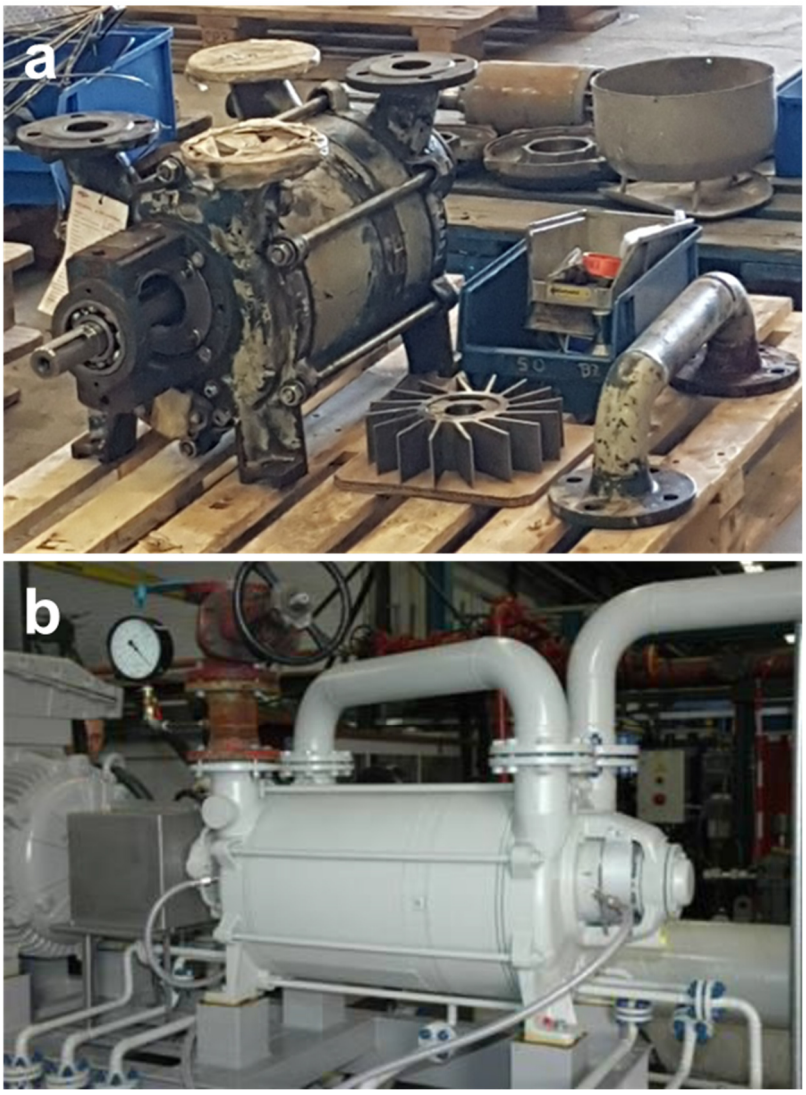

Figure 4.13. Pump O impeller (a) in the mechanical workshop pending to install and (b) already installed in the hydrocarbon plant.

Figure 4.14 shows a scheme of the plant. The pump O creates vacuum in the V-A tank, which is previously connected to the T-A tower. Pump O aspires gas phase of T-A and V-A and, at the same time, has an inlet of liquid ring (water) for its operation. T-A and

V-A are the final distillate tower/tank for the process product where the heavy fraction is removed from the bottom and the gases go through the head. These gases are aspirated by the vacuum pump O together with some incondensable part.

The aspirated gas phase is a mixture of incondensable (liquid + gas) from the process. The pump then sends the gas phase as low gas vent (goes out V-B per upper part) and the process liquid phase (goes out V-B per lower part).

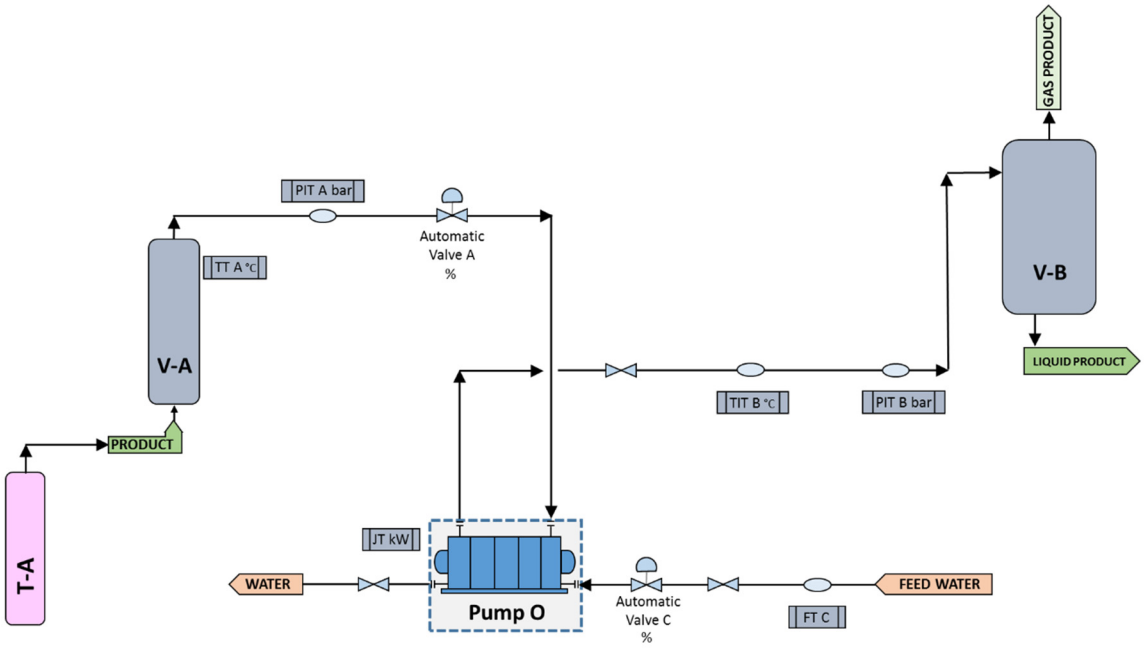

Figure 4.14. Work process flowchart at the Dow Chemical plant. The impeller was mounted in pump O. T-A: pump O aspiration tower, V-A: pump O aspiration vessel, V-B: product destination tank.

In this study, the process parameters were first collected using the original SIHI impeller during specific periods of time. Afterwards, the original impeller was substituted (on 16 June 2022) for the SLM, which was set to operate in identical operational conditions to compare its performance with that of the SIHI impeller. In both cases, a single product recipe was used corresponding to a hydrocarbon mixture. The process was remotely supervised from a control room that collects several process parameters such as process variables (pump power, product flow and pump pressure.

Figures 4.15 shows the results obtained with both impellers for the dependence of pump power on suction and exit pressure, with typical values between 11 and 12 kW. Similarly to the monitoring of pump current in the polyol process (see Chapter 3.9), the pump power

should remain constant since a decrease would indicate a malfunction of mechanical parts of the pump in which the impeller is located, indirectly measuring the performance of the pump throughout the process. The average values in all cases were around 11.5 kW with low standard deviations, indicating similar behaviour of both impellers.

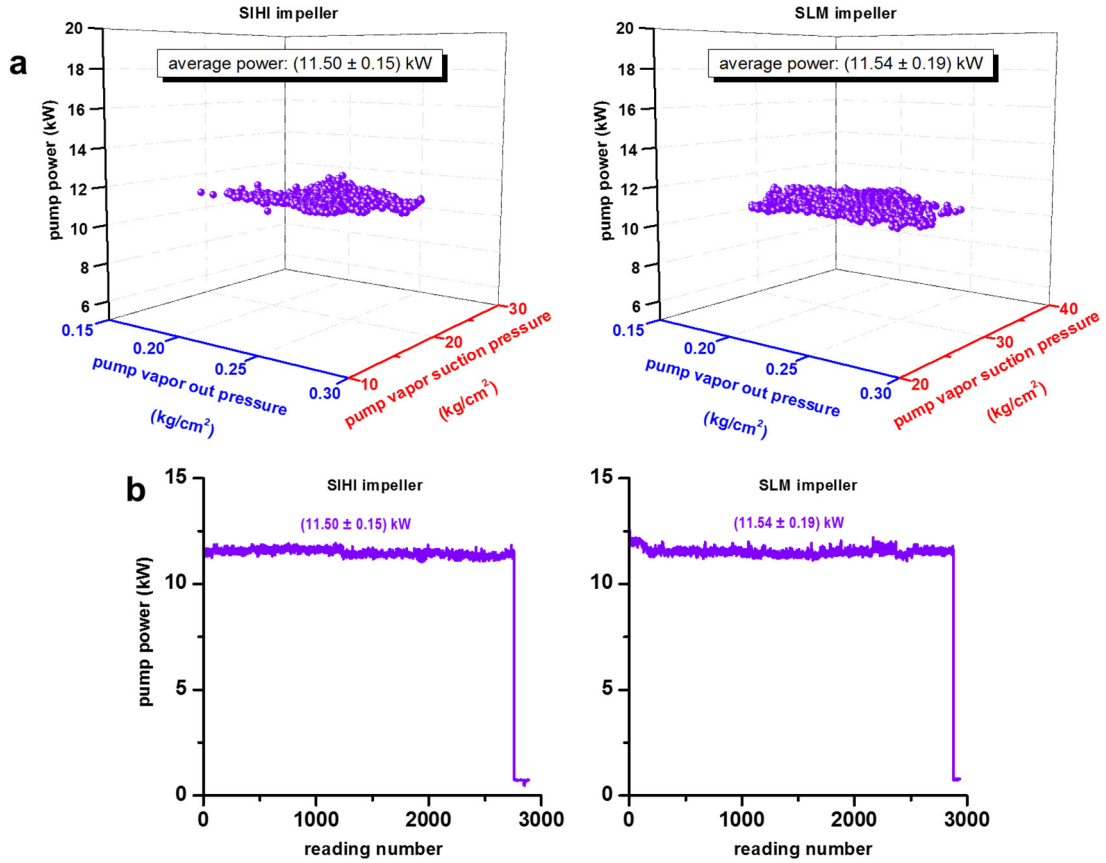

Figure 4.15. a) Dependence of pump power on pump suction and exit pressure for SIHI and SLM impellers, b) pump power raw data for SIHI and SLM impellers corresponding to ~2800 consecutive readings (~4 months of continuous operation).

On the other hand, panels a, b, c in Figures 4.16 show comparisons of the data obtained with both impellers for one typical production cycle. Results for Operations are 100% satisfactory having no clarification for the difference in vapor suction pressure and liquid ring flow. From operations point of view, no changes have been made. Discussion about with Rotating machinery experts justify the difference with small differences in montage (inside tolerances) of the impeller on the shaft that produce such not relevant changes for Operations. In the past they had similar values with another original SIHI impeller.

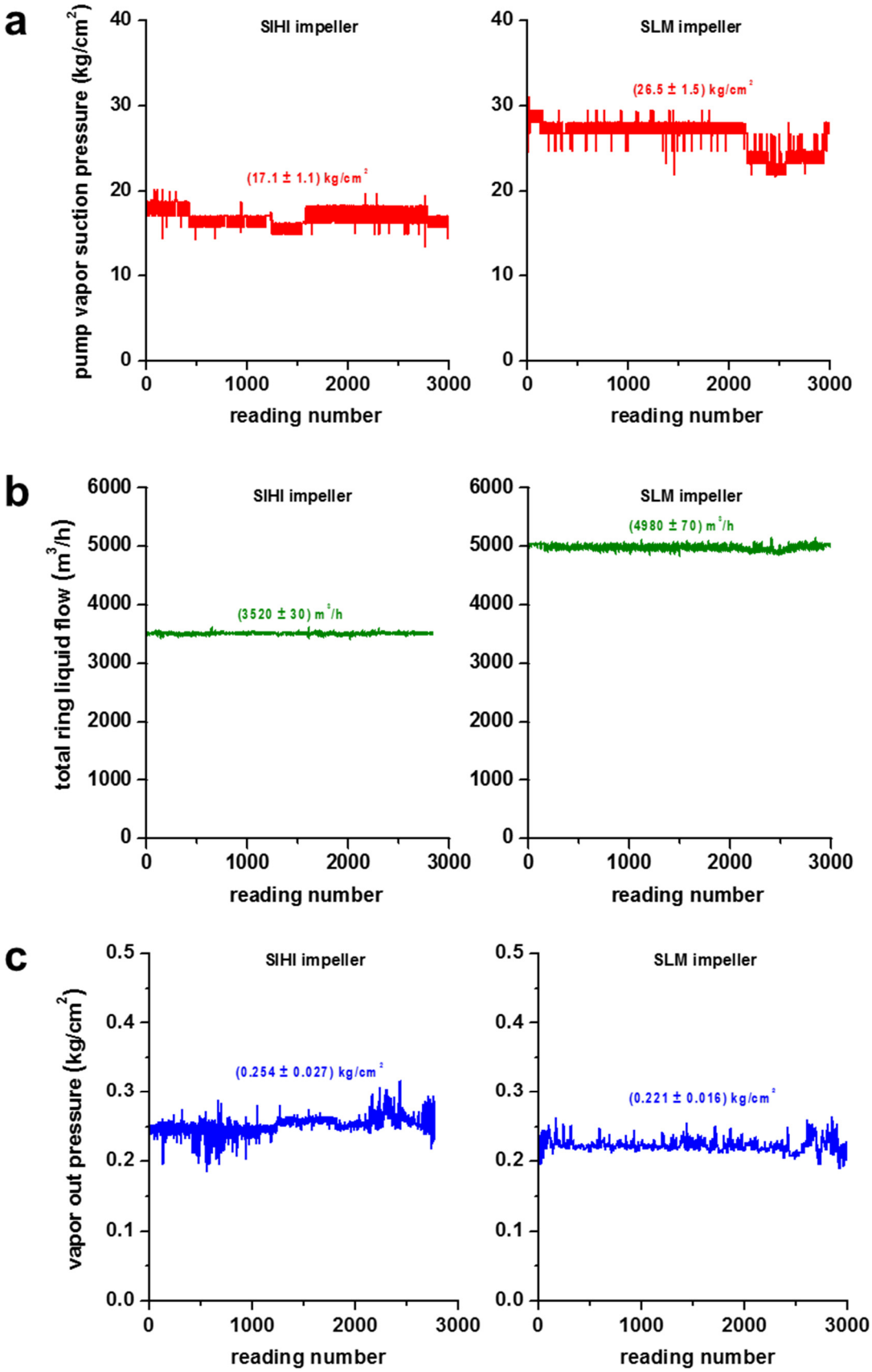

Figure 4.16. Comparison of performance data of SIHI and SLM impellers: a) pump vapor suction pressure, b) pump liquid ring flow, c) pump vapor out pressure.

Hence, the results obtained indicate that the performance of the SLM impeller was similar to that of the original SIHI impeller, demonstrating that the strategy of replacing the original part for a 3D printed copy manufactured using selective laser melting was technically validated, from a design/manufacture point of view to an operational/process point of view. This strategy has thus the advantage of saving the steps of mold printing and casting as in the case of the BJ impeller.

4.8. Economic evaluation of SLM impeller manufacture.

As in the case of the BJ impeller (Chapter 3.10), an economic evaluation is carried out of the manufacture of the new impeller using the SLM technique considering the two options next indicated.

Option 1 involves the calculation and economic balance in case the impellers are kept in stock - as spare part - in warehouse, while *Option 2* involved the economic balance in case the impellers 3D printed are not kept in stock in warehouse.

The results for both economic balance options are given below (Tables 4.2. and 4.3.):

Option 1: **Project economic balance *keeping* units in stock in warehouse**.

Table 4.2. Project economic balance summary for *Option 1* (keeping units in stock).

SIHI *vs*. first 3D impeller manufactured

Purchase order to SIHI manufacturer	
Purchase order (2 pieces)	4000
Total cost (€ / 1 impeller):	**2000**

3D manufactured 1st unit	
3D Development Cost - just once to pay (€)	6260
3D Manufacturing Print Cost (€/1 piece)	-1080
Material analysis - replica (€)	Included
Metallographic study (€)	Included
Impeller balancing (€)	Included
Shaft hole machining (approx. 2 h work) (€)	Included
Total cost (€ / 1 impeller):	**5180**

2nd and 3rd 3D impeller manufactured

3D manufactured 2nd unit	
3D Development Cost - just once to pay (€)	0
3D Manufacturing Print Cost (€/1 pieces)	1080
Material analysis - replica (€)	0
Metallographic study (€)	0
Impeller balancing (€)	0
Shaft hole machining (approx. 2 h work) (€)	0
Total cost (€ / 1 impeller)	**1080**

3D manufactured 3rd unit	
3D Development Cost - just once to pay (€)	0
3D Manufacturing Print Cost (€/1 pieces)	1080
Material analysis - replica (€)	0
Metallographic study (€)	0
Impeller balancing (€)	0
Shaft hole machining (approx. 2 h work) (€)	0
Total cost (€ / 1 impeller) *	**1134**

* Considering an estimated IPC of 5%t.

Total cost per impeller (€) ⇒	**1st unit**	**2nd unit**	**3rd unit**	**4th unit**
Purchase order to SIHI manufacturer	2000	2100*	2205*	2315*
Cumulative cost	2000	4100	6305	8620
3D manufactured units	5180	1080*	1134*	1190*
Cumulative cost	5180	6260	7394	8585

* Considering an estimated IPC of 5%.

The project economic balance keeping units in stock in warehouse indicate that the direct manufacturing of the impeller by 3D printing using SLM is economically profitable from the 4th manufactured unit – comparing with traditional method from SIHI manufacturer - taking into account the total cost invested from the first time study/evaluation and the total development work, but it is very interesting to mention that the 2nd unit is already profitable (cheaper than original SIHI impeller, 2.000 € versus 1.080 €), so making cheaper the initial investment with, for example, a bigger amount of spare parts to evaluate together, it would make much more profitable 3D printing material.

Option 2: **Project economic balance *not keeping* units in stock in warehouse**.

Table 4.3. Project economic balance summary for *Option 2* (not keeping units in stock).

Purchase order to SIHI manufacturer plus stocking costs	
Purchase order	2000
Cost of keeping stock for one year: 1.- Operational costs: Labour costs, maintenance facilities, salaries… 2.- Taxes 3.- Capital charge: a.- Use of inventory + Accounts receivable b.- Physical Assets (buildings, equipment's) c.- Intangible Assets (patents, intellectual property)	
25-30% costs items	550
Total cost (€ / 1 impeller):	**2550**

Project economic balance: 3D impeller manufacturing but none stocked.

3D manufactured 1st unit/year - non stocked	
3D Development Cost - just once to pay (€):	4100
3D Manufacturing Print Cost (€/1 pieces):	Included
Material analysis - replica (€)	Included
Metallographic study (€)	Included
Impeller balancing (€)	Included
Shaft hole machining (approx. 2 h work) (€)	Included
Cost of having stock (€)	0
Total cost (€ / 1 impeller):	**4100**

3D manufactured unit (only when needed it)	
3D Development Cost - just once to pay (€):	0
3D Manufacturing Print Cost (€/1 pieces):	1080
Material analysis - replica (€)	Included
Metallographic study (€)	Included
Impeller balancing (€)	Included
Shaft hole machining (approx. 2 h work) (€)	Included
Cost of having stock (€)	0
Total cost (€ / 1 impeller):	**1080**

* considering an estimated IPC of 5%.

Total cost per impeller (€) ⇒	**Year 1**	**Year 2**	**Year 3**	**Year 4**
Purchase order to KSB manufacturer - stocked	2550	550*	578*	2100*
Cumulative cost	2550	3100	3678	5778
3D manufactured units - non stocked	4100	0	0	1080
Cumulative cost	4100	4100	4100	5180

The results indicate that *Option 2* is economically profitable – comparing with traditional method from SIHI manufacturer - from the 2nd unit taking into account the total cost invested from the first time study/evaluation and total development work but making the 3D printing impeller just when you really need it in plant, not before. Additionally, it is interesting to indicate that 3D printing impeller fabrication (only the manufacture work) is cheaper than original SIHI impeller, cost 1.080 € versus cost 2.000 €.

As more expensive the original manufactured spare part is, the more profitable is the 3D printing project. These impellers have long life in pump. With 3D printing project you have not yet an impeller, because you do not need it really (not yet), and your investment has been 4.100€, the same up to the time you really need to have/print the impeller. There

is no cost increase with the time. With the SIHI impeller in stock, in traditional way, cost increase year by year as time goes by.

Estimation is done for a change impeller in year 4th.

4.9. Conclusions.

In this Chapter, we have presented the fabrication and performance study of a titanium alloy pump impeller manufactured by SLM – Selective Laser Melting - technology. The work is a further example of real application of metal additive manufacturing in a chemical plant with high critical components and environmental conditions around the pump in service. The 3D-printed part worked in severe operating conditions and is now an available real example that extends this technology to create complex features of original parts or replacement parts useful in the chemical industry. The main conclusions of the work can be summarized as follows:

- Reverse engineering of the original impeller was used to create a polyamide copy, used to validate the CAD design by metrological characterization, with a hight dimensional accuracy. Very accurate tolerance adjustments (0.025 to 0.05 mm) were obtained in all measurements. An extra 0.5 mm were added later for last step of impeller manufacture (machining and dimensional control) as per recommendation of the manufacturer for titanium alloys
- The metalic impeller was fabricated in titanium alloy (Ti6Al4V) as best option selected because the material of the original spare part (stainless steel 1.4027.05) is not yet available for additive manufacturing and SLM technology in particular.
- A total of 2056 layers of 60 μm thickness were needed for SLM fabrication, with a total manufacturing time of 40 hours, 37 minutes and 36 seconds, including a cold down of about 5 hours. The heater target temperature was 170°C and absence of oxygen, it was achieved with an argon flow of 190 m^3/h and a total of 60.3 kg of metal powder were needed. The powder packing density was 2.658 g/cm^3.
- The 3D-printed part had a weight of 2.990 kg, which is 43% lighter than the original.
- The operational performance of the produced impeller was tested in a real scenario by installing the impeller in a vacuum pump. The pump is operated in a hydrocarbon plant, and a series of process parameters (pump power, product flow and pump pressure) related to the pump behaviour were measured continuously and remotely supervised from a control room.

- Results obtained with both impellers (original one and 3D printed manufactured) for pump power on suction and exit pressure, were typical values between 11 and 12 kW. Pump power remained constant since a decrease would indicate a malfunction of mechanical parts of the pump in which the impeller is located, average values in all cases were around 11.5 kW with low standard deviations, indicating similar behaviour of both impellers.
- From an operational point of view, the performance results obtained indicate that the performance of the SLM impeller was similar to that of the original SIHI impeller, demonstrating that the strategy of replacing the original part by a 3D-printed copy manufactured using SLM was technically validated, from a design/manufacture point of view to an operational/process point of view.
- This strategy has also the advantage of saving the steps of mould printing and casting as in the case of the BJ impeller.
- The project economic balance for option 1 and option 2 ("keeping units in stock or not keeping units in stock") in warehouse indicate that the direct manufacturing of the impeller by 3D printing using SLM is economically profitable from the 4th manufactured unit – comparing with traditional method from SIHI manufacturer - taking into account the total cost invested from the first time study/evaluation and the total development work. It is especially interesting to mention that the 2nd unit is already profitable (~1000 € cheaper than original SIHI impeller) so reducing the initial investment with, for example, a bigger amount of spare parts to evaluate together would make this strategy much more profitable.

Therefore, this work demonstrated that the implementation of additive manufacturing technologies in chemical process engineering is a useful solution for fabricating spare parts of high added value that are difficult to replicate with other technologies, with consequent economic benefit.

Further work should focus on comparing the initial mechanical and morphological properties of the SLM impeller with those obtained after one year of operation in order to understand possible changes induced by the stress in material associated with continuous operation.

Chapter 5: Conclusions and future work

5.1. Conclusions and future work.

The Metal Additive Manufacturing (AM) Technology can be considered to be is in its birth or starting point from the perspective of industrial applications and worldwide massive divulgation. It is noteworthy that there are high hopes in the near future for this technology, expectations that range from a technological to an economical point of view. The emergence of additive manufacturing is renovating the landscape of available production technologies and these novel technologies have multiple different and potential uses. Among them, in the industrial field it can become an alternative to the process of materials purchasing and price negotiations, manufacturing obsolete (not anymore in the market) or new pieces and storage/custody of technical spare parts in many chemical industries.

The first part of this study has been focused on the application of additive manufacturing for the fabrication of a pump impeller (*Strategy 1)* using molds with additive technology 3D sand printing type BJ (Binder Jetting) plus a casting step for the manufacturing process.

The second part of this study has also been focused on the application of additive manufacturing in the fabrication of another type of pump impeller (*Strategy 2*) but by direct 3D printing (without molds and casting steps) using SLM (Selective Laser Melting), which is a '100%' metal printing technology.

The development of the present work (*Strategy 1* and *Strategy 2*) was based on the following steps: *design* - scanning, drawing and elaboration of constructive 3D plans -, *manufacturing*, pump assembly and commissioning of two different types of metallic impellers for use in pumps P and O with the consequent *analysis of the results* and work data once both pumps have been assembled and *put into operation* in chemical plants for a minimum of 4 months in service. Finally, a *comparison* has been done under normal operating conditions with the same previous service and with the same type of metal impellers but manufactured in a conventional way and hence evaluating *additive vs. conventional* manufacturing methods. In both cases, economic assessments of the implementation of AM technology were done.

On *Strategy 1* we described the fabrication and results of a closed vane pump impeller (ϕ 206 mm, height 68 mm, weight 4 kg) by binder jetting (BJ) 3D printing of a sand mould followed by a casting process using stainless steel 316 to create an identical copy of a part in service in a chemical plant in Tarragona, Spain. The original part from manufacturer KSB was reverse engineered and used to create a sand mould by BJ 3D printing on which new impellers were fabricated by casting. Metallographic studies showed an austenitic matrix with 6.3% of ferritic phase and 40 μm × 8 μm ferrite grains without precipitated carbides. The operational performance of the produced impeller was tested in a real scenario by installing the impeller in a centrifugal pump. The impeller was put into operation in a centrifugal pump at a polyol/polyglycol plant belonging to Dow Chemical Ibérica SL for 6 months from October 2020 to April 2021. Process variables related to the pump behavior were compared with the same variables obtained in previous cycles with the original impeller for three different product concentrations and viscosities. Several monitored parameters (current consumption, pump pressure, product flow and tank level) were similar in both cases, validating the fabrication strategy from an operational point of view. This indicated that both impellers had equivalent performance, thus validating the fabrication strategy of combining additively manufactured sand mould with casting from an operational point of view.

Regarding *Strategy 2*, we described the fabrication and performance results of an open pump impeller (ø 230 mm, height 60 mm, original weight 5.247 kg) using Selective Laser Melting 3D printing technology in Ti6Al4V titanium alloy with the aim to create an identical copy of a part in service at a chemical plant in Tarragona, Spain. The original impeller (from Flowserve SIHI) was made on stainless steel 1.4027.05 but this material is not yet available for AM technology and was thus reverse engineered and used to create a 3D digitized CAD drawing from which the new SLM impellers were manufactured. For the SLM impeller fabrication was needed a total of 2056 layers of 60 μm thickness, a total manufacturing time of over 40 hours. The printed impeller had a final weight 43% lighter than the original stainless steel part. The operational performance of the produced impeller was tested in a real scenario by installing the 3D-printed impeller in a centrifugal pump used to operate under vacuum in a hydrocarbon plant of Dow Chemical Ibérica SL from June 16, 2022 to October 2022 during roughly 4 months. The process variables (pump power, product flow and pump pressure) related to the behavior of the pump were compared with the same variables obtained in previous cycles with the original SIHI

impeller. The pump power remained constant throughout the process with typical values between 11 and 12 kW with average values in all cases around 11.5 kW with low standard deviations, indicating similar behaviour of both impellers. In general, the results obtained indicate that the performance of the SLM impeller was similar to that of the original SIHI impeller from an operational point of view, also demonstrating that the strategy of replacing the original part for a metal 3D printed copy directly manufactured using selective laser melting can be technically validated from design to operation. This strategy has thus the advantage of saving the steps (and, consequently, save time as well) of mould printing and casting process as in the case of the BJ impeller.

Regarding the economic balance for both strategies, we found that the two studied options involving keeping and not keeping units in stock in warehouse for both strategies (*strategy 1* and *strategy 2*) suggest that the manufacturing of the impeller by 3D printing using either BJ or SLM was economically profitable in both cases as compared with traditional method used by KSB or SIHI manufacturers. The balance took into account the total cost invested from the initial study/evaluation and the total development/manufacture work. Especially interesting is to mention that the 2nd unit should be already profitable (cheaper than the original) by about 900€ (3250€ *vs*. 2.312€ for BJ, 2000€ *vs*. 1.080€ for SLM). Hence making a cheaper initial investment with, for example, a bigger amount of spare parts to evaluate together, it would make the employed additive manufacturing technologies much more profitable.

Future work

The promising results obtained in this work are expected to represent starting point in the large scale implementation of AM in the chemical industry. Further work should focus on comparing the initial mechanical and morphological properties of the BJ impeller and SLM impeller with those obtained after one year of operation in order to understand possible changes induced in the materials such as stress/fatigue properties associated with continuous operation.

In addition, a logical further step would thus involve the fabrication of an impeller or any other metallic part by direct 3D printing for use in several plants around the world so that metal additive manufacturing technologies can be validated in the chemical industry at a wider scale.

References

Ahmed A., Boban J., Improving the surface integrity and mechanical properties of additive manufactured stainless steel components by wire electrical discharge polishing. Journal of Materials Processing Tech. 291 (2021) 117013.

Alvarez B. J., Cuesta E., Giganto S., Barreiro J., Martínez-Pellitero S., Meana V., Laser line scanner aptitude for the measurement of Selective Laser Melting parts. Optics and Lasers in Engineering 138 (2021) 106406.

Ameloot R., Parra-Cabrera C., Achile C., Kuhn S., 3D printing in chemical engineering and catalytic technology: Structured catalysts, mixers and reactors. Chemical Society Reviews Open AccessVolume 47, Issue 1, Pages 209 - 2307 January 2018.

Andres N. S., Development of Solar-Powered Water Pump with 3D Printed Impeller. De Gruyter Open Eng. 2021; 11:249–253 https://doi.org/10.1515/eng-2021-0015.

Astafurov, S.; Astafurova, E. Phase Composition of Austenitic Stainless Steels in Additive Manufacturing: A Review. Metals 2021, 11, 1052.

Bandyopadhyay, A.; Zhang, Y.; Bose, S. Recent developments in metal additive manufacturing. Curr. Opin. Chem. Eng. 2020, 28, 96–104.

Belka, M.; Bączek, T. Additive manufacturing and related technologies—The source of chemically active materials in separation science. Trends Anal. Chem. 2021, 142, 116322.

Bhuvanesh Kumar M., Sathiya P., Methods and materials for additive manufacturing: A critical review on advancements and challenges. Thin–Walled Structures 159 (2021) 107228.

Cai D., Mao Y., Li J., Li W., Wei Q., Binder jetting additive manufacturing of 316L stainless-steel green parts with high strength and low binder content: Binder preparation and process optimization. Journal of Materials Processing Tech. 291 (2021) 117020. https://doi.org/10.1016/j.jmatprotec.2020.117020.

Čantrak D. S., Janković N. Z., Ilić D. B., Lečić M. R., Centrifugal pumps' impellers design and digital fabrication. Authorized licensed use limited to: UNIVERSITAT ROVIRA I VIRGILI. Downloaded on February 25,2021 at 20:15:26 UTC from IEEE Xplore. Restrictions apply. Project No. TR 35046, what is gratefully acknowledged.

Printrbot was acquired through the project US Federal Grant SRB100-15-GR-364 what is also acknowledged.

Cimpoes N., Baciu E., Cimpoes,u R., Vit,alariu A., Baciu C., Sodor A., Zegan G., Murariu A., Surface Analysis of 3D (SLM) Co–Cr–W Dental Metallic Materials. MDPI Appl. Sci. 2021, 11, 255. https://doi.org/10.3390/app11010255.

Cosma C., Drstvensek I, Berce P., Prunean S., Legutko S., Popa C and Balc N. Physical–Mechanical Characteristics and Microstructure of Ti6Al7Nb Lattice Structures Manufactured by Selective Laser Melting. MDPI Materials. Materials 2020, 13, 4123; doi:10.3390/ma13184123 ww.mdpi.com/journal/materials.

Che X., Jiang X., Tian Ch., Zhu X., Zhou G., Chen L., Li J., Preparation of 304 Stainless Steel Powder for 3D Printing by Vacuum-Induced Multistage Atomization. Frontiers in materials. ORIGINAL RESEARCH published: 13 January 2021 doi: 10.3389/fmats.2020.623864.

Chen, C.; Mehl, B.; Munshi, A.; Townsend, A.; Spence, D.; Martin, R. 3D-printed microfluidic devices: Fabrication, advantages and limitations—A mini review. Anal. Meth. 2016, 8, 6005–6012.

Chen X., Meng A., Nie J., Gu L., Mao Q., Zhao Y., Microstructure evolution and mechanical properties of commercial pure titanium subjected to rotary swaging. Journal of Alloys and Compounds 859 (2021) 158222.

Chen Z., Wang P., Huang H., Liu J., Liu Q., Microstructure and mechanical properties of Ti6Al4V/AA6061/AZ31 laminated metal composites (LMCs) fabricated by hot roll bonding. Journal of Alloys and Compounds 861 (2021) 157943.

Deng, C.; Kang, J.; Shangguan, H.; Hu, Y.; Huang, T.; Liu, Z. Effects of hollow structures in sand mold manufactured using 3D printing technology. J. Mater. Process. Technol. 2018, 255, 516–523.

Deng S., Dong D., Chang Ch., Wang H., Yan X., Ma W., Liu M., Gardan J., Bolot R., Liao H., Selective laser melting (SLM) of CX stainless steel: Theoretical calculation, process optimization and strengthening mechanism. Journal of Materials Science & Technology 73 (2021) 151–164.

Designation: F2792 − 12a Standard Terminology for Additive Manufacturing Technologies. Copyright © ASTM International, 100 Barr Harbor Drive, PO Box C700,

West Conshohocken, PA 19428-2959. United States. Copyright by ASTM Int'l (all rights reserved); Mon Sep 9 17:52:47 EDT 2013.

Díaz del Castillo Rodríguez F., Materiales y sus propiedades. Facultad de estudios superiores cuautitlán departamento de ingeniería. Laboratorio de tecnología de materiales. Cuautitlán Izcalli 2008.

Dong A., Wang D., Zhu G., Shu D., Sun J., Li F., Sun B., Rapid casting of complex impeller based on 3D printing wax pattern and simulation optimization. The International Journal of Advanced Manufacturing Technology (2019) 100:2629–2635. https://doi.org/10.1007/s00170-018-2736-9.

Fatemi A., Sanaei N., Defect-based fatigue life prediction of L-PBF additive manufactured metals. Engineering Fracture Mechanics 244 (2021) 107541.

Femmer, T.; Flack, I.; Wessling, M. Additive Manufacturing in Fluid Process Engineering. Chem. Ing. Tech. 2016, 88, 535–552.

Fernandez-Abia A. I., Rodriguez-Gonzalez P., Castro-Sastre M. A., Barreiro J., Heat treatments for improved quality binder jetted molds for casting aluminum alloys. Additive Manufacturing 36 (2020) 101524.

Frazier W. E., Metal Additive Manufacturing: A Review. JMEPEG (2014) 23:1917–1928 _ASM International DOI: 10.1007/s11665-014-0958-z.

Galindo M. Fabricación aditiva / Impresión 3D: Procesos con metales y cerámicos. Industrial design and engineering department at Leitat Technological Center – Industrial design and technology 2016 – Terrasa (Barcelona – Spain).

Gal-Or, E.; Gershoni, Y.; Scotti, G.; Nilsson, S.; Saarinen, J.; Jokinen, V.; Strachan, C.; Boije af Gennäs, G.; Yli-Kauhaluoma, J.; Kotiaho, T. Chemical analysis using 3D printed glass microfluidics. Anal. Meth. 2019, 11, 1802–1810.

Gao, W.; Zhang, Y.; Ramanujan, D.; Ramani, K.; Chen, Y.; Williams, C.; Wang, C.; Shin, Y.; Zhang, S.; Zavattieri, P. The status, challenges, and future of additive manufacturing in engineering. Comput. Aided Des. 2015, 69, 65–89.

Gill, S.; Kaplas, M. Comparative Study of 3D Printing Technologies for Rapid Casting of Aluminium Alloy. Mater. Manuf. Proc. 2009, 24, 1405–1411.

Gill, S.S.; Kaplas, M. Efficacy of powder-based three-dimensional printing (3DP) technologies for rapid casting of light alloys. Int. J. Adv. Manuf. Technol. 2011, 52, 53–64.

Gyak, K.; Vishwakarma, N.; Hwang, Y.; Kim, J.; Yun, H.; Kim, D. 3D-printed monolithic SiCN ceramic microreactors from a photocurable preceramic resin for the high temperature ammonia cracking process. React. Chem. Eng. 2019, 4, 1393–1399.

Harvey A. L., 3-D Printing: The Future of Manufacturing and Maintenance. Wright's Media at 877.652.5295 or visit our website at www.wrightsmedia.com. www.powermag.com POWER | May 2017.

Haghdadi N., Laleh M., Moyle M., Primig S., Additive manufacturing of steels: a review of achievements and challenges https://doi.org/10.1007/s10853-020-05109-0J Mater Sci (2021) 56:64–107.

Hedberg Y. S., Atapour M., Wang X., Persson M., Odnevall Wallinder I., Corrosion of Binder Jetting Additively Manufactured 316L Stainless Steel of Different Surface Finish. Journal of The Electrochemical Society, 2020 167 131503.

Hernández F., Intranet info at Dow Chemical – TES Maintenance Technology Center -. Web consulted on 22 August 2022

Herzog D., Seyda V., Wycisk E., Emmelmann C., Additive manufacturing of metals. Acta Materialia 117 (2016) 371e392.

Hock, S.; Rose, M. 3D□Structured Monoliths of Nanoporous Polymers by Additive Manufacturing. Chem. Ing. Tech. 2020, 92, 525–531.

Hoon Kang S., Suh J., Yeob Lim S., Jung S., Woon Jang Y., Soo Jun I., Additive manufacture of 3 inch nuclear safety class 1 valve by laser directed energy deposition. Journal of Nuclear Materials 547 (2021) 152812.

Huang P. W., Wu S. T., Chang T. W., Jiang I. H. Tsai M. Ch., Application of Magnetic Metal 3-D Printing on the Integration of Axial-Flow Impeller Fan Motor Design. IEEE TRANSACTIONS ON MAGNETICS, VOL. 57, NO. 2, FEBRUARY 2021 8201205.

Kam Liu W., Kafka O. L., Jones K. K., Yu Ch., Cheng P., Image-based multiscale modeling with spatially varying microstructures from experiments: Demonstration with

additively manufactured metal in fatigue and fracture. J. Mech. Phys. Solids 150 (2021) 104350.

Kang S. H., Suh J., Lim S. Y., Jung S., Jang Y. W., Additive manufacture of 3 inch nuclear safety class 1 valve by laser directed energy deposition. Journal of Nuclear Materials 547 (2021) 152812.

Khalajzadeh, V.; Beckermann, C. Simulation of Shrinkage Porosity Formation During Alloy Solidification. Metall. Mater. Trans. A 2020, 51, 2239–2254.

Kladovasilakis, N.; Kontodina, T.; Charalampous, P.; Kostavelis, I.; Tzetzis, D.; Tzovaras, D. A case study on 3D scanning, digital reparation and rapid metal additive manufacturing of a centrifugal impeller. IOP Conf. Ser. Mat. Sci. Eng. 2021, 1037, 012018.

Kotz, F.; Risch, P.; Helmer, D.; Rapp, B. High□Performance Materials for 3D Printing in Chemical Synthesis Applications. Adv. Mater. 2019, 31, 1805982.

Kulikov A., Sidorova A. V., Balanovskiy A. E. Process Design for the Wire Arc Additive Manufacturing of a Compressor Impeller. RusMetalCon 2020 IOP Conf. Series: Materials Science and Engineering 969 (2020) 012098 IOP Publishing doi:10.1088/1757-899X/969/1/012098.

Kumar Das A., Anand M., Issues in fabrication of 3D components through DMLS Technique: A review. Optics & Laser Technology 139 (2021) 106914.

Li J., Sun J., Wang X., Shu D., Wang S., Peng P., Mao Q., Liu T., Lu X., Li Y., Zhu D., Wang G., Qin W., Enhanced mechanical properties of ultrafine-lamella 304L stainless steel processed by multidirectional hot forging. Vacuum 187 (2021) 110116.

Li H., Liu Yongsheng, Liu Yangsong, Zeng Q., Liang J., Silica strengthened alumina ceramic cores prepared by 3D printing. Journal of the European Ceramic Society 41 (2021) 2938-2947.

Ligon, S.; Liska, R.; Stampfl, J.; Gurr, M.; Mülhaupt, R. Polymers for 3D Printing and Customized Additive Manufacturing. Chem. Rev. 2017, 117, 10212–10290.

Lipton J. I., Cutler M., Nigl F., Cohen D., Lipson H., Additive manufacturing for the food industry. Trends in Food Science & Technology, Volume 43, Issue 1, May 2015, Pages 114-123 - https://doi.org/10.1016/j.tifs.2015.02.004.

Liu Y., Li H., Liu Y., Zeng Q., Liang J., Silica strengthened alumina ceramic cores prepared by 3D printing. Journal of the European Ceramic Society 41 (2021) 2938–2947.

Lynch, P.; Hasbrouck, C.R.; Wilck, J.; Kay, M.; Manogharan, G. Challenges and opportunities to integrate the oldest and newest manufacturing processes: Metal casting and additive manufacturing, Rapid Prototyp. J. 2020, 26, 1145–1154.

Mathew M. T., Morris D., Kumar Mamidi S., Kamat S., Cheng K., Bijukumar D., Tsai P., Wu P., Espinoza Orías A. A., Mechanical, Electrochemical and Biological Behavior of 3D Printed□Porous Titanium for Biomedical Applications. Journal of Bio- and Tribo-Corrosion (2021) 7:39. https://doi.org/10.1007/s40735-020-00457-5.

Mahmoud D., Al-Rubaie K. S., Elbestawi M. A., The influence of selective laser melting defects on the fatigue properties of Ti6Al4V porosity graded gyroids for bone implants. International Journal of Mechanical Sciences 193 (2021) 106180.

Maier, M.; Lebl, R.; Sulzer, P.; Lechner, J.; Mayr, T.; Zadravec, M.; Slama, E.; Pfanner, S.; Schmölzer, C.; Pöchlauer, P.; et al. Development of customized 3D printed stainless steel reactors with inline oxygen sensors for aerobic oxidation of Grignard reagents in continuous flow. React. Chem. Eng. 2019, 4, 393–401.

Manogharan G., Reddy Sama S., Badamo T., Case studies on integrating 3d sand-printing technology into the production portfolio of a sand-casting foundry. American Foundry Society https://doi.org/10.1007/s40962-019-00340-1 International Journal of Metalcasting/Volume 14, Issue 1, 2020.

Martinez, D.; Bate, C.; Manogharan, G. Towards Functionally Graded Sand Molds for Metal Casting: Engineering Thermo-mechanical Properties Using 3D Sand Printing. JOM 2020, 72, 1340–1354.

Mitchell, A.; Lafont, U.; Hołyńska, M.; Semprimoschnig, C. Additive Manufacturing—A Review of 4D Printing and Future Applications. Addit. Manuf. 2018, 24, 606–626.

Mitra, S.; EL Mansori, M.; Rodríguez de Castro, A.; Costin, M. Study of the evolution of transport properties induced by additive processing sand mold using X-ray computed tomography. J. Mater. Process. Technol. 2020, 277, 116495.

Mitrík L., Hudák R., Schnitzer M., Orságová Králová Z., Gorejová R., Rajťúková V., Tóth T., Kovaˇcevi´c M., Rizni M. Oriˇnaková R. and Živˇcák J. Additive Manufacturing of Porous Ti6Al4V Alloy: Geometry Analysis and Mechanical Properties Testing. MDPI

Applied Sciences. Appl. Sci. 2021, 11, 2611. https://doi.org/10.3390/app11062611 https://www.mdpi.com/journal/applsci.

Miyanaji H., Moshiur Rahman K., Da M., Williams C. B., Effect of fine powder particles on quality of binder jetting parts. Additive Manufacturing 36 (2020) 101587.

Morris D., Kumar Mamidi S., Kamat S., Cheng K., Bijukumar D., Tsai P., Wu M., Espinoza Orías A., Mathew M., Mechanical, Electrochemical and Biological Behavior of 3D Printed Porous Titanium for Biomedical Applications. Journal of Bio- and Tribo-Corrosion (2021) https://doi.org/10.1007/s40735-020-00457-5.

Mostafaei, A.; Elliott, A.; Barnes, J.; Li, F.; Tan, W.; Cramer, C.; Nandwana, P.; Chmielus, M. Binder jet 3D printing—Process parameters, materials, properties, modeling, and challenges. Prog. Mater. Sci. 2021, 119, 100707.

Nishida M., Negishi T., Sakota D., Kosaka R., Maruyama O., Hyakutake T., Kuwana K., Yamane T., Properties of a monopivot centrifugal blood pump manufactured by 3D printing. Artif Organs (2016) 19:322–329. DOI 10.1007/s10047-016-0914-9.

Pagone, E.; Saxena, P.; Papanikolaou, M.; Salonitis, K.; Jolly, M. Sustainability Assessment of Rapid Sand Mold Making Using Multi-criteria Decision-Making Mapping. In Sustainable Design and Manufacturing 2020. Smart Innovation, Systems and Technologies. Scholz, S.G., Howlett, R.J., Setchi, R., Eds.; Springer: Singapore, 2021; Volume 200, pp 345–355.

Pauzon C., Dietrich K., Forêt P., Hryha E., Witt G., Mitigating oxygen pick-up during laser powder bed fusion of Ti-6Al-4V by limiting heat accumulation. Materials Letters 288 (2021) 129365.

Ponticelli, G.; Tagliaferri, F.; Venettacci, S.; Horn, M.; Giannini, O.; Guarino, S. Re-Engineering of an Impeller for Submersible Electric Pump to be Produced by Selective Laser Melting. Appl. Sci. 2021, 11, 7375.

Pumera M., Manzanares Palenzuela C., (Bio)Analytical chemistry enabled by 3D printing: Sensors and biosensors. TrAC - Trends in Analytical Chemistry Volume 103, Pages 110 - 118June 2018.

Quail F. J., Scanlon T., Strickland M., Development of a regenerative pump impeller using rapid manufacturing techniques. Rapid Prototyping Journal. www.emeraldinsight.com/1355-2546.htm.

Redwood B., Schöffer F., Garret B. 3D_Printing_The_Definitive_Guide - The 3D Printing Handbook -Technologies, design and applications. 3D Hubs. Consulted on Feb-17th, 2021: https://www.3dhubs.com/guides/3d-printing/.

Redwood B., Schöffer F., Garret B. The 3D Printing Handbook: Technologies design and applications. 3D Hubs B.V. 2017. Amsterdam, The Netherlands. Edición de Kindle.

Ritter S., Formnext: AM Field Guide – Mesago Messe. ISBN 978-3-9820318-0-4. Oktober 2018 Reutlingen University Frankfurt am Main.

Romero L., Jiménez M., Dominguez I. A., Espinosa K., Dominguez M., Additive Manufacturing Technologies: An Overview about 3D Printing Methods and Future Prospects. Hindawi Complexity Volume 2019, Article ID 9656938, 30 pages. https://doi.org/10.1155/2019/9656938.

Sama, S.; Badamo, T.; Lynch, P.; Manogharan, G. Novel sprue designs in metal casting via 3D sand-printing. Addit. Manuf. 2019, 25, 563-578.

Sama, S.; Badamo, T.; Manogharan, G. Case Studies on Integrating 3D Sand-Printing Technology into the Production Portfolio of a Sand-Casting Foundry. Int. J. Metalcast. 2019, 14, 12-24.

Scime, L.; Beuth, J. Using machine learning to identify in-situ melt pool signatures indicative of flaw formation in a laser powder bed fusion additive manufacturing process. Addit. Manuf. 2019, 25, 151–165.

Senvol - Materials search. Consulted on Feb-20th, 2021: http://senvol.com/material-search/

Service provider. Consulted on Feb-20th, 2021: http://additivemanufacturing.com/am-service-provider/

Shakil, S.; Smith, N.; Yoder, S.; Ross, B.; Alvarado, D.; Hadadzadeh, A.; Haghshenas, M. Post fabrication thermomechanical processing of additive manufactured metals: A review. J. Manuf. Proc. 2022, 73, 757–790.

Shangguan, H.; Kang, J.; Deng, C.; Hu, Y.; Huang, T. 3D-printed shell-truss sand mold for aluminum castings. J. Mater. Proc. Technol. 2017, 250, 247–253.

Shangguan, H.; Kang, J.; Yi, J.; Deng, C.; Hu, Y.; Huang, T. Controlled cooling of an aluminum alloy casting based on 3D printed rib reinforced shell mold. China Foundry 2018, 15, 210–215.

Sharon Nai M. L., Kumar Meenashisundaram G., Xu Z., Lu S., Sheuan Ten J., Wei J., Binder Jetting Additive Manufacturing of High. Porosity 316L Stainless Steel Metal Foams. Materials 2020, 13, 3744; doi: 10.3390/ma13173744 www.mdpi.com/journal/materials.

Shi T., Cheng D., Zhang J., Li G., Shi J., Lu L., Fu G., Microstructure and mechanical properties of additive manufactured Ti-6Al-4V components by annular laser metal deposition in a semi-open environment. Optics & Laser Technology 135 (2021) 106640.

Sivarupan, T.; Balasubramani, N.; Saxena, P.; Nagarajan, D.; El Mansori, M.; Salonitis, K.; Jolly, M.; Dargusch, M. A review on the progress and challenges of binder jet 3D printing of sand molds for advanced casting. Addit. Manuf. 2021, 40, 101889. https://doi.org/10.1016/j.addma.2021.101889

Snelling, D.; Li, Q.; Meisel, N.; Willaims, C.B.; Batra, R.C.; Druschitz, A.P. Lightweight metal cellular structures fabricated via 3D printing of sand cast molds. Adv. Eng. Mater. 2015, 17, 923–932.

Sun G. F., Wang Z. D., Lu Y., Chen M. Z., Lan H. F., Bi K. D., Ni Z. H., High-performance Ti-6Al-4V with graded microstructure and superior properties fabricated by powder feeding underwater laser metal deposition. Surface & Coatings Technology 408 (2021) 126778.

Sundaram, D.; Svidró, J.T.; Svidró, J.; Diószegi, A. On the Relation between the Gas-Permeability and the Pore Characteristics of Furan Sand. Materials 2021, 14, 3803.

Talamona D., Mukhtarkhanov M., Perveen A., Application of Stereolithography Based 3D Printing Technology in Investment Casting. MDPI Micromachines 2020, 11, 946; doi:10.3390/mi11100946 www.mdpi.com/journal/micromachines.

Vaezi M., Drescher P., Seitz H., Beamless Metal Additive Manufacturing. Consulted on Feb-20th, 2021: www.mdpi.com/journal/materials. Materials 2020, 13, 922; doi:10.3390/ma13040922.

Vafadar A., Guzzomi F., Rassau A., Hayward K., Advances in Metal Additive Manufacturing: A Review of Common Processes, Industrial Applications, and Current Challenges. Appl. Sci. 2021, 11, 1213. https://doi.org/10.3390/app11031213

Valdes A. What Is 3D Printing and How Does It Work? | Mashable Explains. Consulted on Feb-21st, 2021: https://www.youtube.com/watch?v=Vx0Z6LplaMU.

Vander Voort, G.; Lucas, G.; Manilova, E. Metallography and Microstructures of Stainless Steels and Maraging Steels. In Metallography and Microstructures; ASM International: Materials Park, OH, USA, 2004; pp. 670–700.

Vitalariu A., Baciu E., Cimpoes,u R., Baciu C., Cimpoes,u N., Sodor A., Zegan G. and Murariu A. Surface Analysis of 3D (SLM) Co–Cr–W Dental Metallic Materials. MDPI Applied Science. Appl. Sci. 2021, 11, 255. https://doi.org/10.3390/app11010255 https://www.mdpi.com/journal/applsci.

Vora, H.D.; Sanyal, S. A comprehensive review: Metrology in additive manufacturing and 3D printing technology. Prog. Addit. Manuf. 2020, 5, 319–353.

Warzocha K., Szura J., Ba¸k P., Rzucidło P. and Rogalski T. Transformative Use of Additive Technology in Design and Manufacture of Hydraulic Actuator for Fly-by-Wire System. MDPI Applied Sciences. Appl. Sci. 2021, 11, 4772. https://doi.org/10.3390/app11114772 https://www.mdpi.com/journal/applsci.

Wei Ch., Zhang Z., Cheng D., Sun S., Zhu M., Li L., An overview of laser-based multiple metallic material additive manufacturing: from macro- to micro-scales. International Journal of Extreme Manufacturing. (2021) 012003 (24pp) https://doi.org/10.1088/2631-7990/abce04

Wohlers, T. Wohlers Report 2020: Additive Manufacturing and 3D Printing, State of the Industry; Wohlers Associates: Fort Collins, CO, USA, 2020, Wohlers Associates, Inc.970-225-0086. Consulted on Feb-20th, 2021: https://wohlersassociates.com/press82.html

Wohlers, T.; Campbell, I.; Diegel, O.; Huff, R.; Kowen, J. 3D Printing and Additive Manufacturing State of the Industry: Annual Worldwide Progress Report; Lund University: Lund, Sweden, 2017.

Wohlers, T.; Campbell, I.; Diegel, O.; Huff, R.; Kowen, J. Wohles Report 2020. Additive Manufacturing and 3D Printing, State of the Industry; Wohlers Associates: Fort Collins, CO, USA, 2020.

Zentel, K.; Fassbender, M.; Pauer, W.; Luinstra, G. 3D printing as chemical reaction engineering booster. Adv. Polym. React. Eng. 2020, 56, 97–137.

Zhang Y., Li X., He L., Ma Ch., Liu X., Mao Y., Research for Process on Investment Casting of Impeller Based on 3D Printing. IOP Conf. Series: Earth and Environmental Science 332 (2019) 042047. doi:10.1088/1755-1315/332/4/042047.

ZHANG Y., LI X. Y., ZHANG L. Y., RONG B. S., Hu Q. CAI, ZHU R. F., XU Y., Simulation and Optimization for Investment Casting of Impeller Based on 3D Printing. IOP Conf. Series: Earth and Environmental Science 186 (2018) 012016. doi :10.1088/1755-1315/186/5/012016.

Zhao, L.; Zeng, G.; Gu, Y.; Tang, Z.; Wang, G.; Tang, T.; Shan, Y.; Sun, Y. Nature inspired fractal tree-like photobioreactor via 3D printing for CO2 capture by microaglae. Chem. Eng. Sci. 2019, 193, 6–14.

Zheng, J.; Chen, A.; Zheng, W.; Zhou, X.; Bai, B.; Wu, J.; Ling, W.; Ma, H.; Wang, W. Effectiveness analysis of resources consumption, environmental impact and production efficiency in traditional manufacturing using new technologies: Case from sand casting. Energy Convers. Manag. 2020, 209, 112671.

Zhou C., Zhang F., Wei M., Viswanathan V., Swart B., Shao Y., Wu G., 3D printing technologies for electrochemical energy storage. Nano Energy Volume 40, Pages 418 - 431October 2017.

Zhu, J.; Wu, P.; Chao, Y.; Yu, J.; Zhu, W.; Liu, Z.; Xu, C. Recent advances in 3D printing for catalytic applications. Chem. Eng. J. 2022, 433, 134341.

WEB´s:

Web: https://www.3dnatives.com/es/inyeccion-aglutinante-te-lo-contamos-23032016/. Consulted on February 2020.

Web: AM Metal landscape. www.am-power.de. Version V5.0 Consulted on February 2020. Source Leitat 2021.

Web: Https://www.voxeljet.com Consulted on April 2020.

Web: AM Polymer landscape. www.am-power.de. Version V5.0 Consulted on July 2020. Source Leitat 2021. Consulted on Feb-20th, 2021.

Web: Stratasys: Background to 3D printing: What is 3D Printing? The Definitive Guide to Additive Manufacturing. Consulted on Feb-20th, 2021: https://www.stratasysdirect.com/manufacturing-services/3d-printing?resources=bb8d0914-1d4e-46d6-9ea5-1b1aefd5991c.

Web: https://www.makeitfrom.com/material-properties/EN-1.4408-GX5CrNiMo19-11-2-Cast-Stainless-Steel Consulted on March-23rd 2021.

Web: acero-inoxidable-alta-resistencia-austenitico-castinox: https://www.castinox.net/materiales/acero-inoxidable/aceros-austeniticos/ Pdf document and Web page consulted on march-23rd 2021.

Web: https://www.gom.com/en/products/3d-measuring-machines/atos-scanbox-series-4 Web page consulted on march-26th 2021.

Web: https://www.aniwaa.com/guide/3d-scanners/3d-scanning-technologies-and-the-3d-scanning-process/ Web page consulted on april-1st 2021.

Web: https://www.aniwaa.com/buyers-guide/3d-printers/best-metal-3d-printer/ Cherdo, Ludivine, 2022. Web page consulted on july-1st 2022.

UNIVERSITAT
ROVIRA i VIRGILI